

AD-A086 348

HEBREW UNIV JERUSALEM (ISRAEL) DEPT OF INORGANIC AND--ETC F/8 20/12  
ENERGY TRANSFER BETWEEN POST-TRANSITION ELEMENTS & RARE EARTHS --ETC(1)  
AUG 79 R REISFELD

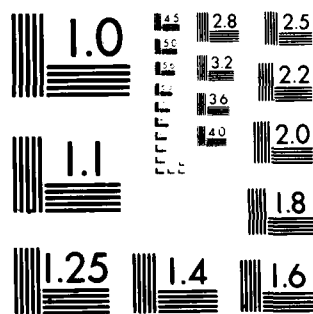
DA-ERO-76-8-066

NL

UNCLASSIFIED

1 of 1  
AD-A086 348

END  
DATE  
FILMED  
8-80  
DTIC



MICROCOPY RESOLUTION TEST CHART  
NATIONAL BUREAU OF STANDARDS-1963-A

**LEVEL IV**

**(12)**

**ENERGY TRANSFER BETWEEN POST-TRANSITION ELEMENTS  
AND RARE EARTHS IN OXIDE AND CHALCOGENIDE GLASSES**

**Final Technical Report**

**by**

**Professor Ronald Reisfeld**

**27 August 1976 - 27 August 1979**

**DEFENSE RESEARCH OFFICE**

**United States Army**

**Fort Monmouth, N.J., England**

**Contract Number DAH04-76-C-0001**

**DTIC  
ELECTE  
JUN 27 1980**

**ADA 086348**

Unclassified  
SECURITY CLASSIFICATION OF THIS PAGE (When Data Entered)

R&D 2280CH

REPORT DOCUMENTATION PAGE		READ INSTRUCTIONS BEFORE COMPLETING FORM	
1. REPORT NUMBER	2. GOVT ACCESSION NO.	3. RECIPIENT'S CATALOG NUMBER	
	AD-A086 348		
4. TITLE (and Subtitle)		5. TYPE OF REPORT & PERIOD COVERED	
Energy Transfer Between Post-Transition Elements & Rare Earths in Oxide & Chalcogenide Glasses		Final Technical rpt. 27 Jul 76 - 27 Aug 79	
6. AUTHOR		7. CONTRACT OR GRANT NUMBER(s)	
Prof. Renata Reisfeld		DAERO-76-G-066	
8. PERFORMING ORGANIZATION NAME AND ADDRESS		9. PROGRAM ELEMENT, PROJECT, TASK AREA & WORK UNIT NUMBERS	
The Hebrew University of Jerusalem Dept. of Inorganic & Analytical Chemistry Jerusalem, Israel		6.11.02A 1T161102BH57-08	
10. CONTROLLING OFFICE NAME AND ADDRESS		11. REPORT DATE	
USARDSG-UK Box 65 FPO, NY 09510		12. NUMBER OF PAGES	
13. MONITORING AGENCY NAME & ADDRESS (if different from Controlling Office)		68	
14. MONITORING AGENCY NAME & ADDRESS (if different from Controlling Office)		15. SECURITY CLASS. (of this report)	
11 27 Aug 79		Unclassified	
16. DISTRIBUTION STATEMENT (of this Report)		15a. DECLASSIFICATION/DOWNGRADING SCHEDULE	
Approved for Public Release - distribution Unlimited			
12 73			
17. DISTRIBUTION STATEMENT (of the abstract entered in Block 20, if different from Report)			
18. SUPPLEMENTARY NOTES			
19. KEY WORDS (Continue on reverse side if necessary and identify by block number)			
Energy Transfer, Luminescence, Rare-Earth Doped Glasses			
20. ABSTRACT (Continue on reverse side if necessary and identify by block number)			
<p>Intensity parameters, radiative transition probabilities and non-radiative relaxation of <math>\text{Ho}^{3+}</math> in various telluride glasses are described.</p> <p>Eigenstates of <math>\text{Tm}^{3+}</math> in an intermediate coupling scheme were obtained by diagonalization of electrostatic matrices of <math>E^1</math>, <math>E^2</math> and <math>E^3</math>, the configurational parameters <math>a</math> and the spin orbit matrix <math>L</math>.</p>			

DD FORM 1 JAN 73


EDITION OF 1 NOV 65 IS OBSOLETE

ALPHA

408527  
SECURITY CLASSIFICATION OF THIS PAGE (When Data Entered)

20. poisoning, were examined for their pharmacokinetic properties. It was found that these sugar derivatives persisted in the blood circulation for a longer period than their non sugar analogs.

The antidotal properties of the two sugar oximes mentioned above against various OP poisoning is now under study and preliminary results (not included in this report) substantiate their superiority to 3- and 4-PAM. The reactivation properties to changes in the antidotal potency of the sugar-oxime vs. its parent substance has been discussed.



ENERGY TRANSFER BETWEEN POST-TRANSITION ELEMENTS  
AND RARE EARTHS IN OXIDE AND CHALCOGENIDE GLASSES

Final Technical Report

by

Professor Renata Reisfeld

27 August 1976 - 27 August 1979

EUROPEAN RESEARCH OFFICE  
United States Army  
London, W.1., England

Contract Number DAERO-76-G-066

The Hebrew University of Jerusalem  
Jerusalem, Israel

Approved for public release; distribution unlimited

# TABLE OF CONTENTS

	<u>Page</u>
Summary and Introduction	1
A. Absorption and emission of $\text{Ho}^{3+}$ in germanate glass	5
B. Calculated radiative and nonradiative transition probabilities and stimulated cross-sections of selected $\text{Er}^{3+}$ lines in oxide glasses	15
C. Intensity parameters and laser analysis of $\text{Pr}^{3+}$ and $\text{Dy}^{3+}$ in oxide glasses	19
D. Radiative transition probabilities and stimulated cross-sections of $\text{Nd}^{3+}$ in $3\text{Ga}_2\text{S}_3 \cdot \text{La}_2\text{S}_3$ (GLS) and $3\text{Al}_2\text{S}_3 \cdot \text{La}_2\text{S}_3$ (ALS) glasses	31
E. Spectral behaviour of $\text{Nd}^{3+}$ doped glasses under narrow-line excitation	37
F. Optical transitions of $\text{Sm}^{3+}$ in oxide glasses	41
G. Energy transfer from $\text{UO}_2^{2+}$ to $\text{Sm}^{3+}$ in phosphate glass	45
H. Transition probabilities of europium(III) in zirconium and beryllium fluoride glasses, phosphate glass and pentaphosphate crystals	50
I. Multiphonon relaxation in glasses	58

Accession For	
NTIS GRA&I	<input checked="" type="checkbox"/>
DDC TAB	<input type="checkbox"/>
Unannounced	
Justification	
By _____	
Distribution/	
Availability Codes	
Dist	Avail and/or special
A	

## Summary and Introduction

This report includes the findings of the research performed under the U.S. Army contract from August 1976 to August 1979.

The findings to August 1978 were reported in two progress reports and included the following information.

Intensity parameters, radiative transition probabilities and non-radiative relaxation of  $\text{Ho}^{3+}$  in various tellurite glasses are described. The results were published in two papers which are presented in this report.

Eigenstates of  $\text{Tm}^{3+}$  in an intermediate coupling scheme were obtained by diagonalization of electrostatic matrices of  $E^1$ ,  $E^2$  and  $E^3$ , the configurational parameters  $\alpha$  and the spin orbit matrix. From these  $U(\lambda)$  matrices between all electronic states of  $\text{Tm}^{3+}$  were obtained.

Multiphonon relaxation rates were calculated for all levels of the  $4f^{12}$  configurations of  $\text{Tm}^{3+}$  incorporated in phosphate, borate, germanate and tellurite glasses. The level fluorescent lifetime was derived from these rates and from the calculated radiative transition probabilities. Using the above results four candidates for laser lines of  $\text{Tm}^{3+}$  in oxide glasses are proposed. These are  $^3\text{H}_4 - ^3\text{H}_5$  at  $2.3\mu$ ,  $^1\text{G}_4 - ^3\text{H}_5$  at  $0.781\mu$ ,  $^1\text{D}_2 - ^3\text{F}_3$  at  $0.760\mu$  and  $^1\text{D}_2 - ^3\text{F}_2$  at  $0.796\mu$ . The results relating to the thulium ion in glasses are presented in three papers below.

Energy transfer was found between antimony and dysprosium in phosphate glasses. Efficiency of transfer was calculated from the measurements of fluorescence intensity and lifetimes.

Energy transfer from  $\text{Bi}^{3+}$  to  $\text{Nd}^{3+}$  is reported in germanate glass. It was found that the excitation range and intensities of the  $^4\text{F}_{3/4} \rightarrow ^4\text{F}_{9/2}$ ,  $^4\text{I}_{11/2}$  emissions are increased several fold when excited through  $^1\text{S}_0 \rightarrow ^3\text{P}_1$  absorption of  $\text{Bi}^{3+}$ . It is shown that the energy transfer is nonradiative. The energy transfer probability and efficiency were calculated from the  $\text{Bi}^{3+}$  fluorescence decay rates and intensities. The  $\text{Bi}^{3+} \rightarrow \text{Nd}^{3+}$  energy transfer may be utilized in  $\text{Nd}^{3+}$  laser glass.

For the measurements of fluorescence in the infrared part of the spectrum an apparatus was assembled.

Chalcogenide glasses of the composition  $0.7\text{Ga}_2\text{S}_3 \cdot 0.27\text{La}_2\text{S}_3 \cdot 0.03\text{Nd}_2\text{S}_3$  doped by 3 mol% of  $\text{Nd}^{3+}$  were prepared. The absorption and emission spectra of these glasses were compared to those of commercial ED-2 3.1wt% Nd-doped silicate glass. The absorption intensities of  $\text{Nd}^{3+}$  in chalcogenide glass are higher than in silicate glass due to the increasing covalency of  $\text{Nd}^{3+}$  in these glasses. Because of the low phonon frequency of the chalcogenide glasses nonradiative relaxation from the  $^4\text{F}_{5/2}$ ,  $^2\text{H}_{9/2}$  to the  $^4\text{F}_{3/2}$  are lower than in other oxide glasses and thus fluorescence from this state is observed.

Based on literature research the prediction of new laser lines in solid and vapor lasers are summarized. These are compared to the characteristics of lasers based on neodymium glasses.

Optical spectra of neodymium in gadolinium molybdate were measured and the optical spectra free-ion wave functions and radiative transition probabilities computed.



The preparation and physical properties of lanthanum-gallium and lanthanum-gallium-sulfide glasses are described. Optical properties such as absorption spectra, fluorescence and radiative and nonradiative transitions of rare-earth ions in these glasses are presented.

A detailed description of the research performed until August 1978 may be found in the following references:

1. R. Reisfeld, J. Hormadaly and A. Muranevich, Chem. Phys. Lett. 38 (1976) 188-191.
2. J. Hormadaly and R. Reisfeld, Chem. Phys. Lett. 45 (1977) 436-440.
3. N. Spector, R. Reisfeld and L. Boehm, Chem. Phys. Lett. 49 (1977) 49-53.
4. R. Reisfeld, L. Boehm and N. Spector, Chem. Phys. Lett. 49 (1977) 251-254.
5. R. Reisfeld, L. Boehm and N. Spector, The Rare Earths in Modern Science and Technology, Ed. G.J. McCarthy and J.J. Rhyne, Plenum (1978) 513-517.
6. R. Reisfeld, N. Roth and L. Boehm, 157th Meeting of the Electrochem. Soc., Pennsylvania, May 8-13, 1977. Abstract No. 145, 77 (1977) 375-377.
7. R. Reisfeld and Y. Kalisky, Chem. Phys. Lett. 50 (1977) 199-201.
8. R. Reisfeld and A. Bornstein, Chem. Phys. Lett. 47 (1977) 194-196.
9. R. Reisfeld, A. Bornstein, J. Flahaut, M. Guittard and A.M. Loireau-Lazac'h, Chem. Phys. Lett. 47 (1977) 408-410.
10. R. Reisfeld and A. Bornstein, J. Noncryst. Solids 27 (1978) 143-145.
11. R. Reisfeld, The 10th Convention of Electrical and Electronics Engineers in Israel, IEEE Papers (1977) 1-3.
12. A. Bornstein, J. Flahaut, M. Guittard, S. Jaulmes, A.M. Loireau-Lazac'h, G. Lucazeau and R. Reisfeld, The Rare Earths in Modern Science and Technology, Ed. G.J. McCarthy and J.J. Rhyne, Plenum (1978) 599-606.
13. N. Spector, C. Guttel and R. Reisfeld, Optica Pura y Aplicada 10 (1977) 197-213.
14. R. Reisfeld, A. Bornstein, J. Bodenheimer and J. Flahaut, J. Luminescence 18/19 (1979) 153-256.

The research performed between August 1978 to August 1979 is presented in detail in this report and includes the following information:

Absorption spectra of  $\text{Ho}^{3+}$  in germanate glass in the range 300-2500 nm and the Judd-Ofelt intensity parameters. Excitation and emission spectra in the visible in temperature range 80-573 K. Radiative transition probabilities from the excited states [ $^5\text{F}_4$ ,  $^5\text{S}_2$ ],  $^5\text{F}_5$ ,  $^5\text{I}_4$ ,  $^5\text{I}_5$  and  $^5\text{I}_6$ , branching ratios and integrated emission cross-sections. Relaxation rates from the ( $^5\text{F}_4$ ,  $^5\text{S}_2$ ) levels estimated to be about  $2 \times 10^5 \text{ s}^{-1}$ .

Radiative transition probabilities for fluorescence bands of  $\text{Er}^{3+}$  in the range  $0.523\mu$  to  $13\mu$  in phosphate, germanate and tellurite glasses. Multiphonon relaxation rates in these glasses and possible laser transitions.

Intensity parameters of  $\text{Pr}^{3+}$  and  $\text{Dy}^{3+}$  in tellurite, borate and phosphate glasses calculated by exclusion of hypersensitive transitions. Branching ratios and integrated cross-sections for stimulated emission for  $^3\text{P}_0$ ,  $^3\text{P}_1$  and  $^1\text{D}_2$  excited states of  $\text{Pr}^{3+}$  and  $^4\text{F}_{9/2}$  of  $\text{Dy}^{3+}$  from intensity parameters and calculated matrix elements. Potential laser transitions.

Radiative transition probabilities, oscillator strengths, radiative lifetimes and branching ratios of  $\text{Nd}^{3+}$  in gallium-lanthanum-sulfide and aluminum-lanthanum-sulfide glasses. Comparison of radiative characteristics of  $\text{Nd}^{3+}$  in oxide and chalcogenide glasses.

$\text{Nd}^{3+}$  doped phosphate, tellurite, ED-2 and germanate glasses excited by laser into different parts of the  $^4\text{I}_{9/2} \rightarrow ^4\text{G}_{5/2}$  inhomogeneously broadened band. Wavelength-dependent decay times in germanate glass and slow diffusion of energy in germanate glass because of large energy mismatch between different sites.

Reduced matrix elements and eigenvectors of the  $4f^5$  electronic configuration of  $\text{Sm}^{3+}$ . Absorption spectra of  $\text{Sm}^{3+}$  in phosphate, borate, germanate and tellurite glasses. Deduction of intensity parameters from measured oscillator strengths by least-squares fitting. Radiative transition probabilities, integrated cross-sections, branching ratios and decay times.

Energy transfer from  $\text{UO}_2^{2+}$  to  $\text{Sm}^{3+}$ . Transfer efficiency from decrease of donor luminescence and lifetimes and from increase of acceptor fluorescence. Higher efficiency when donor excited at higher energy levels. Condition for transfer overlap of excitation levels of donor and acceptor.

$\text{Eu}^{3+}$  in zirconium and beryllium fluoride glasses, phosphate glass and pentaphosphate crystals for which radiation transition probabilities and branching ratios are evaluated for excited states  $^5\text{D}_J$  ( $J = 0, 1, 2, 3$ ) and  $^5\text{L}_6$  to  $^7\text{F}_J$ . Better agreement between calculated and observed lifetimes

and branching ratios than in pentaphosphate crystals and fluoride glasses are obtained.

Experimental data of multiphonon relaxation between electronic levels of rare earth ions in glasses are presented. These are based on measurements of the decay times or quantum efficiencies of the specific levels and subtracting the radiative transition probabilities in oxide, chalcogenide and fluoride glasses. It is shown that the nonradiative transfer in all glasses depends mainly on the energy gap between the emitting and next lower level of the ion incorporated in the glass and that the high energy phonons of the network formers are responsible for the relaxation permitting the lowest order process. The phenomenological parameters  $\alpha$ ,  $\beta$  and  $\epsilon$  appearing in the formulae of multiphonon transfer are computed and compared to these values in crystals. It is also shown that the Huang-Rhys number  $S$  being a measure of the electron-phonon coupling strengths is smaller than 0.1 for the oxide glasses as predicted by the theory of multiphonon relaxation. However it achieves a large value of about 2 in the chalcogenide glasses. The discrepancy in this high value is explained by the covalency of the rare earths incorporated in the chalcogenide glasses with the surrounding sulfur ions, thus the rare earth ions cannot be treated as isolated centers in these glasses. Experimental findings of phonon-assisted energy transfer between uranyl and rare earth ions in phosphate glasses are presented. It is shown that an experimental dependence between multiphonon relaxation rates and the energy gap is obtained similar to the multiphonon relaxation in a single ion. The coupling constant is higher in the case of the energy transfer due to the stronger coupling of uranyl to the glass.

## ABSORPTION AND EMISSION OF $\text{Ho}^{3+}$ IN GERMANATE GLASSES

R. REISFELD, J. HORMADALY and A. MURANEVICH

*Department of Inorganic and Analytical Chemistry, The Hebrew University of Jerusalem, Jerusalem, Israel*

Received 1 February 1978

Absorption spectra of  $\text{Ho}^{3+}$  in germanate glasses were measured in the range 300–2500 nm and the intensity parameters were calculated by the Judd–Ofelt theory. Excitation and emission spectra were measured in the visible at a temperature range of 80–573 K. The radiative transition probabilities from the excited states [ $^5\text{F}_4$ ,  $^5\text{S}_2$ ],  $^5\text{F}_5$ ,  $^5\text{I}_4$ ,  $^5\text{I}_5$  and  $^5\text{I}_6$ , branching ratios and integrated emission cross-sections were calculated. The non-radiative relaxation rate from the ( $^5\text{F}_4$ ,  $^5\text{S}_2$ ) levels is estimated to be about  $2 \times 10^5 \text{ s}^{-1}$ .

### 1. Introduction

Recently it was shown that holmium may play a dominant role in infrared-to-visible conversion [1]. Coherent emission for holmium ions ( $2.1 \mu\text{m}$ ) has been reported in numerous hosts [2]. Optical intensities, radiative transition probabilities and non-radiative relaxation of holmium in tellurite glasses [3], calibo and phosphate glasses have been performed in our laboratory [4]. Analysis of the optical spectra of holmium in  $\text{LiYF}_4$  was performed by Karyanis et al. [5]. Analysis of laser emission in several crystal lattices has been performed by Caird and DeShazer [6]. Of the many solid-state hosts of rare earth ions the germanates appear to be a very promising material [7–9]. Therefore we have performed a detailed analysis of the optical characteristics of holmium in the germanate host using the approach of the Judd–Ofelt theory for calculation of the radiative transition probabilities and stimulated cross-sections.

### 2. Theory

Since the theory and treatment of the radiative and non-radiative transitions of the rare earths have been described in detail in ref. [10], only a brief summary and essential formulas are given below. The free-ion states of an ion having an  $f^n$  electronic configuration are composed of a linear combination of Russell–Saunders

states:

$$|f^n[\alpha SL]J\rangle = \sum_{\alpha SL} C_{\alpha SL} |f^n\alpha SLJ\rangle, \quad (1)$$

where the coupling coefficients  $C$  are obtained from diagonalizing the combined electrostatic, spin-orbit and configuration interaction energy matrices. (The bracketed quantities indicate that in the labeling of states,  $S$  and  $L$  are no longer good quantum numbers.)

Electric dipole transitions are forbidden between states of the same configuration. However, they become allowed if odd order terms in the expansion of the static or dynamic crystalline field potential admix states of higher, opposite parity configurations into  $f^n$ .

Because rare earths enter into the glass at non-centro-symmetric sites [11] ( $C_s$  symmetry) electric dipole transitions of rare earths in glasses become possible.

The electric dipole (ed) line strength in the Judd-Ofelt theory is expressed as the sum of three intensity parameters  $\Omega_\lambda$  and reduced matrix elements of tensor operators  $U^{(\lambda)}$ . The line strength of the transition has the form in Axe notation [12]

$$S_{ed}(aJ; bJ') = e^2 \sum_{\lambda \text{ even}} \Omega_\lambda \langle f^n[\alpha SL]J \| U^{(\lambda)} \| f^n[\alpha' S' L'] J' \rangle^2. \quad (2)$$

The parameters  $\Omega_\lambda$  contain the odd terms in the crystal field expansion, the energy separation of the two opposite-parity configurations and the interconfigurational radial integrals, and include contributions from both static and vibrationally induced electric-dipole transitions. From the selection rule  $|\Delta J| \leq 2l$ ,  $\lambda$  in the summation in eq. (2) is limited to values of 2, 4, 6 for lanthanide ( $l = 3$ ) ions.

The energy levels of  $\text{Ho}^{3+}$  in  $\text{LaF}_3$  up to  $40\,000\text{ cm}^{-1}$  are well established by the work of Caspers et al. [13]. Their results were used by Weber et al. [14] to derive eigenstates for intermediate coupling and subsequently transition matrix elements between  $J$  manifold. It was shown by Reisfeld et al. [15] and by Riseberg and Weber [16] that the matrix elements for a given rare earth ion are insensitive to the host in which the rare earth is situated, therefore the matrix elements obtained by Weber [14] were used in this work.

For calculation of the spontaneous emission probability the relaxation between  $A_{ed}$  (spontaneous emission probability) and the line strengths may be used. This is of the form:

$$A(aJ', bJ') = 64\pi^4 \nu^3 \chi / [3(2J + 1) hc^3] S(aJ; bJ'), \quad (3)$$

where  $\nu$  is the frequency,  $\chi_{ed} = \frac{1}{9}[n(n^2 + 2)^2]$  (electric field correction) and  $n$  is the refractive index.

The oscillator strength  $p$  of a transition of average frequency in terms of the line strength above is given by

$$p(aJ; bJ') = [8\pi^2 m \nu / 3(2J + 1) hc^2] S(aJ; bJ'). \quad (4)$$

Experimentally,  $p$  is obtained from the absorption spectrum by

$$p = 4.318 \times 10^{-9} \int \epsilon(\sigma) d\sigma, \quad (5)$$

where  $\epsilon$  is the molar extinction coefficient and  $\sigma \text{ cm}^{-1}$  is the wavenumber of the absorption band.

The relation between  $A$  and  $p$  is

$$A_{ed} = \frac{8\pi^2 e^2 \nu^2 \chi}{mc^3} \cdot p = \frac{8\pi^2 e^2 \sigma^2 \chi}{mc} \cdot p = \frac{8\pi^2 e^2 \sigma^2 n^2}{mc(2J+1)} \sum_{\lambda=2,4,6} \Omega_{\lambda} \langle f^N \psi_J \| U^{(\lambda)} \| f^N \psi'_{J'} \rangle^2, \quad (6)$$

where  $\tau_{\lambda}/(2J+1) = T_{\lambda}$ .

It should be noted that the intensity parameters  $\Omega_{\lambda}$  [eq. (2)] and the  $\tau_{\lambda}$  parameters [eq. (6)] are related by

$$\Omega_{\lambda} = (3h/8\pi^2 mc)(n^2/\chi) \tau_{\lambda} = 9.2185 \times 10^{-12} (n^2/\chi) \tau_{\lambda}.$$

The probabilities for magnetic-dipole transitions are small compared to the electric dipole of  $\text{Ho}^{3+}$  in glasses, and their contribution to the oscillator strengths of  $\text{Ho}^{3+}$  were not included.

The branching ratio

$$\beta_{ij} = A_{ij} / \sum A_{ij}, \quad (7)$$

which takes the form in the case of thermalization, is given by

$$\beta_{ij} = \frac{\sum_i g_i \exp(-\Delta E_i/kT) A_{ij}}{\sum_i \sum_j g_i \exp(-\Delta E_i/kT) A_{ij}}. \quad (8)$$

The cross-section for stimulated emission integrated over all Stark split components of the upper and lower  $J$ -manifolds is given by [17]

$$\int_{J \rightarrow J'} \sigma(\nu) d\nu = \frac{\bar{\lambda}^2}{8\pi c n^2} A_{JJ'}, \quad (9)$$

where  $\nu = 1/\lambda$ .

Using eq. (6) this is reduced to

$$\int_{J \rightarrow J'} \sigma(\nu) d\nu = \frac{\pi e^2}{mc^2} f_{JJ'}, \quad (10)$$

which shows the significance of the oscillator strength in laser analysis. Without detailed line-shape information eq. (10) cannot be used to predict peak cross-sections, but it is evident that transitions with larger oscillator strengths will generally have larger peak cross-sections.

### 3. Experimental

The germanate glasses of composition  $17 \text{ K}_2\text{O} \cdot 17 \text{ BaO} \cdot 66 \text{ GeO}_2$  were studied. The preparation procedure and starting materials were described earlier [18]. The doping by holmium was made by adding the appropriate amount of  $\text{Ho}_2\text{O}_3$  to the glass-forming base and melting the mixture at  $1150^\circ\text{C}$ . The optical absorption spectra were measured at room temperature. The absorption spectra within the spectral range 300–2500 nm were obtained with a Cary 14 spectrophotometer, samples of about 2 mm thickness containing 1 and 10 wt%  $\text{Ho}^{3+}$  being used. The absorption of  $\text{Ho}^{3+}$  up to 300 nm was not observable because of the high intrinsic absorption of the germanate glasses. The emission and excitation spectra were recorded by an apparatus described elsewhere [19]. The measurements were performed in liquid nitrogen, room temperature up to 573 K (at 50 K intervals). For emission measurements, samples of about 1 mm thickness with holmium content between 0.25 and 5.00 wt% were used.

### 4. Results and discussion

Figure 1 shows the absorption spectrum of  $\text{Ho}^{3+}$  in germanate glass in the range 300–2500 nm. Table 1 compiles the measured and calculated oscillator strengths of  $\text{Ho}^{3+}$  in germanate glasses and compares these results to the previously obtained oscillator strengths in barium tellurite glass [3].

Table 2 gives the calculated intensity parameters from the above oscillator strengths. Intensity parameters of  $\text{Ho}^{3+}$  in other oxide glasses are also given for comparison. It should be noted that while the  $\Omega_2$  parameters are similar in the different hosts a remarkable difference is observed in the  $\Omega_4$  and  $\Omega_6$  parameters.

Table 3 gives the calculated electric dipole radiative transition probabilities  $A_{ij}$ , the branching ratio  $\beta_{ij}$  and integrated cross-sections for stimulated emission using formulae (3), (8) and (10) correspondingly.

The refractive index taken was 1.643 (no wavelength correction was made).

Figure 2 shows the emission spectrum from  $^5\text{F}_4$  and  $^5\text{S}_2$  levels at temperatures of 80, 293, 373, 473 and 573 K. The excitation spectrum of this emission (540 nm) at 80 K is shown in fig. 3. From fig. 2 it can be seen that the relative intensity of the short-wave band to the long-wave band decreases with lowering of temperature, indicating that because of thermalization the contribution of  $^5\text{F}_4$  is smaller at 80 K. Also, a shift to the red is observed in maxima with lowering of temperature owing to different superposition of the bands.

Figure 4 shows the concentration dependence of the  $^5\text{F}_4$ ,  $^5\text{S}_2 \rightarrow ^5\text{I}_8$  emission of  $\text{Ho}^{3+}$  in germanate glass. The concentration quenching in the germanate glass is less pronounced than in the tellurite glass [4]. This means that the  $\text{Ho}^{3+}$  centers are interacting less strongly than in the tellurite glasses.

The mechanism of the quenching of the green fluorescence of  $\text{Ho}^{3+}$  arises from

Fig. 1. Absorption spectrum of  $\text{Ho}^{3+}$  (2 mm thick sample) in  $17 \text{ K}_2\text{O} \cdot 17 \text{ BaO} \cdot 66 \text{ GeO}_2$ . (a) A - 10 wt%  $\text{Ho}^{3+}$ ; B - 1 wt%  $\text{Ho}^{3+}$ . (b) 10 wt%  $\text{Ho}^{3+}$ .



Table 1  
Oscillator strengths of  $\text{Ho}^{3+}$  in germanate and tellurite glasses.

Transition assignment	Wave number ( $\text{cm}^{-1}$ )	Oscillator strength $\times 10^6$			
		17 $\text{K}_2\text{O} \cdot 17 \text{BaO} \cdot 66 \text{GeO}_2$		15 $\text{BaO} \cdot 85 \text{TeO}_2$	
		$f_{\text{meas}}$	$f_{\text{cal}}$	$f_{\text{meas}}$	$f_{\text{cal}}$
$^5\text{I}_8 \rightarrow ^5\text{I}_7$	4717-5555	0.90	—	2.08	—
$^5\text{I}_6$	8064-9090	0.26	0.38	1.15	1.76
$^5\text{I}_5$	10638-11627	—	—	0.28	0.32
$^5\text{I}_4$	—	—	—	—	—
$^5\text{F}_5$	14880-16129	1.24	1.50	4.70	4.76
$^5\text{S}_2$	17857-19230	1.58	1.56	6.40	6.26
$^5\text{F}_4$					
$^5\text{F}_3$	20000-21276	0.51	0.34	2.09	1.91
$^5\text{F}_2$	21052-21739	0.47	0.74	1.29	1.09
$^3\text{K}_8$				0.84	—
$^5\text{G}_6$	21276-22988	24.03	24.03	35.77	35.75
$^5\text{G}_5$	23225-25000	1.36	0.51	5.31	—
$^5\text{G}_4$	25064-26666	0.45	0.35	—	—
$^3\text{K}_7$					
$^3\text{H}_6$	26666-28238	5.57	—	—	—
$^3\text{H}_5$					
$^5\text{G}_2$					
$^3\text{L}_9$	—	—	—	—	—
$^5\text{G}_3$					
$^3\text{K}_6$					
$^3\text{F}_4$	29412-30769	0.78	—	—	—

the following interaction:

$$[^5\text{F}_4 - ^5\text{S}_2] + ^5\text{I}_8 \rightarrow ^5\text{I}_4 + ^5\text{I}_7,$$

and in order that such quenching will occur the interacting centers must be separated by very small differences or a resonance should exist between the energy levels of the two centers. From the absence of strong quenching in the germanate

Table 2  
Intensity parameters of  $\text{Ho}^{3+}$  in various oxide glasses [4]

Host glass	$\Omega_2$ ( $10^{-20} \text{ cm}^2$ )	$\Omega_4$ ( $10^{-20} \text{ cm}^2$ )	$\Omega_6$ ( $10^{-20} \text{ cm}^2$ )	Ref.
germanate	$6.52 \pm 0.47$	$1.71 \pm 0.86$	$0.50 \pm 0.31$	this work
phosphate	$5.60 \pm 0.28$	$2.72 \pm 0.41$	$1.87 \pm 0.26$	
calibo	$6.83 \pm 0.29$	$3.15 \pm 0.42$	$2.53 \pm 0.31$	
barium tellurite	$6.08 \pm 0.27$	$2.61 \pm 0.50$	$1.94 \pm 0.18$	

Table 3  
Radiative transition probabilities, branching ratios and integrated emission cross sections of Ho<sup>3+</sup> in germanate glasses

Transition assignment	Energy (cm <sup>-1</sup> )	$A_{ij}$ (s <sup>-1</sup> ) <sup>a)</sup>	$\beta_{ij}$ <sup>b)</sup>	$f\sigma(\nu) d\nu$ (10 <sup>-18</sup> cm <sup>-1</sup> ) <sup>c)</sup>
<sup>5</sup> F <sub>4</sub> → <sup>5</sup> F <sub>5</sub>	3090	13.68	0.006	0.704
<sup>5</sup> F <sub>4</sub> → <sup>5</sup> I <sub>4</sub>	5380	8.66	0.004	0.147
<sup>5</sup> F <sub>4</sub> → <sup>5</sup> I <sub>5</sub>	7440	62.92	0.029	0.559
<sup>5</sup> F <sub>4</sub> → <sup>5</sup> I <sub>6</sub>	10000	173.68	0.082	0.853
<sup>5</sup> F <sub>4</sub> → <sup>5</sup> I <sub>7</sub>	13500	284.49	0.134	0.766
<sup>5</sup> F <sub>4</sub> → <sup>5</sup> I <sub>8</sub>	18540	1585.78	0.745	2.27
<sup>5</sup> S <sub>2</sub> → <sup>5</sup> F <sub>5</sub>	2740	0.248	0.0003	0.016
<sup>5</sup> S <sub>2</sub> → <sup>5</sup> I <sub>4</sub>	5030	14.46	0.019	0.117
<sup>5</sup> S <sub>2</sub> → <sup>5</sup> I <sub>5</sub>	7090	12.66	0.017	0.124
<sup>5</sup> S <sub>2</sub> → <sup>5</sup> I <sub>6</sub>	9650	59.29	0.078	0.313
<sup>5</sup> S <sub>2</sub> → <sup>5</sup> I <sub>7</sub>	13150	273.70	0.359	0.779
<sup>5</sup> S <sub>2</sub> → <sup>5</sup> I <sub>8</sub>	18190	401.38	0.527	0.596
<sup>5</sup> F <sub>5</sub> → <sup>5</sup> I <sub>4</sub>	2300	0.041	0.00003	0.004
<sup>5</sup> F <sub>5</sub> → <sup>5</sup> I <sub>5</sub>	4350	3.79	0.003	0.098
<sup>5</sup> F <sub>5</sub> → <sup>5</sup> I <sub>6</sub>	6910	46.06	0.035	0.474
<sup>5</sup> F <sub>5</sub> → <sup>5</sup> I <sub>7</sub>	10410	262.11	0.205	1.220
<sup>5</sup> F <sub>5</sub> → <sup>5</sup> I <sub>8</sub>	15450	996.38	0.757	2.050
<sup>5</sup> I <sub>4</sub> → <sup>5</sup> I <sub>5</sub>	2060	2.48	0.076	0.287
<sup>5</sup> I <sub>4</sub> → <sup>5</sup> I <sub>6</sub>	4610	12.62	0.387	0.292
<sup>5</sup> I <sub>4</sub> → <sup>5</sup> I <sub>7</sub>	8110	14.63	0.449	0.109
<sup>5</sup> I <sub>4</sub> → <sup>5</sup> I <sub>8</sub>	13160	2.86	0.088	0.008
<sup>5</sup> I <sub>5</sub> → <sup>5</sup> I <sub>6</sub>	2560	3.86	0.068	0.289
<sup>5</sup> I <sub>5</sub> → <sup>5</sup> I <sub>7</sub>	6060	29.73	0.523	0.398
<sup>5</sup> I <sub>5</sub> → <sup>5</sup> I <sub>8</sub>	11100	23.24	0.409	0.093
<sup>5</sup> I <sub>6</sub> → <sup>5</sup> I <sub>7</sub>	3500	8.71	0.118	0.349
<sup>5</sup> I <sub>6</sub> → <sup>5</sup> I <sub>8</sub>	8540	65.42	0.882	0.441

a) Calculated by eq. (3).

b) Calculated by eq. (8).

c) Calculated by eq. (10).

glasses we conclude that the Ho<sup>3+</sup> centers in the germanate are separated in energy, as can be seen from the splitting in the spectra.

The multiphonon relaxation rates  $W_{NR}$  between the two adjacent levels [<sup>5</sup>F<sub>4</sub>, <sup>5</sup>S<sub>2</sub>] → <sup>5</sup>F<sub>5</sub> were obtained from the formula:  $W_{NR}(0) = B \exp(-\alpha\Delta E)$  where  $W_{NR}(0)$  is the multiphonon relaxation rate at low temperature and  $B$  and  $\alpha$  are host-dependent constants determined previously [20] and are summarized in table 4. Here,  $\Delta E$  is the energy difference in cm<sup>-1</sup> between the levels in which the multiphonon relaxation occurs. In the germanate glass the multiphonon relaxation

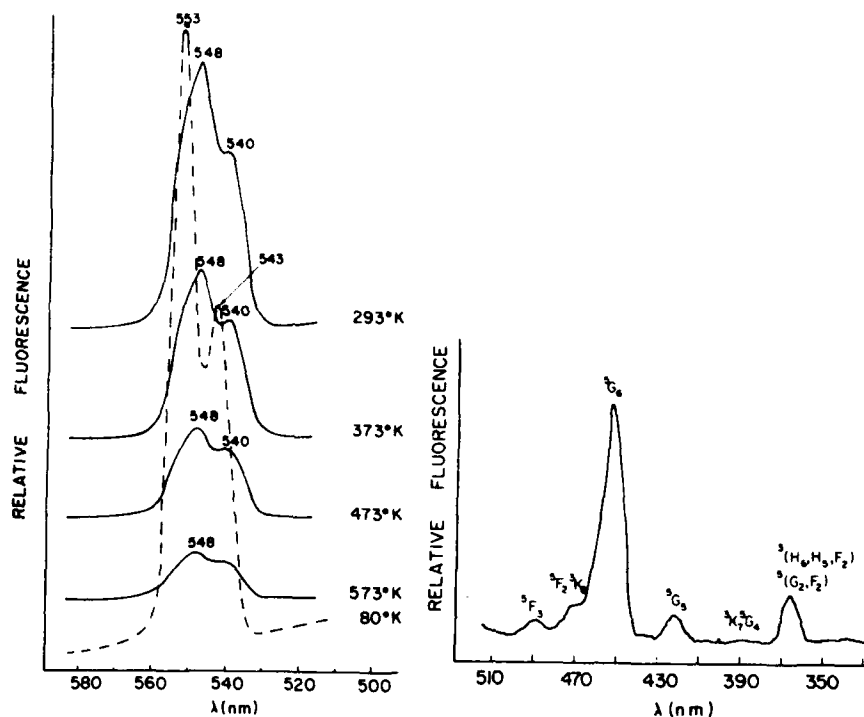


Fig. 2. Emission intensities of  $^5\text{F}_4$ ,  $^5\text{S}_2 \rightarrow ^5\text{I}_8$  transitions under excitation at 450 nm ( $^5\text{I}_8 \rightarrow ^5\text{G}_6$ ) as a function of temperature.

Fig. 3. Excitation spectrum of the  $^5\text{F}_4$ ,  $^5\text{S}_2 \rightarrow ^5\text{I}_8$  emission at room temperature.

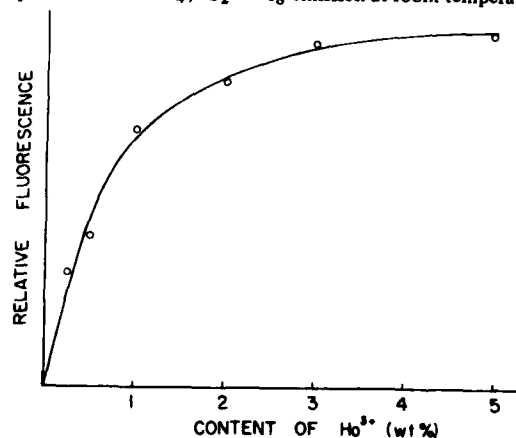


Fig. 4. Concentration dependence of  $\text{Ho}^{3+}$  in  $17 \text{ K}_2\text{O} \cdot 17 \text{ BaO} \cdot 66 \text{ GeO}_2$  glass.

Table 4  
Multiphonon parameters in oxide glasses [20]

	$B$	$\alpha$
borate glass	$2.9 \times 10^{12}$	0.0038
phosphate glass	$5.4 \times 10^{12}$	0.00466
germanate glass	$3.4 \times 10^{11}$	0.00485
tellurite glass	$6.3 \times 10^{10}$	0.0047
$\text{YAlO}_3$ crystal	$6.43 \times 10^9$	0.00469

rate is  $2 \times 10^5 \text{ s}^{-1}$ . The temperature dependence of the transfer rate can be evaluated from fig. 2, and the results confirm those of refs. [21] and [22].

The high multiphonon relaxation rate permits a strong population of the  $^5\text{I}_1$  level from the higher excited electronic levels, and thus a germanate glass may have promising value as a material for a laser at  $2.1 \mu\text{m}$ .

#### Acknowledgement

This research was partially supported by US Army Contract No. DAERO-77-G-066.

#### References

- [1] J.F. Pouradier and F. Auzel, *J. Phys.* 37 (1976) 421.
- [2] R.G. Stafford, H. Masui, R.L. Farrow, R.K. Chang and L.G. Van Uitert, *J. Appl. Phys.* 47 (1976) 2483.
- [3] R. Reisfeld, J. Hormadaly and A. Muranevich, *Chem. Phys. Letters* 38 (1976) 188.
- [4] R. Reisfeld and J. Hormadaly, *J. Chem. Phys.* 64 (1976) 3207.
- [5] N. Karyanis, D.E. Wortman and H.P. Jenssen, *J. Phys. Chem. Solids* 37 (1976) 675.
- [6] J.A. Caird and L.G. DeShazer, *IEEE J. Quantum Electron.* QE-11 (1975) 97.
- [7] H.G. Lipson, J.R. Buckmelter and C.O. Dugger, *J. Non-Crystalline Solids* 17 (1975) 27.
- [8] R. Reisfeld and Y. Eckstein, *Solid State Commun.* 13 (1973) 265.
- [9] R. Reisfeld and Y. Eckstein, *J. Non-Crystalline Solids* 15 (1974) 125.
- [10] R. Reisfeld, *Structure and Bonding* 22 (1975) 123.
- [11] R. Reisfeld, *Structure and Bonding* 13 (1973) 53.
- [12] J.D. Axe, Jr., *J. Chem. Phys.* 39 (1963) 1154.
- [13] H.H. Caspers, H.E. Rast and J.L. Fry, *J. Chem. Phys.* 53 (1970) 3208.
- [14] M.J. Weber, B.H. Matsinger, V.L. Donlan and G.T. Surratt, *J. Chem. Phys.* 57 (1972) 562.
- [15] R. Reisfeld, L. Boehm, N. Lieblich and B. Barnett, *Proc. 10th Rare Earth Res. Conf.* 2 (1973) 1142 (US Atomic Energy Commission Tech. Inf. Center).
- [16] L.A. Riseberg and M.J. Weber, *Relaxation phenomena in rare earth luminescence*, in: *Progress in Optics*, Vol. XIV, ed. E. Wolf (North-Holland, Amsterdam, 1975).
- [17] W.F. Krupke, *IEEE J. Quantum Electron.* QE-10 (1974) 450.

- [18] R. Reisfeld and Y. Eckstein, *J. Non-Crystalline Solids* 12 (1973) 357.
- [19] R. Reisfeld and Y. Eckstein, *J. Solid State Chem.* 5 (1972) 174.
- [20] R. Reisfeld, L. Boehm and N. Spector, in: 13th Rare Earth Res. Conf., W. Virginia, Oct. 1977 Proc. (Plenum Press, New York, 1978).
- [21] J. Hormadaly and R. Reisfeld, *Chem. Phys. Letters* 45 (1977) 436.
- [22] C.B. Layne, W.H. Lowdermilk and M.J. Weber, *Phys. Rev. B* 16 (1977) 10.

CALCULATED RADIATIVE AND NONRADIATIVE TRANSITION PROBABILITIES AND  
STIMULATED CROSS-SECTIONS OF SELECTED  $\text{Er}^{3+}$  LINES IN OXIDE GLASSES\*

R. Reisfeld, L. Boehm, E. Greenberg and N. Spector\*\*

Department of Inorganic and Analytical Chemistry  
The Hebrew University of Jerusalem, Israel

\*\*Soreq Research Center, Yavne, Israel

ABSTRACT

Radiative transition probabilities for fluorescence bands extending from  $0.523\mu$  to  $13\mu$  of  $\text{Er}^{3+}$  in phosphate, germanate and tellurite glasses were calculated using the Judd-Ofelt approach. Multiphonon relaxation rates from these levels were also calculated using the phenomenological parameters of multiphonon relaxation theory in glasses. Possible laser transitions of  $\text{Er}^{3+}$  in those glasses are discussed.

Stimulated emission of several infrared lines of erbium above  $1\mu$  has been obtained in a variety of solid hosts. See Weber (1) et al. and references therein. In addition to these transitions, stimulated emission arising from the  $^4\text{S}_{3/2}$ - $^4\text{I}_{13/2}$  at  $0.85\mu$  was observed in YLF by Chicklis et al. (2).

Erbium can also be used as a donor in energy transfer to Ho and Tm in activating fluorescence of these ions (3).

In order to predict the possible laser lines in Er doped glasses, we have performed the calculation of the relevant spectroscopic properties using the Judd-Ofelt parameters obtained by us previously (4,5). All the relevant formulae for the calculation of radiative transition probabilities by the Judd-Ofelt method can be found in the preceding paper (6) in this volume, and a detailed description of the method in ref. 7. In the specific case of the two levels of erbium  $^4\text{S}_{3/2}$ ;  $^2\text{H}_{11/2}$  which are separated in the glasses by an energy gap of approximately  $700\text{ cm}^{-1}$  the effect of thermalization

---

\*Partially supported by U.S. Army Contract No. DAERO-76-G-066

at room temperature must be taken into account. In this case effective radiative transition probabilities  $A_{eff}^R$  and lifetimes  $\tau_{eff}$  are obtained by

$$A_{ijeff}^R = \frac{\sum_{ij} g_i A_{ij}^R \exp-(E_1-E_i)/kT}{\sum_{ij} g_i \exp-(E_1-E_i)/kT}$$

$$i = {}^2H_{11/2}, {}^4S_{3/2}$$

j = terminal level

$$\frac{1}{\tau_{eff}} = \sum_{ij} A_{ij}^R + \sum_{ij} W_{ij}^{NR}$$

The formula for nonradiative transfer is given in ref. 8.

In Table I we present the oscillator strengths, transition probabilities A, branching ratios  $\beta$  and effective life time  $\tau_{eff}$  for transitions which have been shown to lase in crystals and in three oxide glasses: phosphate, tellurite, and germanate. (The composition of the glasses was described in ref. 5). The calculated values are compared to those of  $CaF_2$ ,  $YAlO_3$  and YAG.

As can be seen from the Table, the radiative transition probabilities in the glasses, in particular the tellurite glass, compare well with those of  $CaF_2$  and  $YAlO_3$ . Also, the branching ratios are quite favourable in the glasses.<sup>3</sup> Therefore, those glasses can be considered as good materials for erbium lasers.

#### REFERENCES

1. M.J. Weber, M. Bass & G.A. de Mars, J.Appl.Phys. 42, 301 (1971).
2. E.P. Chicklis, C.S. Naiman & H.P. Jenssen, J.Q.E. QE-13, 893 (1977).
3. D. Pacheco & B. Di Bartolo, J.Lumin. 16, 1 (1978).
4. R. Reisfeld & Y. Eckstein, J.Non-Crys.Solids 15, 125 (1974).
5. R. Reisfeld & Y. Eckstein, J.Chem.Phys. 63, 4001 (1975).
6. R. Reisfeld, A. Bornstein, J. Flahaut & A.M. Loireau-Lazac'h, This volume.
7. R. Reisfeld & C.K. Jørgensen, Lasers & Excited States of Rare-Earths, Springer Verlag, 1977.
8. R. Reisfeld, L. Boehm & N. Spector, The Rare Earths in Modern Science & Technology, Ed. G.J. McCarthy & J.J. Rhyne, Plenum Press 1977, p. 513.

Table I. Spectral characteristics for the observed laser line of  $\text{Er}^{3+}$  in various matrices.

Matrix	$f \times 10^6$	$A$ $s^{-1}$	$\beta$	$\tau_{i, \text{eff}}$ sec	$f\sigma(\nu) d\nu$ $\times 10^{-18}$	Comments
1. Transition ${}^2H_{11/2}, {}^4S_{3/2} \rightarrow {}^4I_{9/2}$ at $\sim 1.67\mu$ .						
$\text{YAlO}_3$	1.21	107	0.015	$0.14 \times 10^{-3}$		pulse laser at room temperature
Phosphate glass	1.19	68	0.032	$0.20 \times 10^{-3}$	1.02	
Germanate glass	0.65	63*	0.041*	$0.60 \times 10^{-3}$	0.61	
Tellurite glass	1.55	50	0.03	$0.68 \times 10^{-4}$	1.33	
		42*	0.05*			
		188	0.03			
		172*	0.04*			
2. Transition ${}^2H_{11/2}, {}^4S_{3/2} \rightarrow {}^4I_{11/2}$ at $1.2\mu$ .						
$\text{YAlO}_3$	0.38	51.2	0.007	$0.14 \times 10^{-3}$		pulse laser at 77°K
$\text{CaF}_2$	0.31	51.2	0.007	$0.14 \times 10^{-3}$		
Phosphate glass	0.33	37	0.017	$0.20 \times 10^{-3}$	0.30	
Germanate glass	0.16	32*	0.021	$0.6 \times 10^{-3}$	0.17	
Tellurite glass	0.45	25	0.216	$0.68 \times 10^{-4}$	0.42	
		19*				
		107	0.017			
		95*	0.021			
3. Transition ${}^2H_{11/2}, {}^4S_{3/2} \rightarrow {}^4I_{13/2}$ at $0.85\mu$ .						
$\text{CaF}_2$	1.61	557	0.078	$0.14 \times 10^{-3}$		operating at 77°K
Phosphate glass	2.13	421	0.20	$0.20 \times 10^{-3}$	1.70	
Germanate glass	0.991	440*	0.283*	$0.60 \times 10^{-3}$	0.82	
Tellurite glass	3.01	248	0.149	$0.68 \times 10^{-4}$	2.40	
		251*	0.281*			
		1252	0.199			
		1310*	0.284*			
4. Transition ${}^4I_{11/2} \rightarrow {}^4I_{13/2}$ at $2.75\mu$ .						
$\text{YAlO}_3$	1.29	41.0	0.22	$1.63 \times 10^{-3}$		room temperature
YAG	1.29	41.0	0.067	$1.63 \times 10^{-3}$		
Phosphate glass	1.35	26.0	0.147	$5.02 \times 10^{-6}$	1.19	
Germanate glass	0.98	23.3	0.163	$1.57 \times 10^{-4}$	----	
Tellurite glass	1.86	76.0	0.144	$3.16 \times 10^{-4}$	0.16	



Matrix	$f \times 10^6$	$A$ $s^{-1}$	$\beta$	$\tau_i$ eff sec	$\int \sigma(\nu) d\nu$ $\times 10^{-18}$	Comments
5. Transition ${}^4I_{13/2} \rightarrow {}^4I_{15/2}$ at $1.54\mu$ .						
YAlO <sub>3</sub>	2.04	211.0	1.00	$4.75 \times 10^{-3}$		pulse laser, room temperature
YAG	2.04	211.0	1.00	$4.75 \times 10^{-3}$		
Phosphate glass	2.19	134.0	1.0	$7.42 \times 10^{-3}$	1.93	
Germanate glass	1.46	119.0	1.0	$9.1 \times 10^{-3}$	1.19	
tellurite glass	3.05	396	1.0	$2.53 \times 10^{-3}$	2.71	

\*The position of the  ${}^2H_{11/2}$  is  $713 \text{ cm}^{-1}$  above the  ${}^4S_{3/2}$  level.  
The value of thermalization was calculated using this energy gap.

	<u>Phosphate</u>	<u>Germanate</u>	<u>Tellurite</u>
$\sigma$	10.27, 2.52, 1.08	8.49, 0.63, 0.64	7.49, 1.26, 1.22
$n$	1.48	1.64	2.15

## INTENSITY PARAMETERS AND LASER ANALYSIS OF Pr<sup>3+</sup> AND Dy<sup>3+</sup> IN OXIDE GLASSES \*

J. HORMADALY and R. REISFELD

*Department of Inorganic and Analytical Chemistry, The Hebrew University of Jerusalem,  
Jerusalem, Israel*

Received 6 July 1978

Revised 19 September 1978

Intensity parameters ( $\Omega_\lambda$ ) of Pr<sup>3+</sup> and Dy<sup>3+</sup> have been obtained in tellurite, borate and phosphate glasses. It has been found that  $\Omega_\lambda$  calculated by exclusion of hypersensitive transitions, gives a better fit between measured and calculated lifetimes and branching ratios than those including hypersensitive transitions. Using these parameters and calculated matrix elements  $U(\lambda)$ , radiative transition probabilities, branching ratios and integrated cross sections for stimulated emission were calculated for <sup>3</sup>P<sub>0</sub>, <sup>3</sup>P<sub>1</sub> and <sup>1</sup>D<sub>2</sub> excited states of Pr<sup>3+</sup> and <sup>4</sup>F<sub>9/2</sub> excited state of Dy<sup>3+</sup>. Potential laser transitions are indicated.

### 1. Introduction

It has been shown [1] earlier that the desirable conditions for good laser materials are large stimulated cross section, high quantum efficiency and branching ratios of the emitting level. Also in order to retain the population inversion, a fast depopulation of the terminal laser level is required. Prediction of these transitions is possible by use of the Judd-Ofelt [2,3] approach, as was shown [4] in the case of Tm<sup>3+</sup>. In the present paper we show that the Judd-Ofelt approach should be restricted to non-hypersensitive transitions in the case of Pr<sup>3+</sup> and Dy<sup>3+</sup> doped oxide glasses.

### 2. Theory

Oscillator strengths were calculated from the absorption spectra via the relationship:

$$f_{\text{meas}} = 4.318 \times 10^{-9} \int_{\text{band}} \epsilon(\bar{\nu}) d\bar{\nu}, \quad (1)$$

\* Partially supported by U.S. Army Contract no. DAERO 76-G-066.

where  $\epsilon(\bar{\nu})$  is the decadic molar extinction coefficient at wavenumber  $\bar{\nu}(\text{cm}^{-1})$ .

According to the Judd-Ofelt model the oscillator strength is given by [5]:

$$f_{JJ'} = \frac{8\pi^2 mc}{3h(2J+1)\bar{\lambda}} \left( \frac{n^2+2}{9n} \right)^2 \sum_{\lambda=2,4,6} \Omega_{\lambda} \langle 4f^n[S, L] J || U^{(\lambda)} || 4f^n[S', L'] J' \rangle^2 \quad (2)$$

where  $n$  is the index of refraction,  $\bar{\lambda}$  is the mean wavelength of the transition,  $\Omega_{\lambda}$  intensity parameters,  $\langle || U^{(\lambda)} || \rangle$  doubly reduced matrix elements of tensor operator,  $J$  and  $J'$  refer to the degeneracies of the initial and final levels respectively.

The electric dipole spontaneous emission probability is given by:

$$A_{JJ'} = \frac{8\pi^2 e^2 n^2}{mc\bar{\lambda}^2} \times f_{JJ'} \quad (3)$$

The branching ratio is given by:

$$\beta_{ij} = A_{ij} / \sum_j A_{ij} \quad (4)$$

where  $i$  is the emitting level and  $j$  stands for all the underlying levels.

Laser analysis of rare earth materials makes use of the following equation [5,6]:

$$\int_{J \rightarrow J'} \sigma(\bar{\nu}) d\bar{\nu} = \frac{\bar{\lambda}^2}{8\pi c n^2} \times A_{JJ'} \quad (5)$$

where the left hand side of (5) represents the integrated cross section for stimulated emission.

Another useful relation is obtained by combining eqs. (3) and (5):

$$\int_{J \rightarrow J'} \sigma(\bar{\nu}) d\bar{\nu} = (\pi e^2 / mc^2) f_{JJ'} \quad (6)$$

The last equation shows the connection between the oscillator strength and the integrated cross section for stimulated emission. In practice it is found that laser lines have  $\sigma(\nu_0)$  of the order  $10^{-19} \text{ cm}^2$  or greater (integrated cross sections of order  $10^{-18} \text{ cm}$ ).  $\sigma(\nu_0)$  can be approximated by dividing the left hand side of eq. (6) by the halfwidth of the emission band

### 3. Experimental details and fitting procedure

The glasses studied were binary tellurite borate and phosphate glasses of the following compositions: 20 Na<sub>2</sub>O · 80 TeO<sub>2</sub>, 15 BaO · 85 TeO<sub>2</sub>, 35 ZnO · 65 TeO<sub>2</sub>, X<sub>2</sub>O · 2 B<sub>2</sub>O<sub>3</sub> where X = Li, Na, K, and Na<sub>2</sub>O · P<sub>2</sub>O<sub>5</sub>.

The details of tellurite and phosphate glass preparations and the techniques of optical measurements have been described elsewhere [7,8].

Binary borate glasses were prepared by melting the following salts:  $\text{Na}_2\text{B}_4\text{O}_7 \cdot 10 \text{H}_2\text{O}$ ,  $\text{K}_2\text{B}_4\text{O}_7 \cdot 5 \text{H}_2\text{O}$  and  $\text{Li}_2\text{B}_4\text{O}_7$  respectively.

In the present study no correction was made for the dispersion of the index of refraction. The indices of refraction used for tellurite glasses were: 2.15, 2.10 and 2.036 for sodium [9], barium [9] and zinc [10] respectively. For borate and phosphate glasses the value 1.51 [11] was used.

Intensity parameters were obtained by least squares analysis, the  $\Omega_\lambda$  were those giving the best fit between the measured [eq. (1)] and calculated [eq. (2)] oscillator strengths. The reduced matrix elements used were those calculated by Weber [12] for  $\text{Pr}^{3+}$  in  $\text{LaF}_3$ . Matrix elements for  $\text{Dy}^{3+}$  were kindly supplied by Dr. J. Caird [13]. A calculation of reduced matrix elements of  $\text{Pr}^{3+}$  in 20  $\text{Na}_2\text{O} \cdot 80 \text{TeO}_2$  glass [14] showed that they differ slightly from data of ref. [12] however, the difference is less than 1%, much smaller than the experimental error in the determination of oscillator strengths.

#### 4. Results

Intensity parameters of  $\text{Pr}^{3+}$  in tellurite glasses were calculated by three fits:

(a) Nine transitions were used in the fitting procedure, the transitions included were  $^3\text{H}_4 \rightarrow ^3\text{H}_6$ ,  $^3\text{F}_2$ ,  $^3\text{F}_3$ ,  $^3\text{F}_4$ ,  $^1\text{G}_4$ ,  $^1\text{D}_2$ ,  $^3\text{P}_0$ ,  $^3\text{P}_1 \rightarrow ^1\text{I}_6$  and  $^3\text{H}_4 \rightarrow ^3\text{P}_2$ .

(b) Eight transitions, by excluding the hypersensitive transition  $^3\text{H}_4 \rightarrow ^3\text{P}_2$  from the data of fit (a).

(c) Seven transitions, where the transitions  $^3\text{H}_4 \rightarrow ^3\text{H}_6$ ,  $^3\text{P}_2$  were excluded from the data of fit (a).

The only reason for excluding  $^3\text{H}_4 \rightarrow ^3\text{H}_6$  transition in the fitting procedure was the uncertainty in the measured oscillator strength due to the overlap with the strong band  $^3\text{H}_4 \rightarrow ^3\text{F}_2$ .

Measured and calculated oscillator strengths, the resulting intensity parameters and RMS deviations obtained by the three fits are collected in table 1.

A similar treatment has been carried out to calculate the intensity parameters of  $\text{Dy}^{3+}$  in tellurite glasses. In this case intensity parameters were obtained by two fits:

(a) Seven transitions were used; the transitions were:  $^6\text{H}_{15/2} \rightarrow ^6\text{H}_{11/2}$ ,  $^6(\text{F}_{11/2} + \text{H}_{9/2})$ ,  $^6(\text{F}_{9/2} + \text{H}_{7/2})$ ,  $^6(\text{F}_{7/2} + \text{H}_{5/2})$ ,  $^6\text{F}_{5/2}$ ,  $^6\text{F}_{3/2}$  and  $^6\text{H}_{15/2} \rightarrow ^3\text{F}_{9/2}$ .

(b) Six transitions were included, where the hypersensitive transitions  $^6\text{H}_{15/2} \rightarrow ^6(\text{F}_{11/2} + \text{H}_{9/2})$  was excluded from the data of fit (a). The hypersensitive transitions as first predicted by Jørgensen are dependent on the surrounding ligands and cannot be fitted straightforwardly to the Judd-Ofelt treatment [15].

Measured and calculated oscillator strengths, intensity parameters and RMS deviations for  $\text{Dy}^{3+}$  are presented in table 2.

Comparisons between measured and calculated lifetimes and branching ratios as

Table 1  
Measured and calculated oscillator strengths and intensity parameters of  $\text{Pr}^{3+}$  in tellurite glasses

Transition	Glass							
	35 ZnO · 65 TeO <sub>2</sub>				20 Na <sub>2</sub> O · 80 TeO <sub>2</sub>			
	$f \times 10^6$				$f \times 10^6$			
	$f_{\text{meas}}$	$f_{\text{cal}}^a$	$f_{\text{cal}}^b$	$f_{\text{cal}}^c$	$f_{\text{meas}}$	$f_{\text{cal}}^a$	$f_{\text{cal}}^b$	$f_{\text{cal}}^c$
$^3\text{H}_4 \rightarrow ^3\text{H}_6$	1.56	1.65	1.12	—	2.06	1.56	1.08	—
$^3\text{F}_2$	6.15	5.56	6.24	6.25	6.36	5.79	6.45	6.46
$^3\text{F}_3$	11.36	14.00	10.57	10.53	11.06	13.45	10.20	10.12
$^3\text{F}_4$	3.92	8.17	5.41	5.38	3.41	7.74	5.13	5.06
$^1\text{G}_4$	0.35	0.33	0.25	0.25	0.51	0.32	0.24	0.24
$^1\text{D}_2$	3.13	2.30	1.65	1.64	3.28	2.20	1.58	1.56
$^3\text{P}_0$	5.66	6.12	6.36	6.36	5.98	6.10	6.32	6.33
$^3\text{P}_1 + ^1\text{F}_6$	9.16	8.93	8.95	8.95	8.75	8.86	8.88	8.89
$^3\text{P}_2$	16.43	8.12	—	—	15.60	7.72	—	—
$^3\text{P}_1$								
RMS ( $10^{-6}$ )		4.00	1.07	1.19			1.24	1.30
$\Omega_\lambda (10^{-20} \text{ cm}^2)$		$f_{\text{cal}}^a$		$f_{\text{cal}}^b$		$f_{\text{cal}}^c$		
$\Omega_2$ 35 ZnO · 65 TeO <sub>2</sub>		$1.46 \pm 6.42$		$2.57 \pm 1.81$		$2.59 \pm 1.97$		
$\Omega_4$		$6.96 \pm 2.73$		$7.26 \pm 0.76$		$7.26 \pm 0.84$		
$\Omega_6$		$8.29 \pm 2.13$		$5.49 \pm 0.81$		$5.45 \pm 0.90$		
$\Omega_2$ 20 Na <sub>2</sub> O · 80 TeO <sub>2</sub>		$0.86 \pm 6.07$		$2.73 \pm 1.90$		$2.83 \pm 1.86$		
$\Omega_4$		$6.36 \pm 2.58$		$6.56 \pm 0.81$		$6.50 \pm 0.77$		
$\Omega_6$		$8.01 \pm 2.42$		$4.68 \pm 0.95$		$4.60 \pm 0.83$		

<sup>a</sup>) Refers to the oscillator strengths calculated by fits a, b and c, respectively; the corresponding intensity parameters are given in the lower part of the table.

obtained by the different sets of intensity parameters are presented in tables 3 and 4 for  $\text{Pr}^{3+}$  and  $\text{Dy}^{3+}$  respectively.

Comparison between measured and calculated lifetimes for  $\text{Pr}^{3+}$  has not been made, since the probe level ( $^3\text{P}_0$ ) has significant nonradiative losses which preclude such comparison.

## 5. Discussion

From table 1 it is seen that by excluding the hypersensitive transition  $^3\text{H}_4 \rightarrow ^3\text{P}_2$  from the fitted transitions, the intensity of the remaining bands is well accounted for by the Judd-Ofelt model.

The situation is more complicated for  $\text{Dy}^{3+}$  (table 2); it is difficult to choose the

Table 2  
Measured and calculated oscillator strengths and intensity parameters of  $Dy^{3+}$  in tellurite and phosphate glasses

Transition	Glass		$Na_2O \cdot P_2O_5$ $f \times 10^6$		$f_{cal}^a$		$f_{cal}^b$	
	$f_{meas}$	$f_{cal}^a$	$f_{meas}$	$f_{cal}^a$	$f_{meas}$	$f_{cal}^a$	$f_{meas}$	$f_{cal}^b$
$6H_{15/2} \rightarrow 6H_{11/2} + 6H_{9/2}$	1.52	1.72	1.06	1.23	1.06	1.06	1.06	1.06
$6F_{11/2} + 6H_{9/2}$	10.63	10.62	7.11	7.10	7.11	7.10	7.11	7.10
$6F_{9/2} + 6H_{7/2}$	3.27	3.28	2.59	2.59	2.56	2.56	2.56	2.56
$6F_{7/2} + 6H_{5/2}$	2.81	2.75	2.09	2.12	2.19	2.19	2.19	2.19
$6F_{5/2}$	1.53	1.43	1.27	1.08	1.13	1.13	1.13	1.13
$6F_{3/2}$	0.30	0.27	0.19	0.21	0.22	0.22	0.22	0.22
$4F_{9/2}$	0.20	0.31	0.21	0.24	0.24	0.24	0.24	0.24
RMS ( $10^{-6}$ )		0.131		0.131		0.10		0.10
$\Omega_\lambda (10^{-20} \text{ cm}^2)$								
$\Omega_2$		8.59 ± 0.24		4.28 ± 1.36		1.46 ± 1.99		1.46 ± 1.99
$\Omega_4$		1.48 ± 0.24		1.32 ± 0.14		1.16 ± 0.21		1.16 ± 0.21
$\Omega_6$		2.43 ± 0.11		2.53 ± 0.07		1.97 ± 0.10		1.97 ± 0.10

a) See comments in table 1.

Table 3  
Comparison of measured and calculated decay times and branching ratios of 0.5 wt.% Dy<sup>3+</sup> in 35 ZnO · 65 TeO<sub>2</sub> glass

Transition	$\beta_{ij}$ <sup>a)</sup>		$\tau_0$ ( $\mu$ s)		Experi- mental branching ratios	$\tau_{\text{meas}}$ ( $\mu$ s)
	a <sup>b)</sup>	b	a	b		
<sup>4</sup> I <sub>9/2</sub> → <sup>6</sup> H <sub>15/2</sub>	0.249 ± 0.026	0.387 ± 0.089			0.488	
→ <sup>6</sup> H <sub>13/2</sub>	1	1	261 ± 12	371.4 ± 60	1	365 ± 5%
→ <sup>6</sup> H <sub>11/2</sub>	0.241 ± 0.017	0.190 ± 0.093			0.146	

<sup>a)</sup> Branching ratios normalized to strongest transition.

<sup>b)</sup> Columns a and b refer to branching ratios calculated by intensity parameters of table 2.

best set of intensity parameters, as the fit between measured and calculated oscillator strengths is very good in both fits (a and b, table 2).

In order to select the best set of intensity parameters we have compared the calculated lifetimes and branching ratios with the experimental values. The results are presented in tables 3 and 4.

The practical conclusion from the inspection of these tables is that the intensity parameters obtained by the exclusion of hypersensitive transitions predicted correctly the experimental lifetime and branching ratios.

From this we conclude that in the case of Pr<sup>3+</sup> and Dy<sup>3+</sup> in tellurite glasses hypersensitive transitions are not accounted for by the Judd-Ofelt model.

This conclusion is of practical value in predicting the laser characteristics of Pr<sup>3+</sup> and Dy<sup>3+</sup> in oxide glasses.

Table 4  
Comparison of measured and calculated branching ratios of 0.25 wt.% Pr<sup>3+</sup> in 20 Na<sub>2</sub>O · 80 TeO<sub>2</sub> glass

Transition	a <sup>a)</sup> $\beta_{ij}$	b	c	Experimental branching ratios
<sup>3</sup> P <sub>0</sub> → <sup>3</sup> H <sub>4</sub>	1	1	1	1
→ <sup>3</sup> H <sub>6</sub>	0.253	0.143	0.142	b)
→ <sup>3</sup> F <sub>2</sub>	0.098	0.302	0.305	0.33

<sup>a)</sup> a, b and c refer to the branching ratios calculated by intensity parameters of table 1.

<sup>b)</sup> This value has not been measured because strong overlap with other bands excludes meaningful value.

## 6. Laser analysis of $\text{Pr}^{3+}$ and $\text{Dy}^{3+}$ and doped oxide glasses

The intensity parameters used for laser analysis were those obtained by the exclusion of hypersensitive transitions (table 5). Predicted transition probabilities, branching ratios and integrated cross sections (of electric dipole emission) for  $\text{Pr}^{3+}$  in tellurite and borate glasses, are presented in tables 6 and 7. Corresponding predictions for  $\text{Dy}^{3+}$  in tellurite and phosphate glasses are collected in table 8.

Figure 1 presents the emission spectrum of  $\text{Pr}^{3+}$  in sodium tellurite glass; similar emission curves are obtained in the other tellurite glasses presented in this work. The integrated cross sections of the stimulated emissions from the  $^3\text{P}_1 \rightarrow ^3\text{F}_2$  ( $0.647 \mu$ ) are  $318 \text{ cm}^{-1}$  and  $155 \text{ cm}^{-1}$  respectively. Hence the peak cross sections for these transitions are estimated as  $1.2 \times 10^{-19}$  and  $1.6 \times 10^{-19} \text{ cm}^2$ . The peak cross section for  $\text{Nd}^{3+}$  laser in YAG [16] is  $9 \times 10^{-19} \text{ cm}^2$  and in ED-2 glass [17] is  $2.71 \times 10^{-20} \text{ cm}^2$ , therefore the transitions at  $0.486 \mu$  and  $0.647 \mu$  look promising as laser transitions.

These transitions are characterized by large integrated cross sections for stimulated emission and reasonable branching ratios. The radiative lifetime of the  $^3\text{P}_0$  state,  $8 \mu\text{s}$  is rather short however laser operation was found [18,19] for  $\text{Pr}^{3+}$  excited states with lifetimes shorter than  $1 \mu\text{s}$ .

It should be noted that the terminal level for  $^3\text{P}_0 \rightarrow ^3\text{H}_4$  transition is the ground-state, therefore only at low temperatures the upper Stark components are unoccupied and population inversion may be expected.

The terminal levels  $^3\text{H}_6$ ,  $^3\text{F}_2$  and  $^3\text{F}_4$  have short lifetimes due to fast multiphonon relaxation rates which are  $1.76 \times 10^6 \text{ s}^{-1}$ ,  $3.70 \times 10^9 \text{ s}^{-1}$  and  $6.26 \times 10^9 \text{ s}^{-1}$  respectively.

The multiphonon relaxation rates were calculated using the formulae:  $W_{\text{NR}}(0) = B e^{-\alpha \Delta E}$ , where  $W_{\text{NR}}(0)$  is the multiphonon relaxation rate at low temperature and

Table 5  
Intensity parameters of  $\text{Pr}^{3+}$  and  $\text{Dy}^{3+}$  in oxide glasses

Ion	$\Omega_2(10^{-20} \text{ cm}^2)$	$\Omega_4(10^{-20} \text{ cm}^2)$	$\Omega_6(10^{-20} \text{ cm}^2)$	Glass
$\text{Pr}^{3+}$	$2.59 \pm 1.97$	$7.26 \pm 0.84$	$5.45 \pm 0.90$	35 ZnO · 65 TeO <sub>2</sub>
$\text{Pr}^{3+}$	$4.95 \pm 2.40$	$6.46 \pm 1.09$	$5.44 \pm 1.09$	15 BaO · 85 TeO <sub>2</sub>
$\text{Pr}^{3+}$	$2.83 \pm 1.86$	$6.50 \pm 0.79$	$4.60 \pm 0.83$	20 Na <sub>2</sub> O · 80 TeO <sub>2</sub>
$\text{Pr}^{3+}$	$2.14 \pm 0.94$	$2.91 \pm 0.41$	$1.67 \pm 0.43$	K <sub>2</sub> O · 2 B <sub>2</sub> O <sub>3</sub>
$\text{Pr}^{3+}$	$0.77 \pm 1.45$	$4.13 \pm 0.62$	$3.07 \pm 0.65$	Na <sub>2</sub> O · 2 B <sub>2</sub> O <sub>3</sub>
$\text{Pr}^{3+}$	$0.77 \pm 1.35$	$3.84 \pm 0.58$	$3.58 \pm 0.61$	Li <sub>2</sub> O · 2 B <sub>2</sub> O <sub>3</sub>
$\text{Dy}^{3+}$	$4.28 \pm 1.36$	$1.32 \pm 0.14$	$2.53 \pm 0.07$	35 ZnO · 65 TeO <sub>2</sub>
$\text{Dy}^{3+}$	$3.20 \pm 0.86$	$1.35 \pm 0.09$	$2.47 \pm 0.04$	15 BaO · 85 TeO <sub>2</sub>
$\text{Dy}^{3+}$	$3.70 \pm 1.35$	$1.15 \pm 0.14$	$2.22 \pm 0.07$	20 Na <sub>2</sub> O · 80 TeO <sub>2</sub>
$\text{Dy}^{3+}$	$1.46 \pm 1.99$	$1.16 \pm 0.21$	$1.97 \pm 0.10$	Na <sub>2</sub> O · P <sub>2</sub> O <sub>5</sub>



Table 6  
Radiative transition probabilities, branching ratios and integrated cross-sections for stimulated emission of the  $^3P_1$ ,  $^3P_0$  and  $^1D_2$  excited states of  $Pt^{3+}$  in tellurite glasses

Transition	Energy (cm <sup>-1</sup> )	35 ZnO · 65 TeO <sub>2</sub>			15 BaO · 85 TeO <sub>2</sub>			20 Na <sub>2</sub> O · 80 TeO <sub>2</sub>		
		$A_{ij}$ (s <sup>-1</sup> )	$\beta_{ij}$	$\Sigma(10^{-18} \text{ cm}^{-1})$	$A_{ij}$ (s <sup>-1</sup> )	$\beta_{ij}$	$\Sigma(10^{-18} \text{ cm}^{-1})$	$A_{ij}$ (s <sup>-1</sup> )	$\beta_{ij}$	$\Sigma(10^{-18} \text{ cm}^{-1})$
$^3P_0 \rightarrow ^3H_4$	20576	66993	0.606	50.6	66886	0.509	47.5	74315	0.593	50.4
$\rightarrow ^3H_5$	18148	0	0	0	0	0	0	0	0	0
$\rightarrow ^3H_6$	16221	10122	0.012	12.8	11332	0.086	13.2	10474	0.084	11.7
$\rightarrow ^3F_2$	15456	17374	0.157	23.6	37220	0.283	46.9	22723	0.181	27.3
$\rightarrow ^3F_3$	14074	0	0	0	0	0	0	0	0	0
$\rightarrow ^3F_4$	13583	13646	0.126	24.0	13624	0.104	22.2	15138	0.121	23.4
$\rightarrow ^1G_4$	10773	2385	0.022	6.7	2381	0.018	6.2	2646	0.021	6.4
$\rightarrow ^1D_2$	3769	11	0.0001	0.3	25	0.0002	0.5	15	0.0001	0.3
$^3P_1 \rightarrow ^3H_4$	21119	24258	0.235	17.7	24219	0.198	16.3	26909	0.231	17.3
$\rightarrow ^3H_5$	18692	34472	0.334	32.0	35211	0.288	30.3	37751	0.324	31.0
$\rightarrow ^3H_6$	16594	6399	0.062	7.5	7164	0.059	7.8	6621	0.057	6.9
$\rightarrow ^3F_2$	15991	5887	0.057	7.5	12612	0.103	14.8	7699	0.066	8.6
$\rightarrow ^3F_3$	14617	18705	0.181	28.4	29571	0.242	41.6	22640	0.194	30.4
$\rightarrow ^3F_4$	14126	12030	0.117	19.6	12011	0.098	18.1	13345	0.115	19.2
$\rightarrow ^1G_4$	11316	1312	0.013	3.3	1310	0.011	3.1	1455	0.012	3.3
$\rightarrow ^1D_2$	4313	32	0.0003	0.6	69	0.0005	1.1	42	0.0004	0.6
$^1D_2 \rightarrow ^3H_4$	16807	2312	0.310	2.7	2534	0.249	2.7	2453	0.287	2.5
$\rightarrow ^3H_5$	14379	57	0.008	0.1	57	0.006	0.1	62	0.007	0.1
$\rightarrow ^3H_6$	12282	1152	0.155	2.5	1159	0.114	2.3	1272	0.149	2.4
$\rightarrow ^3F_2$	11679	1231	0.165	2.9	1305	0.128	2.9	1379	0.161	2.9
$\rightarrow ^3F_3$	10305	270	0.036	0.8	390	0.038	1.1	32	0.038	0.9
$\rightarrow ^3F_4$	9823	1654	0.222	5.6	3444	0.339	10.7	2137	0.250	6.4
$\rightarrow ^1G_4$	7003	773	0.101	5.1	1282	0.126	7.9	927	0.108	5.4

Table 7  
Radiative transition probabilities, branching ratios and integrated cross-sections for stimulated emission of the  $^1D_2$  excited state of  $Pt^{3+}$  in binary borate glasses

Transition	$Li_2O \cdot 2 B_2O_3$				$Na_2O \cdot 2 B_2O_3$				$K_2O \cdot 2 B_2O_3$			
	Energy ( $cm^{-1}$ )	$A_{ij}$ ( $s^{-1}$ )	$\beta_{ij}$	$\Sigma(10^{-18} cm^{-1})$	Energy ( $cm^{-1}$ )	$A_{ij}$ ( $s^{-1}$ )	$\beta_{ij}$	$\Sigma(10^{-18} cm^{-1})$	Energy ( $cm^{-1}$ )	$A_{ij}$ ( $s^{-1}$ )	$\beta_{ij}$	$\Sigma$ ( $10^{-18} cm^{-1}$ )
$^1D_2 \rightarrow ^3H_4$	17094	812	0.331	1.62	17094	727	0.349	1.45	17241	451	0.212	0.90
$\rightarrow ^3H_5$	14818	19	0.009	0.05	14812	19	0.009	0.05	14966	14	0.006	0.04
$\rightarrow ^3H_6$	12778	397	0.181	1.41	12778	394	0.189	1.40	12925	280	0.131	1.00
$\rightarrow ^3F_2$	11858	381	0.174	1.58	11803	378	0.181	1.58	11865	289	0.136	1.21
$\rightarrow ^3F_3$	10471	72	0.033	0.38	10427	70	0.034	0.38	10485	85	0.040	0.46
$\rightarrow ^3F_4$	10027	327	0.149	1.89	9951	319	0.153	1.87	10047	748	0.351	4.37
$\rightarrow ^1G_4$	6993	188	0.086	2.24	6993	179	0.086	2.13	7140	265	0.124	3.06

Table 8  
Radiative transition probabilities, branching ratios and integrated cross-sections for stimulated emission of the  $^4F_{9/2}$  excited state of  $Dy^{3+}$  in tellurite and phosphate glasses

Transition	Energy ( $cm^{-1}$ )	35 ZnO · 65 TeO <sub>2</sub>			15 BaO · 85 TeO <sub>2</sub>			Na <sub>2</sub> O · P <sub>2</sub> O <sub>5</sub>		
		$A_{ij}$	$\beta_{ij}$	$\Sigma(10^{-18} cm^{-1})$	$A_{ij}$	$\beta_{ij}$	$\Sigma(10^{-18} cm^{-1})$	$A_{ij}$	$\beta_{ij}$	$\Sigma(10^{-18} cm^{-1})$
$^4F_{9/2} \rightarrow ^6H_{15/2}$	20747	579	0.125	0.43	638	0.243	0.45	243	0.284	0.33
$\rightarrow ^6H_{13/2}$	17361	1496	0.556	1.59	1410	0.537	1.41	435	0.508	0.85
$\rightarrow ^6H_{11/2}$	15068	284	0.105	0.40	236	0.090	0.31	57	0.066	0.15
$\rightarrow ^6H_{11/2} + ^6H_{9/2}$	12934	186	0.069	0.36	189	0.072	0.47	65	0.076	0.23
$\rightarrow ^6F_{9/2} + ^6H_{7/2}$	11623	111	0.041	0.26	119	0.045	0.26	44	0.051	0.19
$\rightarrow ^6F_{7/2} + ^6H_{5/2}$	9667	22	0.008	0.07	24	0.007	0.08	9	0.010	0.06
$\rightarrow ^6F_{5/2}$	8286	12	0.004	0.05	10	0.004	0.04	2	0.003	0.02
$\rightarrow ^6F_{3/2}$	7467	1	0.0005	0.008	2	0.0006	0.009	1	0.0007	0.006
$\rightarrow ^6F_{1/2}$	7024	0	0.0001	0.002	0	0.0001	0.002	0	0.00002	0.001

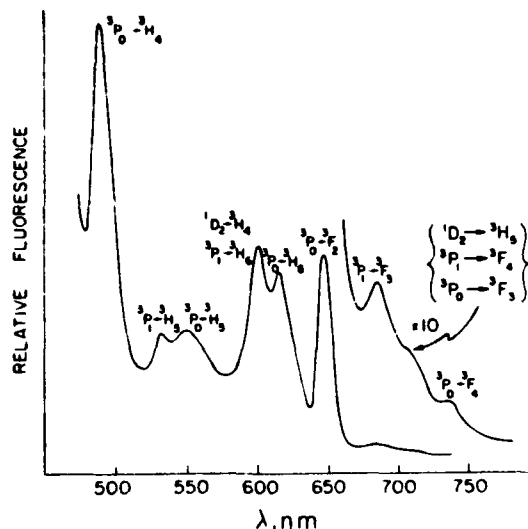


Fig. 1. Corrected emission spectrum of 0.25 wt%  $\text{Pr}^{3+}$  in  $20 \text{ Na}_2\text{O} \cdot 80 \text{ TeO}_2$  at room temperature.

$B$  and  $\alpha$  are the host-dependent constants which were determined previously [20], for tellurite glasses [20]  $B = 6.3 \times 10^{10}$  and  $\alpha = 0.0047$ .

By the same line of reasoning other potential laser transitions are:  $^3\text{P}_1 \rightarrow ^3\text{H}_4$  ( $0.478 \mu$ ),  $^3\text{H}_5$  ( $0.531 \mu$ ),  $^3\text{F}_3$  ( $0.684 \mu$ ) and  $^3\text{P}_1 \rightarrow ^3\text{F}_4$  ( $0.708 \mu$ ) for  $^3\text{P}_1$  excited state and  $^1\text{D}_2 \rightarrow ^3\text{H}_4$  ( $0.602 \mu$ ),  $^3\text{H}_6$  ( $0.834 \mu$ ),  $^3\text{F}_2$  ( $0.856 \mu$ ) and  $^1\text{D}_2 \rightarrow ^3\text{F}_4$  ( $1.019 \mu$ ).

Because of the high multiphonon relaxation rate (for  $^3\text{P}_0 \rightarrow ^1\text{D}_2$  transition) in borate and phosphate glasses [21], only the  $^1\text{D}_2$  state is expected to show laser operation.

The  $^1\text{D}_2$  state in borate and phosphate glasses is populated [21] by fast non-radiative decay from the higher lying  $^3\text{P}_0$ ,  $^3\text{P}_1$ ,  $^1\text{I}_6$ , and  $^3\text{P}_2$  states. An additional advantage of borate and phosphate glasses may be the possibility of increasing population by energy transfer to  $^3\text{P}_{0,1,2}$  and  $^1\text{I}_6$  states. Such energy transfer between donor  $\text{UO}_2^{2+}$  ion to  $\text{Pr}^{3+}$  was recently demonstrated to take place [22].

#### Acknowledgement

The author (RR) is deeply grateful to Professor C.K. Jørgensen and to Professor B.R. Judd for fruitful discussions concerning the hypersensitive transitions and to Mrs. Esther Greenberg for her kind help in preparation of the manuscript.

## References

- [1] R. Reisfeld and C.K. Jørgensen, *Lasers and Excited States of Rare Earths* (Springer-Verlag, Berlin, Heidelberg, New York, 1977).
- [2] B.R. Judd, *Phys. Rev.* 127 (1962) 750.
- [3] G.S. Ofelt, *J. Chem. Phys.* 37 (1962) 511.
- [4] J.A. Caird, L.G. DeShazer and J. Nella, *IEEE J. Quant. Elect.* QE-11 (1975) 874.
- [5] W.F. Krupke, *Phys. Rev.* 145 (1966) 325.
- [6] W.F. Krupke, *IEEE J. Quant. Elect.* QE-10 (1974) 450.
- [7] R. Reisfeld and J. Hormadaly, *J. Chem. Phys.* 64 (1976) 3207.
- [8] R. Reisfeld, J. Hormadaly and A. Muranevich, *Chem. Phys. Lett.* 38 (1976) 188.
- [9] A.K. Yakhind, *J. Am. Ceram. Soc.* 40 (1966) 670.
- [10] M.J. Redman and J.H. Chen, *J. Am. Ceram. Soc.* 50 (1967) 523.
- [11] R. Reisfeld, *Structure and Bonding*, 22 (1975) 123.
- [12] M.J. Weber, *J. Chem. Phys.* 48 (1969) 4774.
- [13] J.A. Caird, private communication.
- [14] J. Hormadaly, Ph.D. Thesis, submitted 1977.
- [15] R.D. Peacock, *Structure and Bonding* 22 (1975) 83.
- [16] T. Kushida, H.M. Marcos and J.E. Geusic, *Phys. Rev.* 167 (1968) 1289.
- [17] W.F. Krupke, *IEEE J. Quant. Electron.* QE-10 (1974) 450.
- [18] K.R. German, A. Kiel and H. Guggenheim, *Appl. Phys. Lett.* 22 (1973) 87.
- [19] K.R. German, A. Kiel and H. Guggenheim, *Phys. Rev. B* 11 (1974) 2436.
- [20] R. Reisfeld, L. Boehm and N. Spector, *Proc. 13th Rare Earth Conf.*, (W. Virginia, Oct., 1977).
- [21] R. Reisfeld and J. Hormadaly, to be published.
- [22] R. Reisfeld and N. Lieblich-Sofer, in preparation.

RADIATIVE TRANSITION PROBABILITIES AND STIMULATED CROSS-SECTIONS OF  
 $\text{Nd}^{3+}$  in  $3\text{Ca}_2\text{S}_3 \cdot \text{La}_2\text{S}_3$  (GLS) AND  $3\text{Al}_2\text{S}_3 \cdot \text{La}_2\text{S}_3$  (ALS) GLASSES\*

R. Reisfeld\*\*, A. Bornstein\*\*, J. Flahaut\*\*\* and A.M.  
Loireau-Lazac'h\*\*\*.

\*\*Department of Inorganic and Analytical Chemistry,  
The Hebrew University of Jerusalem, Israel.

\*\*\*Laboratoire de Chimie Minérale Structurale associé  
au CNRS, Faculté des Sciences Pharmaceutiques et  
Biologiques, 4 avenue de l'Observatoire, 75006 Paris  
Cedex 06, France.

ABSTRACT

Radiative transition probabilities, oscillator strengths, radiative lifetimes and branching ratios of  $\text{Nd}^{3+}$  in GLS and ALS glasses were calculated for levels ranging between  $160\text{cm}^{-1}$  -  $18\,000\text{cm}^{-1}$ . The matrix elements for the transitions were calculated in the intermediate coupling scheme using the measured energies in the glasses. The intensity parameters were obtained from these matrix elements and experimentally obtained oscillator strengths. The cross sections of the  ${}^4\text{F}_{3/2} \rightarrow {}^4\text{I}_{9/2}$ ,  ${}^4\text{I}_{11/2}$  and  ${}^4\text{F}_{3/2} \rightarrow {}^4\text{I}_{13/2}$  were calculated and compared to the equivalent quantities in oxide glass. The similarity and difference in the radiative characteristics of  $\text{Nd}^{3+}$  between oxide and chalcogenide glasses will be discussed.

The importance of chalcogenide glasses doped by  $\text{Nd}^{3+}$  (1),  $\text{Ho}^{3+}$  (2) and  $\text{Er}^{3+}$  (3) has been emphasized. The qualitative behaviour of these glasses has been described recently (4,5).

In the present work we have calculated the relevant optical properties of the ALS and GLS glasses and compared them with similar properties in oxide (6) and fluorophosphate glasses (7).

The spectroscopic properties were calculated by the use of the Judd-Ofelt theory (8,9) as described in ref. 10.

---

\*Partially supported by U.S. Army Contract No. DAERO-76-G-066

The formulae used for the calculations are:

Line strength of electronic transitions

$$S_{ed}(aJ; bJ') = e^2 \Sigma \Omega_{\lambda} | \langle f^N [\gamma SL] J || U^{(\lambda)} || f^N [\gamma' S' L'] J' \rangle |^2 \quad (1)$$

$\lambda = 2, 4, 6$

Line strength of magnetic transitions

$$S_{md}(aJ; bJ') = (e^2 h^2 / 4 m^2 c^2) | \langle f^N [\gamma SL] J || L + 2S || f^N [\gamma' S' L'] J' \rangle |^2 \quad (2)$$

For the calculation of the spontaneous transition probability

$$A(aJ; bJ') = [64 \pi^4 \nu^3 e^2 / 3 h c^3 (2J+1)] \times [1/9 n (n^2+2)^2 S_{ed} + n^3 S_{md}] \quad (3)$$

$n = \text{refractive index, for ALS} = 2.15, \text{ for GLS} = 2.5$

The branching ratio

$$B_{ij} = \frac{A_{ij}}{\Sigma A_{ij}} \quad (4)$$

Experimentally the oscillator strength is obtained from the absorption spectrum by  $f = 4.318 \times 10^{-9} \int \epsilon(\nu) d\nu$

Intensity parameters  $\Omega_{\lambda}$  are obtained from

$$f(aJ; bJ') = \frac{8 \pi^2 m c \nu}{3 h (2J+1)} \frac{(n^2+2)^2}{9n} \Sigma \Omega_{\lambda} | \langle f^N [S, L] J || U^{(\lambda)} || f^N [S' L'] J' \rangle |^2 \quad (5)$$

In the least square fitting of the intensity parameters a statistical weight was given for various bands. This is especially important for the transition  ${}^4I_{9/2} \rightarrow {}^4F_{3/2}$  as the lasing occurs from this level.

The  $\Omega_{\lambda}$  parameters and the predicted spectral intensity together with the matrix elements (11) are presented in Table I, for the transitions from  ${}^4F_{3/2}$ ,  ${}^4I_{15/2}$ ,  ${}^4I_{13/2}$  and  ${}^4I_{11/2}$ . The complete set of levels will be published later. The measured and calculated oscillator strengths together with the absorption and intensity parameters are presented in Table II.

The integrated cross-sections were calculated from

$$d = \frac{\lambda^4 A}{8 \pi c n^2} \quad (6)$$

The radiative properties of  $Nd^{3+}$  in chalcogenide glass compared to Ed-2 glass and other oxide glasses are presented in Table III.

While the branching ratio is slightly in favor of  ${}^4F_{3/2} \rightarrow {}^4F_{11/2}$  (the lasing transition) the significant fluorescence of  ${}^4F_{3/2} \rightarrow {}^4F_{13/2}$  should also be mentioned. This transition is responsible for the

emission at 1.37 microns and is of importance as a light source for the IR region.

A striking property of chalcogenide glass is the cross-section of stimulated emission which is higher in chalcogenide glass as compared to ED-2 glass. It should be noted that this property of the glass enables its use as a laser material.

Thermal and mechanical stability of these glasses should also be mentioned. The glass transition temperature is  $t_g = 530^\circ\text{C}$ .

#### REFERENCES

1. R. Reisfeld & A. Bornstein. Chem.Phys.Lett. 47 194 (1977).
2. R. Reisfeld, A. Bornstein, J. Flahaut, M. Guittard & A.M. Loireau-Lozac'h. Chem.Phys.Lett. 47 408 (1977).
3. R. Reisfeld & A. Bornstein. J.Noncryst.Solids 27 143 (1978).
4. A. Bornstein, J. Flahaut, M. Guittard, S. Jaulmes, A.M. Loireau-Lozac'h, G. Lucareau & R. Reisfeld. The Rare Earths in Modern Science & Technology. Ed. G.J. McCarthy & J.J. Rhyne, Plenum 599 (1978.)
5. R. Reisfeld, A. Bornstein, J. Bodenheimer & J. Flahaut. J. Luminescence 18/19 253 (1979).
6. W.F. Krupke. IEEE J. Quant.Electron. QE-10 450 (1974).
7. R.R. Jacobs & J.M. Weber. IEEE J.Quant.Electron. QE-12 102 (1976).
8. B.R. Judd. Phys.Rev. 127 750 (1962).
9. G.S. Ofelt. J.Chem.Phys. 37 511 (1962).
10. R. Reisfeld & C.K. Jørgensen. Lasers and Excited States of Rare Earths. Springer-Verlag, Heidelberg 1977.
11. N. Spector, C. Gittel and R. Reisfeld. Optica Pura y Aplic. 10 197 (1979).

THIS PAGE IS BEST QUALITY PRACTICABLE  
FROM COPY FURNISHED TO DDC



Table I. Predicted intensities and  $U_{\lambda}^{(2)}$  matrix elements of  $\text{Nd}^{3+}$  in GLS and ALS.

Transi- tion	U <sub>2</sub> <sup>2</sup>	U <sub>4</sub> <sup>2</sup>	U <sub>6</sub> <sup>2</sup>	GLS			ALS							
				Energy of level cm <sup>-1</sup>	S <sub>ed</sub> ×10 <sup>20</sup> cm <sup>2</sup>	S <sub>md</sub> ×10 <sup>22</sup> cm <sup>2</sup>	A sec <sup>-1</sup>	E	Energy of level cm <sup>-1</sup>	S <sub>ed</sub> ×10 <sup>20</sup> cm <sup>2</sup>	S <sub>md</sub> ×10 <sup>22</sup> cm <sup>2</sup>	A sec <sup>-1</sup>		
<u><sup>4</sup>F<sub>3/2</sub> →</u>														
<sup>4</sup> I <sub>15/2</sub>	-	-	0.0190	6139	0.08	-	39	0.0028	6075	0.13	-	55	0.0053	
<sup>4</sup> I <sub>13/2</sub>	-	-	0.2357	4016	1.03	-	1350	0.0993	4012	1.55	-	1110	0.1112	
<sup>4</sup> I <sub>11/2</sub>	-	0.1421	0.3772	2048	2.28	-	6120	0.4494	2048	3.17	-	4670	0.4759	
<sup>4</sup> I <sub>9/2</sub>	-	0.2298	0.0670	165	1.30	-	6110	0.4485	165	1.55	-	4000	0.4076	
<u><sup>4</sup>I<sub>15/2</sub> →</u>														
<sup>4</sup> I <sub>13/2</sub>	0.0196	0.1136	1.4545	4016	7.04	71.00	62	0.2994	4012	10.30	71.00	46	0.2339	
<sup>4</sup> I <sub>11/2</sub>	-	0.0110	0.4172	2048	1.88	-	110	0.5283	2048	2.80	-	87	0.5372	
<sup>4</sup> I <sub>9/2</sub>	-	0.0001	0.0448	165	0.20	-	36	0.1725	165	0.30	-	29	0.1790	
<u><sup>4</sup>I<sub>13/2</sub> →</u>														
<sup>4</sup> I <sub>11/2</sub>	0.0257	0.1352	1.2390	2048	6.20	93.30	52	0.3117	2048	9.06	93.30	41	0.3013	
<sup>4</sup> I <sub>9/2</sub>	0.0001	0.0136	0.4545	165	2.06	-	115	0.6883	165	3.06	-	94	0.6982	
<u><sup>4</sup>I<sub>11/2</sub> →</u>														
<sup>4</sup> I <sub>9/2</sub>	0.0195	0.1072	1.1651	165	5.72	69.60	48	1.0000	165	8.38	69.60	38	1.0000	

Table II  
Oscillator strengths (f), radiative transition possibilities (A) and integrated cross-sections ( $\Sigma od\lambda$ ) of the absorption bands of Nd<sup>3+</sup> in GLS and ALS

Transition	Energy of level cm <sup>-1</sup>	$\lambda$ nm	GLS			Energy of level cm <sup>-1</sup>	$\lambda$ nm	ALS		
			f <sub>meas.</sub> x10 <sup>6</sup>	f <sub>cal.</sub> x10 <sup>6</sup>	A sec <sup>-1</sup>			f <sub>meas.</sub> x10 <sup>6</sup>	f <sub>cal.</sub> x10 <sup>6</sup>	A sec <sup>-1</sup>
<u><math>4I_{9/2} \rightarrow</math></u>										
$4G_{9/2}$	18755	533	-	10.33	4220	18721	534	9.51	9.81	2980
$4G_{7/2}$			2.62		10600					7450
$2G_{7/2}$	16843	593.5	52.15	51.59	9730	16798	595	52.21	51.45	6700
$4G_{5/2}$					50200					37300
$2H_{11/2}$	15950	627	0.49	0.30	313	15895	629	-	0.32	243
$4F_{9/2}$	14505	689.5	0.75	1.08	924	14695	681	-	1.17	759
$4F_{7/2}$	13212	757	11.12	8.86	6250	13222	756	11.01	9.37	5090
$4S_{3/2}$					46.1					32
$2H_{9/2}$	12306	827	12.95	13.52	1490	12316	812	13.06	13.86	1210
$4F_{5/2}$					6820					5120
$4F_{3/2}$	11272	887	4.89	4.75	2440	11239	890	4.14	4.23	1600
$4I_{15/2}$	6139	1629	0.17	0.39	57.4	6075	1646	-	0.43	46.2
$4I_{13/2}$	4016	2490	1.97	2.60	161	4012	2493	-	2.89	132
$4I_{11/2}$	2048	4883	-	3.88	57.5	2048	4883	-	4.18	45.8
					64.37					74.71

Table III

Radiative properties of neodymium in glasses as a function of network forming anion.

The last three parameters are for  $^4F_{3/2} \rightarrow ^4I_{11/2}$ 

	Chalcogenide glass									
	GLS	ALS	Phosphate LHG5	Borate H13	Germanate H12	Silicate ED2	Tellurite 162M	Aluminate LG5	Titanate L220	Fluoro- phosphate L223
$\tau_{\text{rad}}(^4F_{3/2})$ , ms	0.077	0.100	0.346	0.419	0.435	0.326	0.239	0.392	0.309	0.371
$\lambda_{\text{p, nm}}$	1.077	1.077	1,054	1,061	1,062	1,062	1,063	1,069	1,064	1,054
$\Delta\lambda_{\text{eff, nm}}$	22	22	25.5	36.8	34.7	34.0	28.9	43.1	38.6	27.2
$\sigma_{\text{p}}(10^{-20} \text{ cm}^2)$	7.95	8.2	3.9	2.2	1.9	2.9	2.9	1.8	2.5	3.5

# SPECTRAL BEHAVIOUR OF Nd<sup>3+</sup> DOPED GLASSES UNDER NARROW-LINE EXCITATION \*

Y. KALISKY, R. REISFELD

*Department of Inorganic and Analytical Chemistry, The Hebrew University of Jerusalem, Jerusalem, Israel*

and

Y. HAAS

*Department of Physical Chemistry, The Hebrew University of Jerusalem, Jerusalem, Israel*

Received 18 September 1978

Nd<sup>3+</sup> doped phosphate, tellurite, ED-2 and germanate glasses were excited by a laser into different parts of the <sup>4</sup>I<sub>9/2</sub> → <sup>4</sup>G<sub>5/2</sub> inhomogeneously broadened band. It was found that the germanate glass exhibited wavelength-dependent decay times even at room temperature. It is concluded that the diffusion of energy in the germanate glass is slow because a large energy mismatch between different sites decreases the probability of energy diffusion between them.

## 1. Introduction

Nd<sup>3+</sup> doped glasses have been studied extensively in view of their importance as laser materials [1]. Recently, the technique of laser-induced fluorescence line narrowing (FLN) was used for the study of Nd<sup>3+</sup> [2,3] and Eu<sup>3+</sup> [4-7] spectroscopy in glasses. This technique makes it possible to distinguish between different groups of sites in the inhomogeneously broadened spectrum of Nd<sup>3+</sup>. Using this technique, Brecher et al. [3,8] showed that the radiative and non-radiative transition probabilities in the commercial ED-2 glass as well as borate, phosphate and fluoride glasses depend on the specific site in which the Nd<sup>3+</sup> ion is situated. This arises from the differences in the crystal-field parameters between the various sites that contribute to the inhomogeneous band.

In the present paper we compare the spectral behaviour of phosphate, germanate and tellurite glasses with that of ED-2 glass. As a result of this study, it is possible to draw conclusions about the character and inter-

action between various sites in different glasses as reflected by the lifetime dependence on excitation wavelength.

## 2. Experimental

Nd<sup>3+</sup> doped glasses of the following compositions were prepared:

0.045 mole per liter in phosphate NaPO<sub>3</sub> [9];

0.097 mole per liter Nd<sup>3+</sup> in tellurite 15BaO·85TeO<sub>2</sub> [10],

0.054 mole per liter and 0.54 mole per liter Nd<sup>3+</sup> in germanate glass 17K<sub>2</sub>O·17BaO·66GeO<sub>2</sub> [11].

ED-2 glass containing 3 weight % Nd<sup>3+</sup> was kindly provided by Dr. C.F. Rapp of Owens Illinois. The doped glasses were excited with tunable dye laser (Molelectron DL-200) equipped with a scan control unit and pumped by a pulsed N<sub>2</sub>-laser (Molelectron UV-400). The dye laser linewidth at 570-600 nm was about 1 cm<sup>-1</sup> and pulse duration 5 ns.

The fluorescence was passed through a monochromator (6 nm/nm) and detected with an R777 Hamamatsu photomultiplier (890 nm emission) or

\* Partially supported by U.S. Army Contract: DAKO-76-G-066.

with an RCA 7102 photomultiplier (1060 nm emission). The signal was fed into a PAR 162/164 boxcar averager and recorded on an X-Y recorder. Good signal-to-noise ratio was obtained in about 1000 s.

Excitation spectra were taken using a scanning rate of the grating of 2 nm/min. The fluorescence spectra after different time delays were measured by setting the boxcar integrator on the appropriate times and recording the integrated spectra. In steady state experiments, fluorescence was excited by an Ar<sup>+</sup> laser (Spectra Physics 164) at 4880 Å, dispersed by Spex 1401 double monochromator and detected by an RCA C31034 photomultiplier, using a photon counting system. Absorption spectra were taken with a Cary 14 spectrophotometer with undoped glass as a blank.

Emission spectra were measured using an apparatus built in this laboratory\* which consists of an Oriel xenon dc 150 W source and excitation monochromator (Oriel 7240) with a resolution of 6 nm/min blazed at 500 nm, a Spex 1704 analyzing monochromator and an RCA 7102 cooled photomultiplier coupled with a PAR 189 selective amplifier and a PAR 128 lock-in amplifier. The fluorescence spectra were not corrected for the spectral response of the instrument. All measurements were performed at room temperature.

### 3. Results and discussion

Fig. 1 presents the laser excitation spectra of Nd<sup>3+</sup> doped glasses monitored at 890 nm. The same spectra were obtained when monitored at 1060 nm. Note the pronounced splitting of Nd<sup>3+</sup> in germanate glass. It should be noted that germanate glasses have a stronger tendency of devitrification than other glasses [12]. We therefore believe that Nd<sup>3+</sup> is situated at a variety of distinct sites which are well separated in energies in germanate glasses, possibly making the interaction between the various sites weaker than in other glasses.

Fig. 2 presents the fluorescence spectra of the four glasses. Irradiation with broad band light source (250 cm<sup>-1</sup>) leading to excitation of all the sites, results in broad spectrum. The width of the spectrum decreases upon lowering the concentration as the number of different sites decreases. At higher concentration,

\* The detailed descriptions of the instrument will be published shortly.

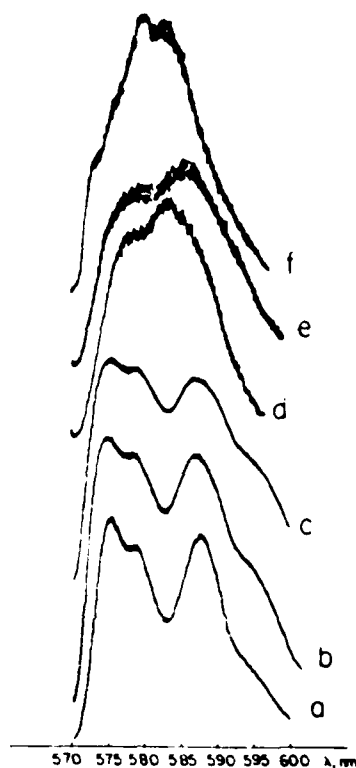
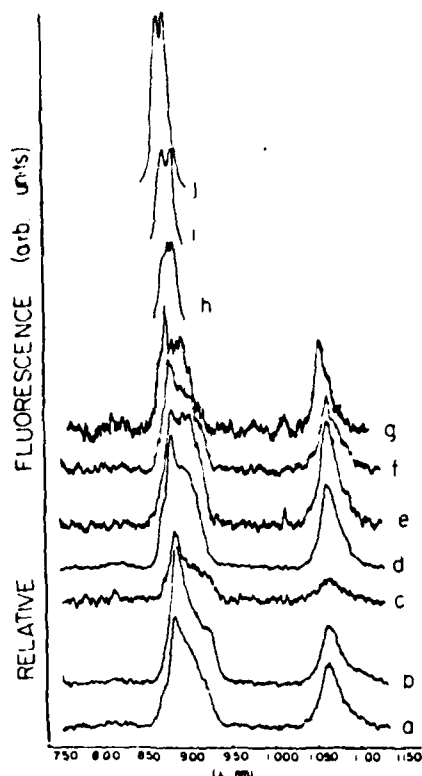


Fig. 1. Laser excitation spectra of various Nd<sup>3+</sup> doped oxide glasses in the region of the  $^4I_{9/2} \rightarrow ^4G_{5/2}$  absorption band: (a) 0.054 mole/liter Nd<sup>3+</sup> in germanate; (b) 0.54 mole/liter Nd<sup>3+</sup> in germanate; (c) 0.81 mole/liter Nd<sup>3+</sup> in germanate; (d) 0.097 mole/liter Nd<sup>3+</sup> in tellurite; (e) ED-2 glass; (f) 0.045 mole/liter Nd<sup>3+</sup> in phosphate. Emission monitored at 890 nm.

the intensity of the short wavelength part of the  $^4F_{3/2} \rightarrow ^4I_{9/2}$  band (880 nm) diminishes because of self-absorption. In contrast to the broad band excitation, the excitation by an Ar<sup>+</sup> laser at 4880 Å results in a narrower emission band of Nd<sup>3+</sup> in germanate and tellurite glasses peaking at 877 and 873 respectively which constitutes a subset of sites\*\*. The ratio of  $I_{880}/I_{1060}$  fluorescence decreases with the concentration of Nd<sup>3+</sup> because of self-trapping of the fluorescence.

\*\* In order to compare the relative intensities of the  $^4F_{3/2} \rightarrow ^4I_{11/2}$  we have used the results of Lipson et al. [13], who measured a corrected spectrum. Thus, our results of the 880 nm fluorescence have to be multiplied by a factor of 1.36 in order to get the corrected values of the 1060 nm fluorescence.



The shape of the emission band did not change after different delay times (0.5–700  $\mu$ s) within the experimental error. This brings us to the conclusion that the relaxation process from the state initially excited to the  $^4F_{3/2}$  state leading to the population distribution of the emitting sites, occurs much faster than 0.5  $\mu$ s (the time resolution of the experimental set-up).

#### 4. Lifetimes

The decay curves of  $Nd^{3+}$  in tellurite glasses were single exponentials with a lifetime of  $155 \pm 6 \mu$ s. Similar results were obtained by Singh et al. [14], and no excitation wavelength dependence of lifetime was observed. In phosphate and ED-2 glasses, non-exponential decays were observed but there still was no dependence on excitation wavelength. By contrast, the decay times for germanate glasses were found to be dependent on the exciting wavelength. In all cases the lifetimes were

Fig. 2. Fluorescence spectra of  $Nd^{3+}$  in various oxide glasses: (a) ED-2 glass; (b) 0.54 mole/liter  $Nd^{3+}$  in germanate; (c) 0.054 mole/liter  $Nd^{3+}$  in germanate; (d) 0.58 mole/liter  $Nd^{3+}$  in tellurite; (e) 1.55 mole/liter  $Nd^{3+}$  in tellurite; (f) 0.097 mole/liter  $Nd^{3+}$  in tellurite; (g) 0.045 mole/liter  $Nd^{3+}$  in phosphate; (h) 0.54 mole/liter  $Nd^{3+}$  in germanate; (i) ED-2 glass; (j) 0.58 mole/liter  $Nd^{3+}$  in tellurite. (a)–(g) were excited at 580 nm under broad band excitation. (h)–(j) were excited under narrow-line (4880 Å)  $Ar^+$  laser excitation.

Table I

Lifetimes of the first, second and third e-folding times of  $Nd^{3+}$  doped germanate glass excited at various wavelengths in the  $^4I_{9/2} \rightarrow ^4G_{5/2}$  region (estimated error  $\pm 2\%$ )

$\lambda_{exc}$ (nm)	0.054 M $Nd^{3+}$ in germanate			0.54 M $Nd^{3+}$ in germanate		
	$t_1$ ( $\mu$ s)	$t_2$ ( $\mu$ s)	$t_3$ ( $\mu$ s)	$t_1$ ( $\mu$ s)	$t_2$ ( $\mu$ s)	$t_3$ ( $\mu$ s)
572	480	630	770	360	415	470
574	450	540	650	340	380	435
577	360	420	500	301	345	415
580	340	430	450	282	340	375
583	315	395	470	275	325	385
585	—	—	—	285	335	405
587	340	440	520	290	345	400
590	300	390	510	—	—	—
592	320	400	480	272	317	400
594	325	405	490	—	—	—
596	—	—	—	286	353	445

clearly non-exponential as shown in table 1 for some excitation wavelengths. The first, second and third e-folding times,  $t_1$ ,  $t_2$  and  $t_3$  where  $I_0/I_1 = e$ ,  $I_0/I_2 = e^2$ ,  $I_0/I_3 = e^3$  are given in table 1 for  $\text{Nd}^{3+}$  doped germanate glass. The lifetimes of  $\text{Nd}^{3+}$  doped phosphate and ED-2 glass are independent of the excitation wavelength (in the range 572–596 nm). The following values were obtained: for phosphate glass  $t_1 = 230 \pm 3 \mu\text{s}$ ,  $t_2 = t_3 = 275 \pm 7 \mu\text{s}$ , and for ED-2 glass  $t_1 = 255 \pm 5 \mu\text{s}$  and  $t_2 = t_3 = 292 \pm 9 \mu\text{s}$ . The fact that germanate glass is the only one displaying a dependence of fluorescence lifetime on excitation wavelength indicates that the interaction between various sites may be weaker in this glass than in the others studied. One possibility is that the phonon assisted energy transfer is less efficient than in other glasses but evidently this phenomenon warrants further study.

### 5. Conclusions

From a comparison of the excitation spectra of the four glasses (fig. 1), it can be seen that the splitting in the spectra of the germanate glasses is larger than that in the spectra of the other glasses, reflecting the trend found in the absorption spectra. This splitting indicates that in germanate glass the energetic separation between the different sites is large and more pronounced than in the other glasses. Therefore, the interaction between the sites is weaker, leading to a lower diffusion rate of energy between the different sites. Thus we observe the phenomenon of different lifetimes dependence on excitation wavelength in germanate glasses at room temperature, while in ED-2, phosphate, borate and fluoride glasses [3,8] this could be seen only at 15 K. It thus appears that qualitatively, the behaviour of germanate glass at room temperature corresponds to that of other glasses at cryogenic temperatures. This, in turn, suggests that energy diffusion experiments may be conducted at room temperature using germanate glasses, allowing a considerable simplification of the experimental set-up. Excitation of  $\text{Nd}^{3+}$  doped germanate and tellurite glasses gives narrower emission peaks than excitation by a broad band source. The narrow-line fluorescence linewidths are much broader than the homogeneous widths, because the excitation is not made into the resonant transition allowing for accidental coincidence [15] during the relaxation process between the various Stark levels.

Thus  $\text{Nd}^{3+}$  doped germanate glasses are expected to show narrow band laser emission, more similar to crystals than the other glasses. From the above we conclude that the interaction between various sites in the phosphate, tellurite and silicate glass is much stronger at room temperature than similar interaction in the germanate glasses. It is worthwhile to note the analogy between the germanate glass and other systems in which Anderson localization occurs [16]. The other glasses resemble in their behaviour organic systems exhibiting the phenomenon of energy percolation [17].

### Acknowledgement

The authors are grateful to Dr. A. Loewenschuss and Mr. A. Givan for their assistance in narrow-line fluorescence measurements.

### References

- [1] R. Reisfeld and C.K. Jørgensen, *Lasers and excited states of rare earths* (Springer, Berlin, 1977).
- [2] L.A. Riseberg, *Phys. Rev. A* 7 (1973) 671.
- [3] C. Brecher, L.A. Riseberg and M.J. Weber, *Phys. Rev.* (1978), to be published.
- [4] N. Motegi and S. Shionoya, *J. Luminescence* 8 (1973) 1.
- [5] T. Kushida and E. Takushi, *Phys. Rev. B* 12 (1975) 824.
- [6] M.J. Weber, in: *Spectroscopie des éléments de transition et des éléments lourds dans les solides*, ed. F. Gaume, Lyon (1976) p. 283.
- [7] P. Avouris, A. Campion and M.A. El-Sayed, *Chem. Phys. Letters* 50 (1977) 9.
- [8] C. Brecher, L.A. Riseberg and M.J. Weber, *Appl. Phys. Letters* 30 (1977) 475.
- [9] R. Reisfeld, R.A. Velapoldi and L. Boehm, *J. Phys. Chem.* 76 (1972) 1293.
- [10] R. Reisfeld, J. Hormadaly and A. Muranevich, *Chem. Phys. Letters* 38 (1977) 188.
- [11] R. Reisfeld and Y. Kalisky, *Chem. Phys. Letters* 50 (1977) 199.
- [12] R. Reisfeld, J. Hormadaly and A. Muranevich, *J. Non-Cryst. Solids* 29 (1978) 323.
- [13] H.G. Lipson, J.R. Buckmelter and C.O. Dugger, *J. Non-Cryst. Solids* 17 (1975) 27.
- [14] S. Singh, L.G. van Uitert and W.H. Grodkiewicz, *Opt. Commun.* 17 (1976) 315.
- [15] M.J. Weber, J.A. Paisner, S.S. Sussman, W.M. Yen, L.A. Riseberg and C. Brecher, *J. Luminescence* 12/13 (1976) 729.
- [16] R. Orbach, *Phys. Letters* 48A (1974) 417.
- [17] R. Kopelman, in: *Topics in applied physics: radiationless processes in molecular and condensed phases*, ed. F.K. Fong (Springer, Berlin, 1976) p. 298.

## Optical Transitions of $\text{Sm}^{3+}$ in Oxide Glasses

L. BOEHM, R. REISFELD, AND N. SPECTOR\*

*Department of Inorganic and Analytical Chemistry, The Hebrew University of Jerusalem, Jerusalem, Israel*

Received April 20, 1978; in revised form July 12, 1978

Eigenvectors of the  $4f^5$  electronic configuration of  $\text{Sm}^{3+}$  were calculated in intermediate coupling, and used to obtain the reduced matrix elements  $U^{(A)}$ . Absorption spectra of  $\text{Sm}^{3+}$  were recorded in phosphate, borate, germanate and tellurite glasses. The Judd-Ofelt  $\Omega_k$ 's intensity parameters were then deduced from the measured oscillator strengths by least-squares fitting. Radiative transition probabilities and integrated cross-sections of stimulated emissions are obtained. Calculated branching ratios and decay lifetimes are compared with the experimental values.

### I. Introduction

Samarium ion has valuable fluorescence properties, that make it useful as laser material and phosphor. At room temperature the absorption and fluorescence study of  $\text{Sm}^{3+}$  in phosphate (1), borate (1) and germanate (2) oxide glasses was performed at this laboratory. The effect of temperature on the fluorescence properties of  $\text{Sm}^{3+}$  in tellurite glass is now in progress (3).

The fluorescence of samarium is quenched at higher concentration because of ion-ion cross relaxation (1). However, this difficulty can be circumvented by utilizing the increase of  $\text{Sm}^{3+}$  population via energy transfer (4).

Therefore, it is of interest to obtain predictions of the radiative transition probabilities and branching ratios of  $\text{Sm}^{3+}$  emission, and verify them with experimental results.

\* Partially supported by U.S. Army Contract No. DAERO-76-G-066.

† Permanent address: Soreq Research Center, Yavne 60700, Israel.

### II. Matrix Element Calculations

As a first step of this calculation the  $4f^5$  "free ion" eigenvectors were obtained, in the intermediate coupling scheme, by diagonalizing<sup>1</sup> the energy matrices for each  $J$  using radial parameters obtained by linear interpolation between  $\text{Nd}^{3+}$  (5) and  $\text{Tm}^{3+}$  (6) ions. Justification of such procedure will be discussed in connection with experimental results. The values of these parameters are given in Table I. The resulting eigenvectors were then introduced into a code by A. Caird and resulted in the reduced matrix elements  $U^{(A)}$  presented in Table II. Recently, matrix elements of  $\text{Sm}^{3+}$  in  $\text{LaF}_3$  were computed by Carnall *et al.* (7), using different radial parameters for calculation of the eigenvectors. Maximum deviation between the reduced matrix elements obtained in this work and the reference cited, do not exceed 10%.

It should be remarked that the lowest fluorescent level of  $J = \frac{5}{2}$  is sometimes

<sup>1</sup> The diagonalization was performed using a code kindly provided to us by Dr. Frey.



TABLE I  
RADIAL PARAMETERS FOR THE  $4f^5$  CON-  
FIGURATION OF  $\text{Sm}^{3+}$

Parameter	Diag ( $\text{cm}^{-1}$ )
A	79643
$F_2$	370
$F_4$	56
$F_6$	62
$\alpha$	30
$\beta$	-900
$\zeta$	1200

referred to as  $^4F$  and sometimes as  $^4G$  (8). According to our calculation the percentage composition of this level is  $^4F$  27% and  $^4G$  25%. Therefore the assignment of this level is a matter of taste.

### III. Intensity Parameters

The intensity parameters  $\Omega_\lambda$ 's were obtained by least-squares fit to the experimental oscillator strengths  $f$  in the spectral region  $0.5 \mu$ - $2.2 \mu$  using Eq. (1)

$$f_{JJ} = \frac{8\pi^2 m c \sigma}{3h(2J+1)} \left[ \frac{(n^2+2)^2}{9n} \right] \sum_{\lambda=2,4,6} \Omega_\lambda \frac{|\langle J^N \psi J \| U^{(\lambda)} \| f^N \psi' J' \rangle|^2}{(1)} \quad (1)$$

TABLE II  
 $(SLJ \| U^{(\lambda)} \| S'L'J')^2$  FOR SOME TRANSITIONS OF  
THE  $f^5$  CONFIGURATION

Designation	$U(2)^2$	$U(4)^2$	$U(6)^2$
$^6H_{5/2} \rightarrow ^6F_{1/2}$	0.1947	0.0	0.0
$^6F_{3/2}$	0.1389	0.1329	0.0
$^6F_{5/2}$	0.0346	0.2594	0.0
$^6F_{7/2}$	0.0042	0.1099	0.3939
$^6F_{9/2}$	0.0001	0.0183	0.3526
$^6F_{11/2}$	0.0	0.0006	0.0527
$^4G_{5/2} \rightarrow ^6H_{5/2}$	0.0002	0.0006	0.0
$^6H_{7/2}$	0.0	0.0067	0.0081
$^6H_{9/2}$	0.0112	0.0066	0.0021
$^6H_{11/2}$	0.0	0.0056	0.0030
$^6H_{13/2}$	0.0	0.0	0.0022
$^6F_{1/2}$	0.0008	0.0	0.0
$^6F_{3/2}$	0.0013	0.0001	0.0

where  $\sigma$  (in  $\text{cm}^{-1}$ ) is the baricenter of the absorption band,  $n$  is the index of refraction of the glass taken as constant over the range of observation and  $2J+1$  are the degeneracies of the  $J$  manifold.

Experimentally,  $f$  is obtained from the absorption spectrum by

$$f = 4.318 \times 10^{-9} \int \epsilon(\sigma) d\sigma \quad (2)$$

where  $\epsilon$  is the molar extinction coefficient.

In our previous work (9, 10) we have found that for calculation of the  $\Omega_\lambda$  parameters of  $\text{Sm}^{3+}$  the levels of this ion must be divided into a low set of energies ( $< 10,000 \text{ cm}^{-1}$ ) and a high lying set of levels ( $> 17,000 \text{ cm}^{-1}$ ), and only the low set is compatible with Judd-Ofelt theory. Recalculation has shown that three additional upper levels, namely  $^4G_{5/2}$ ,  $^4F_{3/2}$  and  $^4G_{7/2}$  can still be fitted into the low lying set of levels, without affecting the values of the low set of  $\Omega_\lambda$  parameters.

The slight difference between the intensity parameters obtained in this work, as presented in Table III, and those reported in Ref. 2, arises from the reidentification of the  $\text{Sm}^{3+}$  transition in the infrared part of the spectrum.

### IV. Radiative Spectral Characteristics

The radiative transition probability  $A_{JJ}$ , is obtained from the oscillator strength  $f_{JJ}$

TABLE III  
INTENSITY PARAMETERS  $\Omega_\lambda$  OF  $\text{Sm}^{3+}$  IN OXIDE  
GLASSES

Glass Matrix	$\Omega_2 \times 10^{20} \text{ cm}^2$	$\Omega_4 \times 10^{20} \text{ cm}^2$	$\Omega_6 \times 10^{20} \text{ cm}^2$	$n$
Borate	6.36	6.02	3.51	1.46
Phosphate	4.31	4.28	5.78	1.48
Germanate	6.48	4.98	3.18	1.64
Tellurite	3.17	3.65	1.61	2.04

OPTICAL TRANSITIONS OF  $\text{Sm}^{3+}$ 

77

TABLE IV  
RADIATIVE TRANSITION PROBABILITIES  $A$ , AND STIMULATED CROSS-SECTIONS OF SOME  
SELECTED TRANSITIONS OF  $\text{Sm}^{3+}$

Transition	Wavelength $\mu$	Borate		Phosphate		Germanate		Tellurite	
		$A(s^{-1}) \int \sigma(\nu) d\nu$ $\times 10^{18} \text{ cm}$	$A(s^{-1}) \int \sigma(\nu) d\nu$ $\times 10^{18} \text{ cm}$	$A(s^{-1}) \int \sigma(\nu) d\nu$ $\times 10^{18} \text{ cm}$	$A(s^{-1}) \int \sigma(\nu) d\nu$ $\times 10^{18} \text{ cm}$	$A(s^{-1}) \int \sigma(\nu) d\nu$ $\times 10^{18} \text{ cm}$	$A(s^{-1}) \int \sigma(\nu) d\nu$ $\times 10^{18} \text{ cm}$	$A(s^{-1}) \int \sigma(\nu) d\nu$ $\times 10^{18} \text{ cm}$	$A(s^{-1}) \int \sigma(\nu) d\nu$ $\times 10^{18} \text{ cm}$
$^4G_{5/2} \rightarrow ^6H_{5/2}$	0.560	20.2	0.039	17.7	0.034	26.8	0.041	45.1	0.045
$^4G_{5/2} \rightarrow ^6H_{7/2}$	0.596	119.0	0.263	133.0	0.286	147.0	0.258	206.0	0.233
$^4G_{5/2} \rightarrow ^6H_{9/2}$	0.642	152.0	0.390	117.0	0.292	205.0	0.417	247.0	0.325
$^4G_{5/2} \rightarrow ^6H_{11/2}$	0.702	43.8	0.134	41.6	0.124	52.5	0.128	76.2	0.120

using Eq. (3)

$$A_{JJ} = \frac{8\pi^2 e^2 n^2}{mc \lambda^2} \times f_{JJ} \quad (3)$$

where  $\bar{\lambda}$  is the mean wavelength of the relevant transition. The integrated emission cross-section is related to the radiative transition probability by (11):

$$\int_{J \rightarrow J'} \sigma(\nu) d\nu = \frac{\bar{\lambda}^2}{8\pi c n^2} A_{JJ} \quad (4)$$

The values of these two quantities in four oxide glasses are given in Table IV. It should be remarked that the four transitions in the Table account for 85% of the total fluorescence.

The branching ratio  $\beta_{ij}$  for a transition  $i \rightarrow j$  is given by

$$\beta_{ij} = \frac{A_{ij}}{\sum_i A_{ij}} \quad (5)$$

The values of the calculated decay lifetimes from the  $^4G_{5/2}$  at  $17\,700 \text{ cm}^{-1}$  of  $\text{Sm}^{3+}$  are given in Table V and compare with the measured ones, taken at concentrations at which quenching does not occur yet. In Table VI we compare the calculated and experimental values of the branching ratio of the three strongest emission bands of  $\text{Sm}^{3+}$  in phosphate glass. The contributions of these

three transitions to the total branching ratio is more than 75%. The reasonable agreement between both values justifies the method of calculation of the eigenvectors.

## V. Conclusions

In the present work we predict the radiative transition probabilities and other spectroscopic characteristics of  $\text{Sm}^{3+}$  ion in the four oxide glasses, based on the intensity parameters which are the average values for the inhomogeneously broadened bands. It is shown that these values predict correctly the experimental data. Similar results may be expected if the  $\text{Sm}^{3+}$  were excited by a laser instead of a broad band xenon source, because of the fast diffusion of energy among the different sites in the Sm system.

Another feature of the present treatment is the possibility to control the red ( $^4G_{5/2} \rightarrow ^6H_{9/2}$  at 642 nm) to orange ( $^4G_{5/2} \rightarrow ^6H_{7/2}$  at 596 nm) intensity ratio by varying the glass host. The phosphate glass is

TABLE V  
DECAY LIFETIMES OF THE  $^4G_{5/2}$  LEVEL OF  $\text{Sm}^{3+}$   
IN OXIDE GLASS

Matrix	$\tau_{\text{exp}}$ (msec)	$\tau_{\text{cal}}$ (msec)
Borate	2.63	3.54
Phosphate	2.34	2.80
Germanate	2.15	1.97

TABLE VI  
BRANCHING RATIOS FROM THE  $^4G_{5/2}$  LEVEL TO  
THE  $^6H$  MANIFOLD OF  $\text{Sm}^{3+}$  IN PHOSPHATE  
GLASS

Transition	$\beta_{\text{exp}}$	$\beta_{\text{cal}}$
$^4G_{5/2} \rightarrow ^6H_{5/2}$	0.07	0.05
$\rightarrow ^6H_{7/2}$	0.35	0.37
$\rightarrow ^6H_{9/2}$	0.33	0.33

characterized by having the orange emission, stronger than the red emission while in the other glasses the opposite holds. This fact may be of practical value in phosphors and related devices.

The stimulated emission cross-section at 650 nm is  $\sigma_p \sim 5 \times 10^{-21} \text{ cm}^2$ , assuming a  $\Delta\nu$  value of  $200 \text{ cm}^{-1}$ . This  $\sigma_p$  is lower by almost one order of magnitude than stimulated emission cross-section of the  $^4F_{3/2} \rightarrow ^4I_{11/2}$  transition of  $\text{Nd}^{3+}$  in silicate glass (11). Thus, larger excited state population densities will be required for efficient laser operation. For this purpose energy transfer from ions having large absorption cross-section such as  $\text{Bi}^{3+}$ - $\text{Sm}^{3+}$  (12) or  $\text{UO}_2^{2+}$ - $\text{Sm}^{3+}$  (4) can be utilized.

## References

1. R. REISFELD, L. BOEHM, AND E. GREENBERG, Proc. 10th Rare Earth Res. Conf., Arizona, 1973, 1149.
2. R. REISFELD, A. BORNSTEIN, AND L. BOEHM, *J. Solid State Chem.* **14**, 14 (1975).
3. H. BILL AND R. REISFELD, unpublished results.
4. R. REISFELD AND N. SOFER, unpublished results.
5. N. SPECTOR, C. GUTFIELD, AND R. REISFELD, *Opt. Pura Appl.* (1978), **10**, 197 (1977).
6. N. SPECTOR, R. REISFELD, AND L. BOEHM, *J. Chem. Phys. Lett.* **49**, 49 (1977).
7. W. T. CARNALL, HANNAH CROSSWHITE AND H. M. CROSSWHITE, Argonne National Laboratory Research Report No. 000, U. of C-AU-A-USERDA.
8. M. J. TREADWAY AND R. C. POWELL, *Phys. Rev. B* **11**, 862 (1975).
9. R. REISFELD, L. BOEHM, N. LIEBLICH, AND B. BARNETT, Proc. 10th Rare Earth Res. Conf., Arizona (1973), 1142.
10. R. REISFELD, A. BORNSTEIN, AND L. BOEHM, *J. Solid State Chem.* **9**, 224 (1974).
11. W. F. KRUPKE, IEEE, *J. Quant. Electron.* **QE-10**, 450 (1974).
12. R. REISFELD, N. LIEBLICH, L. BOEHM, AND B. BARNETT, *J. Luminescence* **12**, 749 (1976).

## Energy Transfer from $\text{UO}_2^{2+}$ to $\text{Sm}^{3+}$ in Phosphate Glass\*

R. REISFELD AND N. LIEBLICH-SOFFER

*Department of Inorganic and Analytical Chemistry, The Hebrew University, Jerusalem, Israel*

Received June 5, 1978; in revised form August 29, 1978

Energy transfer from  $\text{UO}_2^{2+}$  to  $\text{Sm}^{3+}$  is described. The transfer efficiencies are calculated from the decrease of donor luminescence and lifetimes and from the increase of the acceptor fluorescence. It is shown that the transfer is nonradiative. The energy transfer efficiencies are greater when the donor is excited at higher energy levels due to stronger overlap between electronic levels of donor  $\text{UO}_2^{2+}$  and acceptor  $\text{Sm}^{3+}$ . From the comparison of energy transfer efficiencies from  $\text{UO}_2^{2+}$  to  $\text{Sm}^{3+}$  and  $\text{Eu}^{3+}$  it is deduced that the overlap between excitation levels of donor and acceptor is a sufficient condition for the transfer.

### Introduction

The visible emission of  $\text{Sm}^{3+}$  is of practical value as it may be utilized in various fluorescence devices.  $\text{Sm}^{3+}$  as a single dopant in borate (1), phosphate (1), germanate (2), and tellurite (3) glasses has been studied. The radiative transition probabilities along with the transition matrix elements have been calculated recently in these glasses (4). The intensity of fluorescence is ruled by the product of radiative transition probabilities and the population of the excited levels. Since radiative transition probabilities of  $\text{Sm}^{3+}$  from  $^4G_{5/2}$  are  $3.57 \times 10^{-2}$  per second, the way to increase  $\text{Sm}^{3+}$  fluorescence is to increase the population of its levels via energy transfer (5). It has been shown previously (6) that the best way to achieve high population of excited states of rare earth ions is to use donors with high absorption coefficients. In this paper we report the phenomenon of energy transfer (E.T.) from

$\text{UO}_2^{2+}$  to  $\text{Sm}^{3+}$  in phosphate glass and compare the results to E.T. from the same donor to  $\text{Eu}^{3+}$ .

Energy transfer from  $\text{UO}_2^{2+}$  to other rare earth ions in solutions (7, 8), crystals (9, 10), and glasses (11-16) was studied. To the best of our knowledge there is no quantitative study of transfer from  $\text{UO}_2^{2+}$  to  $\text{Sm}^{3+}$ . The fluorescence characteristics of glasses doped with  $\text{UO}_2^{2+}$  only which are needed for such a study are reported in Ref. (17).

### Experimental

Reagents  $\text{NaH}_2\text{PO}_4 \cdot \text{H}_2\text{O}$  (Mallinckrodt), 99.5% purity,  $\text{UO}_2(\text{CH}_3\text{COO})_2 \cdot 2\text{H}_2\text{O}$  (BDH Chemicals),  $\text{Eu}_2\text{O}_3$ , and  $\text{Sm}_2\text{O}_3$  (MolyCorp), 99% purity, were used.

A mixture of phosphate with the appropriate weight of rare earth (R.E.) was homogenized in an electric vibrator and melted in a platinum crucible at  $900^\circ\text{C}$ . Drops of hot melt were poured on a glazed ceramic plate into a ring of 1-cm diameter and pressed with another glazed ceramic.

\* Partially supported by U.S. Army Contract DAERO 76-G-066.

Fluorescence spectra were recorded by a spectrofluorimeter built in our laboratory (18).

Lifetime measurements were performed using an EGG-FX-6AU flash lamp, having an average pulse duration of 3  $\mu$ sec. The pulsed fluorescence was transmitted into a 162 PAR boxcar integrator and recorded on an XY recorder.

### Results

The appearance of the  $\text{UO}_2^{2+}$  excitation bands in the excitation spectrum of  $\text{Sm}^{3+}$  (Fig. 1) is the proof for the energy transfer from  $\text{UO}_2^{2+}$  to  $\text{Sm}^{3+}$ . The excitation bands of  $\text{UO}_2^{2+}$  in phosphate glass are at 330, 430, and 470 nm when monitored at one of the five fluorescence peaks between 500 and 600 nm, as can be seen from Fig. 2.

The emission of  $\text{UO}_2^{2+}$  was quenched in the presence of  $\text{Sm}^{3+}$  as a result of the E.T. The decrease was observed in all five peaks and in the same amount, indicating the nonradiative character of the transfer. The transfer efficiencies were calculated according to Ref. (19) by

$$\eta_t = 1 - \frac{\tau_d}{\tau_d^0} \quad (1)$$

where  $\eta_t$  is energy transfer efficiency,  $\tau_d^0$  the fluorescence efficiency of the pure donor, and  $\tau_d$  the fluorescence efficiency of the donor with acceptor present. The values of  $\eta_t$  are given in Table I. In this table we also give the results of E.T. efficiencies from  $\text{UO}_2^{2+}$  to  $\text{Eu}^{3+}$  in phosphate glass.

The decay time of  $\text{UO}_2^{2+}$  was measured alone and with the presence of  $\text{Sm}^{3+}$  and  $\text{Eu}^{3+}$ . The decay was not a simple exponential in all cases. Examples of the decay curves of  $\text{UO}_2^{2+}$  in the presence of  $\text{Sm}^{3+}$  and  $\text{Eu}^{3+}$  are presented in Figs. 3 and 4, where the shortening of the  $\text{UO}_2^{2+}$  lifetime is demonstrated.  $\tau$  was taken where the intensity fell to  $1/e$  of its initial value.

Transfer efficiencies were calculated according to the equation

$$\eta_t = 1 - \frac{\tau_d}{\tau_d^0} \quad (2)$$

where  $\tau_d^0$  is the lifetime of the pure donor and  $\tau_d$  is the lifetime of the donor in the presence of the acceptor. The efficiencies thus calculated are given in Table II.

The enhancement of  $\text{Sm}^{3+}$  fluorescence in the presence of  $\text{UO}_2^{2+}$  obtained by measuring the relative fluorescence of the 645-nm

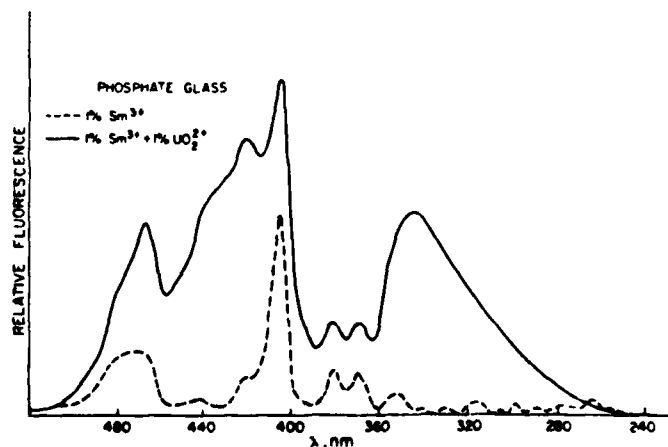


FIG. 1. Excitation spectrum of  $\text{Sm}^{3+}$  (---) and  $\text{Sm}^{3+}$  in presence of  $\text{UO}_2^{2+}$  (—) monitored at 645 nm.

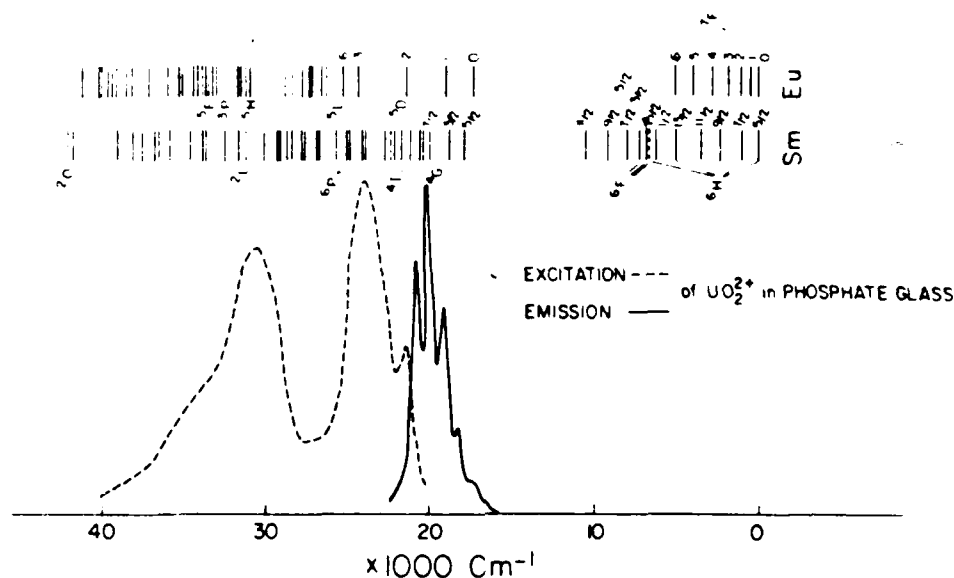


FIG. 2 Excitation and emission of  $\text{UO}_2^{2+}$  in phosphate glass compared to the electronic energy levels of  $\text{Sm}^{3+}$  and  $\text{Eu}^{3+}$  according to Ref. (5, p. 93)

peak when excited at 330, 405, 430, and 470 nm given in Table III.

The relation between the increase of  $\text{Sm}^{3+}$  fluorescence  $\Delta\eta_a$  to the transfer efficiency  $\eta_t$  is shown in Eq. (3):

$$\Delta\eta_a = kAd_\lambda\phi d_\lambda S_\lambda\eta_{ia} \quad (3)$$

where  $Ad_\lambda$  is the absorption of the donor at the excitation wavelength  $\lambda$ ,  $\phi d_\lambda$  the quantum efficiency of the donor fluorescence where excited at wavelength  $\lambda$ ,  $S_\lambda$  the spectral sensitivity of the spectrofluorimeter (including light source and monochromator), and  $k$  the proportionality constant, obtained by equating  $\eta_{ia}$  ( $\lambda = 330$  nm) from

Eq. (1) to  $\eta_{ia}$  obtained by Eq. (3). The three factors  $Ad_\lambda$ ,  $\phi d_\lambda$ ,  $S_\lambda$  are intrinsically included in the excitation curve of  $\text{UO}_2^{2+}$  and are eliminated by dividing  $\Delta\eta_a$  by the intensity of  $\text{UO}_2^{2+}$  peaks at wavelength  $\lambda$  in the excitation spectrum. The values thus obtained are given in Table IV.

TABLE I  
EFFICIENCIES OF E.T. BETWEEN  $\text{UO}_2^{2+} \rightarrow \text{Sm}^{3+}$   
AND  $\text{UO}_2^{2+} \rightarrow \text{Eu}^{3+}$  OBTAINED FROM STEADY  
STATE FLUORESCENCE CALCULATED BY EQ (1)

1% wt $\text{UO}_2^{2+}$ +	$\eta_t$	1% wt $\text{UO}_2^{2+}$ +	$\eta_t$
0.5% $\text{Sm}^{3+}$	0.18	0.5% $\text{Eu}^{3+}$	0.27
1% $\text{Sm}^{3+}$	0.25	1% $\text{Eu}^{3+}$	0.36

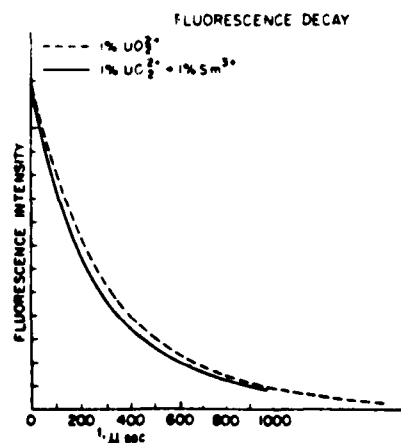


FIG. 3. Fluorescence decay curves of  $\text{UO}_2^{2+}$  and with presence of 1 wt%  $\text{Sm}^{3+}$ .

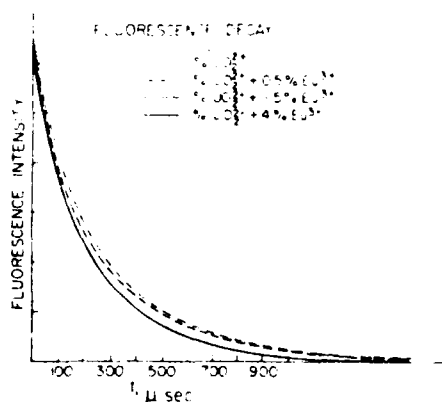


FIG. 4. Fluorescence decay curves of  $\text{UO}_2^{2+}$  and with presence of various concentrations of  $\text{Eu}^{3+}$ .

From Table IV it can be seen that the transfer efficiencies are greater when the excitation level is at higher energy. This can be connected with the stronger overlap between electronic levels of  $\text{Sm}^{3+}$  and  $\text{UO}_2^{2+}$  at higher energies as presented in Fig. 2. In this figure we also see that for  $\text{Sm}^{3+}$  electronic levels there is a good overlap between both excitation and emission bands of  $\text{UO}_2^{2+}$ , while in case of  $\text{Eu}^{3+}$  there exists a good overlap only between the excitation of  $\text{UO}_2^{2+}$  and the electronic levels of  $\text{Eu}^{3+}$ . Since transfer efficiencies are somewhat higher for  $\text{Eu}^{3+}$  (Table I) we can deduce that overlap of the excitation spectrum of the donor with the acceptor electronic levels satisfies the condition that energy transfer will occur.

It is worthwhile to note the highest increase of  $\text{Sm}^{3+}$  fluorescence in the presence of  $\text{UO}_2^{2+}$  at excitation 405 nm (Table III).

TABLE II

EFFICIENCIES OF E.T. BETWEEN  $\text{UO}_2^{2+} \rightarrow \text{Sm}^{3+}$ ,  $\text{UO}_2^{2+} \rightarrow \text{Eu}^{3+}$  CALCULATED FROM LIFETIME MEASUREMENTS BY USING EQ (2)

1% wt $\text{UO}_2^{2+}$ +	$\eta_i$	1% wt $\text{UO}_2^{2+}$ +	$\eta_i$
—	—	0.5% $\text{Eu}^{3+}$	0.14
1% $\text{Sm}^{3+}$	0.22	1% $\text{Eu}^{3+}$	0.17

TABLE III

$\text{Sm}^{3+}$  FLUORESCENCE INTENSITY AT 645 nm EXCITED AT VARIOUS WAVELENGTHS

λ Excitation (nm)	Rf			
	0.5% $\text{Sm}^{3+}$	0.5% $\text{Sm}^{3+}$ + 1% $\text{UO}_2^{2+}$	1% $\text{Sm}^{3+}$	1% $\text{Sm}^{3+}$ + 1% $\text{UO}_2^{2+}$
330	93	480	96	630
405	300	600	430	760
430	32	500	36	590
470	167	330	196	403

\* Rf = Relative fluorescence, arbitrary unit

where the excitation of  $\text{UO}_2^{2+}$  is relatively low. This can arise from a linear combination of the electronic state of  $\text{Sm}^{3+}$  with the wavefunction of  $\text{UO}_2^{2+}$ , thus increasing the transition probability of this state origination from the  $^6P_J$  multiplet of  $\text{Sm}^{3+}$ . This can be seen in the excitation spectrum of  $\text{Sm}^{3+}$  codoped with  $\text{UO}_2^{2+}$  (Fig. 1).

The energy transfer from  $\text{UO}_2^{2+}$  to  $\text{Sm}^{3+}$  mainly occurs in a nonradiative way. This can be seen from the decrease of the  $\text{UO}_2^{2+}$  decay time in the presence of  $\text{Sm}^{3+}$  and from the equivalent decrease in the five fluorescent peaks of  $\text{UO}_2^{2+}$  in the presence of  $\text{Sm}^{3+}$ .

The detailed nonradiative mechanism of the energy transfer cannot be calculated. The various sites of ions present in the glass host create many distances for pairs of  $\text{UO}_2^{2+}$ – $\text{Sm}^{3+}$ , and thus they interact in a different fashion (6). For instance, at very small dis-

TABLE IV

EFFICIENCIES OF E.T. OBTAINED FROM THE INCREASE OF  $\text{Sm}^{3+}$  FLUORESCENCE CALCULATED BY EQ (3)

λ Excitation (nm)	$\eta_{\text{ET}}$ 0.5% $\text{Sm}^{3+}$ + 1% $\text{UO}_2^{2+}$	$\eta_{\text{ET}}$ 1% $\text{Sm}^{3+}$ + 1% $\text{UO}_2^{2+}$
330	0.18	0.25
430	0.17	0.21
470	0.12	0.15

tances quadrupole-quadrupole or exchange interactions may be effective, whereas at larger distances a dipole-dipole interaction would predominate. In addition diffusion of energy between equivalent sites of  $\text{UO}_2^{2+}$  and  $\text{Sm}^{3+}$  may be important at the concentration measured. In order to elucidate this problem it is advisable to perform energy transfer measurements under laser excitation using time-resolved spectroscopy.

# References

- 1 R. REISFELD, L. BOEHM, AND E. GREENBERG, in "Proc. 10th Rare Earth Research Conference, Arizona," p. 1149 (1973).
- 2 R. REISFELD, A. BORNSTEIN, AND L. BOEHM, *J. Solid State Chem.* **14**, 14 (1975).
- 3 H. BILL AND R. REISFELD, unpublished results.
- 4 L. BOEHM, R. REISFELD, AND N. SPECTOR, to be published.
- 5 R. REISFELD AND C. K. JORGENSEN, "Rare-Earth Lasers and Excited States," Springer-Verlag, Berlin-New York (1977).
- 6 R. REISFELD, *Struct. Bonding (Berlin)* **30**, 65 (1976).
- 7 J. L. KROPP, *J. Chem. Phys.* **46**, 843 (1967).
- 8 B. O. JOSHI, A. G. I. DAIVE, AND T. R. BANGIA, *J. Lumin.* **10**, 261 (1975).
- 9 G. BLASSE, *J. Electrochem. Soc.* **115**, 738 (1968).
- 10 M. V. HOFFMAN, *J. Electrochem. Soc.* **117**, 227 (1970).
- 11 H. W. GANDY, R. J. GINTHER, AND J. J. WELLER, *Appl. Phys. Lett.* **4**, 188 (1964).
- 12 N. T. MELAMED, C. HIRAYAMA, AND P. W. FRENCH, *Appl. Phys. Lett.* **6**, 43 (1965).
- 13 L. G. DESHAZER AND A. Y. CABEZAS, *Proc. IEEE* **52**, 1355 (1964).
- 14 A. KITAMURA, *J. Phys. Soc. Japan* **20**, 1283 (1965).
- 15 J. C. JOSHI, B. C. JOSHI, N. C. PANDEY, AND J. JOSHI, *Indian J. Pure Appl. Phys.* **15**, 326 (1977).
- 16 J. C. JOSHI, N. C. PANDEY, B. C. JOSHI, AND J. JOSHI, *Indian J. Pure Appl. Phys.* **15**, 519 (1977).
- 17 N. LIEBLICH-SOFFER, R. REISFELD, AND C. K. JORGENSEN, *Inorg. Chim. Acta* (1978).
- 18 R. REISFELD, A. HONIGBAUM, G. MICHAELI, I. HAREL, AND M. ISH-SHALOM, *Isr. J. Chem.* **7**, 613 (1969).
- 19 R. REISFELD, *Struct. Bonding (Berlin)* **13**, 53 (1973).



## Transition Probabilities of Europium(III) in Zirconium and Beryllium Fluoride Glasses, Phosphate Glass, and Pentaphosphate Crystals\*

B. BLANZAT

*Laboratoire CNRS de Chimie métallurgique et spectroscopie des terres rares, F 92190  
Bellevue-Meudon, France*

L. BOEHM

*Department of Inorganic and Analytical Chemistry, Hebrew University, Jerusalem,  
Israel*

C. K. JORGENSEN AND R. REISFELD

*Département de Chimie minérale, analytique et appliquée, University of Geneva,  
Switzerland*

AND N. SPECTOR

*Soreq Nuclear Research Center, Yavne, Israel*

Received December 13, 1978; in revised form June 18, 1979

Eigenvectors of  $\text{Eu}^{3+}$  were obtained by a least-squares fitting procedure to the measured transitions from the two lowest  $J$  levels to a multitude of excited levels up to  $41\,000\text{ cm}^{-1}$ . The Judd-Ofelt parameters  $\Omega_4$  ( $\lambda = 2, 4, 6$ ) were obtained by comparison between the  $U^{(2)}$  calculated from the eigenvectors, and the observed oscillator strengths. Radiative transition probabilities and branching ratios were evaluated for the excited states  ${}^5D_0$  ( $J = 0, 1, 2, 3$ ) and  ${}^7F_1$  to  ${}^7F_7$ . The agreement between the calculated and observed lifetimes and branching ratios is better in oxide glasses than in the pentaphosphate crystal and fluoride glasses. This can be understood on the basis of the higher variety of sites and hence, better averaging.

### 1. Introduction

Rare earth-doped glasses and crystals are of both theoretical and practical interest because of their properties as lasers (1, 2). It was pointed out that owing to the low multiphonon relaxation rate of fluoride glasses (3)

their luminescent quantum efficiencies will be increased in comparison to those of oxide glasses in the cases where the distances between the fluorescent level and the adjacent lower levels are small. Recently, this hypothesis was verified (4) in lanthanide-doped beryllium fluoride glasses, where an exponential dependence of the multiphonon relaxation rates on this energy gap was observed, typically five times lower than in oxide glasses.

The spectroscopic properties of neodymium in various fluorozirconate glasses were

\* Partially supported by the Israel Scientific Council of Research and Development and by U.S. Army Contract DAERO-76-G-066. Correspondence should be addressed to: Professor R. Reisfeld, Department of Inorganic and Analytical Chemistry, The Hebrew University, Jerusalem, Israel.

page 2

studied by Lucas *et al.* (5) who suggest that because of the relatively low refractive index, such materials may find applications in high-intensity lasers, owing to the absence of self-focusing due to nonlinear effect. The local symmetry of the lanthanide ions in fluoride glasses is somewhat controversial. Hence, it is interesting to study the absorption and emission spectra of  $\text{Eu}^{3+}$  in such glasses, and compare them with oxide glasses. The levels with  $J = 0, 1$ , and  $2$  (spherical symmetry being a remarkably good approximation) of the two lowest terms  ${}^7F$  and  ${}^5D$  of the ground configuration  $4f^6$  are particularly suitable (6-8) for investigating the influence of the nearest-neighbor atoms on  $\text{Eu}^{3+}$ . Pentaphosphate crystals (also called ultraphosphates) such as  $\text{EuP}_5\text{O}_{14}$  (9, 10) have the advantage of high optical transparency for wavelengths down to 240 nm. Therefore, the set of observed  $J$ -levels could be extended up to  $41\,000\text{ cm}^{-1}$ . These newly observed energy levels were incorporated in the least-squares fit thus providing new radial parameters, better established free-ion eigenvectors, and reduced matrix elements which are used in the calculation of spectroscopic properties.

## II. Materials

The beryllium glass was kindly provided by Dr. J. Portier, CNRS, Talence (Bordeaux), and its composition (as mole percentage) is

25%  $\text{BeF}_2$ , 35%  $\text{AlF}_3$ , 24%  $\text{CaF}_2$ ,  
15%  $\text{BaF}_2$ , and 1%  $\text{EuF}_3$ .

The zirconium fluoride glass was kindly provided by Dr. J. Lucas, Université de Rennes. Its preparation is described in Ref. (5) and its composition (as mole percentage) is

60%  $\text{ZrF}_4$ , 33%  $\text{BaF}_2$ , 5%  $\text{LaF}_3$ , and  
2%  $\text{EuF}_3$ .

The crystal of  $\text{EuP}_5\text{O}_{14}$  was grown as described in Ref. (9).

The phosphate glasses (6) were prepared by melting a mixture of  $\text{NaH}_2\text{PO}_4 \cdot \text{H}_2\text{O}$  with 0.5 to 3.5 wt%  $\text{Eu}_2\text{O}_3$  in a platinum crucible at  $1000^\circ\text{C}$  producing  $\text{NaPO}_3$  glass containing 0.4 to 2.8 mole% europium. The absorption spectra were measured on a sample containing 2 wt%  $\text{Eu}_2\text{O}_3$ .

## III. Spectroscopic Measurements

The fluorescence spectra of all the samples were measured on a 50-cm Jarrel Ash grating monochromator equipped with a cooled photomultiplier. As previously described (9) the absorption spectrum of crystalline  $\text{EuP}_5\text{O}_{14}$  was measured on the same instrument, whereas the absorption spectra of the glasses were measured (at room temperature) on a Cary 17 recording spectrophotometer.

Narrow-line selective excitation of the europium excited levels were performed with a dye laser Moletron DL100 using Rhodamine 6G for  ${}^7D_0$  in the yellow, and various substituted coumarines for  ${}^7D_1$  and  ${}^7D_2$  in the green and the blue. The rise time of the laser flash is  $5 \cdot 10^{-9}$  sec.

The lifetimes  $\tau$  were determined by feeding the luminescence signal (after passing a monochromator) in a PAR 162/164 boxcar averager.

Figures 1 and 2 give the observed fluorescence spectra of the zirconium fluoride and beryllium fluoride glasses. In the latter case the broad emission centered around 400 nm is due to a small part of the europium present in its divalent form.

## IV. Energy Levels and Eigenvectors

Table I gives the barycenters of  $J$ -levels of  $\text{Eu}^{3+}$  (in  $\text{cm}^{-1}$ ) derived from the absorption spectra of  $\text{EuP}_5\text{O}_{14}$  relative to the (structureless) ground state  ${}^7F_0$  as zero point. In the next nine  $J$ -levels, the individual  $(2J+1)$  sublevels have all been observed and assigned symmetry types in the site symmetry

${}^7F_0$

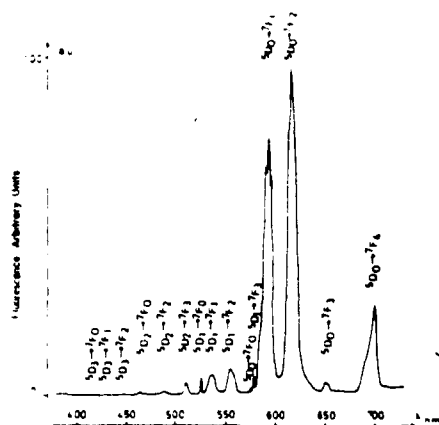


FIG. 1. Steady-state luminescence spectrum of  $\text{Eu}^{3+}$  in the zirconium fluoride glass under 254-nm ultraviolet excitation by a mercury lamp.

$C_2$ , based on absorption spectra in polarized light. Thus, the levels of  $^7F_1$  occur at 267, 403, and  $480 \text{ cm}^{-1}$  and those of  $^7F_2$  at 940, 960, 1075, 1101, and  $1180 \text{ cm}^{-1}$ , whereas the total spreading is around  $300 \text{ cm}^{-1}$  in  $^7F_4$  and  $^7F_5$  and  $466 \text{ cm}^{-1}$  in  $^7F_6$ . As usual,  $^5D_1$  is only split to a very small extent, with sublevels at 19,026, 19,053, and  $19,072 \text{ cm}^{-1}$ . The barycenters of the 30 subsequent  $J$ -levels (from  $^5D_3$  to  $^5G_5$  have

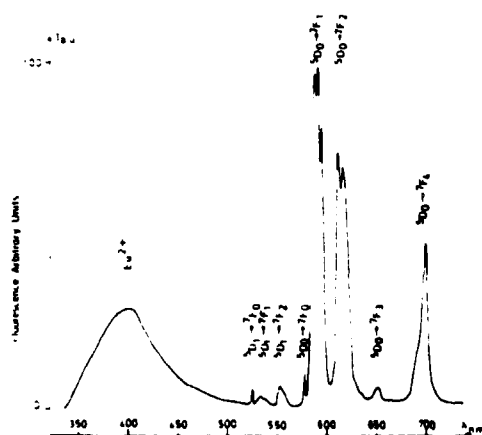


FIG. 2. Luminescence spectrum of  $\text{Eu}^{3+}$  in beryllium fluoride glass under the same conditions as in Fig. 1.

been obtained from the centre of gravity of the (very narrow) absorption band. In the two cases, where two  $J$ -levels are indicated with a distance smaller than  $40 \text{ cm}^{-1}$ , the calculated distances are given.

The manifold of 40 observed  $J$ -level barycenters was compared with the Condon-Shortley parameters (including the Trees corrections,  $\alpha$ ,  $\beta$ , and  $\gamma$  of comparatively minor importance) with a least-squares fitting program like that previously used for the  $4f^{12}$  system  $\text{Tm}^{3+}$  (11) and for  $4f^3\text{Nd}^{3+}$  incorporated in  $\text{Gd}_2(\text{MoO}_4)_3$  (12) resulting in the parameters (in  $\text{cm}^{-1}$ )

$$\begin{aligned} F_2 &= 381.0, & F_4 &= 61.3, & F_6 &= 6.2, \\ \alpha &= 36, & \beta &= -815, & \gamma &= 700, & (1) \\ \zeta_{4f} &= 1327, \end{aligned}$$

with an rms deviation of  $\sim 100 \text{ cm}^{-1}$ . The corresponding eigenvectors of the  $J$ -levels were also evaluated, and Table II gives the predominant components in terms of Russell-Saunders coupling with the last integer being a file number in the standard order of diagonal elements in Rahcch's theory. The calculation is done in full intermediate coupling.

## V. Matrix Elements of Intensities

The qualitative ideas (from 1945) of Broer *et al.* (13) or the origin of the finite transition probabilities (as electric dipolar transitions) from the ground state to excited  $J$ -levels (observed in absorption spectra) were expressed independently by Judd (14) and Ofelt (15) in a theory, where the oscillator strength  $P$  of a given transition is the sum of three contributions

$$P = \frac{8\pi^2 m c \sigma}{3h(2J+1)} \cdot \frac{(n^2+2)^2}{9n} \cdot \sum_{i=2,4,6} \Omega_i |U^{(i)}|^2, \quad (2)$$

where  $\sigma$  is the wavenumber,  $(2J+1)$  the number of states in the lower level, and  $n$  the refractive index. The matrix elements  $U^{(i)}$ ,

page 4

TABLE I  
OBSERVED ENERGY LEVELS (*J*-LEVEL BARYCENTERS) OF  $\text{Eu}^{3+}$  IN  $\text{EuP}_6\text{O}_{14}$

Level	$E(\text{cm}^{-1})$	Level	$E(\text{cm}^{-1})$	Level	$E(\text{cm}^{-1})$	Level	$E(\text{cm}^{-1})$
${}^7F_0$	0	${}^5D_3$	24,490	${}^5H_4$	31,250	${}^5K_6$	37,425
${}^7F_1$	383	${}^5L_6$	25,379	${}^5H_6$	31,526	${}^5P_1$	38,117
${}^7F_2$	1,051	${}^5G_2$	26,410	${}^5P_0$	32,793	${}^5K_5$	38,410
${}^7F_3$	1,927	${}^5L_7$	26,420	${}^5F_2$	33,134	${}^5G_2$	38,760
${}^7F_4$	2,896	${}^5G_3$	26,573	${}^5F_1$	33,452	${}^5K_8$	38,956
${}^7F_5$	3,922	${}^5G_4$	26,594	${}^5F_4$	33,596	$({}^5K, {}^5I)_6$	39,093
${}^7F_6$	5,026	${}^5G_6$	26,715	${}^5I_4$	33,852	${}^5G_3$	39,162
${}^7D_0$	17,289	${}^5D_4$	27,643	${}^5F_5$	34,137	${}^5G_4$	39,850
${}^7D_1$	19,050	${}^5H_3$	30,675	$({}^5L, {}^5H)_6$	35,014	$({}^5D, {}^5P)_3$	40,000
${}^7D_2$	21,528	${}^5H_7$	31,056	${}^5K_4$	36,206	${}^5G_5$	40,399

$U^{4+}$ , and  $U^{6+}$  can be evaluated, for instance, in Russell-Saunders coupling (where they are constrained by several selection rules:  $U^{(n)}$  can only be different from zero if  $J$  is changed by at most  $n$  units and if  $S$  does not change at all). Such matrix elements do not depend on chemical bonding to the neighbor atoms and were tabulated (16, 17) and compared with absorption spectra of aqua ions. In this work matrix elements of  $U^{2+}$ ,  $U^{4+}$ , and  $U^{6+}$  were evaluated with the new eigenvectors of Table II for more than 50 transitions and used for all subsequent spec-

troscopic calculations. They differ by several percent from previously tabulated ones and are available upon request.

At first, it may seem surprising that the absorption band intensities can be described by a fixed set of  $U^{(n)}$  for a given  $M^{3+}$  combined with only three parameters  $\Omega$ , characterizing the compound or (solid or liquid) solution, when it is realized that the energy levels (neglecting their separation in sublevels by "ligand field" effects) depend on four to seven parameters, as in Eq. (1). A general trend is recognized from a large

TABLE II  
EIGEN VECTORS OF LOW-LYING *J*-LEVELS OF  $\text{Eu}^{3+}$  IN INTERMEDIATE COUPLING

$E(\text{cm}^{-1})$	<i>J</i>	
0	0	$0.9713 {}^7F_0 - 0.1736 {}^5D_1 - 0.1561 {}^5D_0$
17,289	0	$-0.2247 {}^7F_0 - 0.5465 {}^5D_1 - 0.1787 {}^5D_2 - 0.6949 {}^5D_0$
383	1	$0.9766 {}^7F_1 - 0.1580 {}^5D_1 + 0.1388 {}^5D_0$
19,050	1	$-0.1992 {}^7F_1 - 0.5674 {}^5D_1 - 0.1889 {}^5D_2 - 0.7268 {}^5D_0$ $-0.1183 {}^5P_1 + 0.1539 {}^5P_0 - 0.1769 {}^5P_2$
1,051	2	$0.9832 {}^7F_2 - 0.1313 {}^5D_1 - 0.1102 {}^5D_0$
21,527	2	$-0.1557 {}^7F_2 - 0.5835 {}^5D_1 - 0.1883 {}^5D_2 - 0.7488 {}^5D_0 - 0.1010 {}^5P_0$
1,927	3	$0.9888 {}^7F_3 - 0.0973 {}^5D_1$
24,490	3	$-0.1049 {}^7F_3 - 0.5912 {}^5D_1 - 0.1699 {}^5D_2 - 0.7539 {}^5D_0 - 0.0862 {}^5F_1 - 0.1348 {}^5F_2$
2,896	4	$0.9903 {}^7F_4 - 0.0591 {}^5D_1 - 0.0738 {}^5F_2$
3,922	5	$0.9888 {}^7F_5 - 0.0709 {}^5F_2 - 0.0853 {}^5G_1 - 0.0824 {}^5G_0$
5,026	6	$0.9839 {}^7F_6 - 0.1175 {}^5G_1 - 0.1168 {}^5G_0$
25,379	6	$-0.0652 {}^5G_1 - 0.0713 {}^5G_2 - 0.0761 {}^5G_3 - 0.0623 {}^5H_1$ $-0.1098 {}^5K_1 - 0.9396 {}^5L_1 - 0.1377 {}^5K_2 - 0.1286 {}^5K_3 - 0.1637 {}^5K_4$

number of examples. Thus, crystalline fluorides, and aqua ions in water, have values of  $\Omega_4$  and  $\Omega_6$  of comparable magnitude, whereas  $\Omega_2$  usually is not larger than the experimental uncertainty. On the other hand, more covalent compounds (1) have much higher  $\Omega_2$ , producing "hypersensitive pseudoquadrupolar transitions" having intensities (proportional to the genuine electric quadrupolar transitions, but with a huge factor) dependent almost exclusively on the square of  $U^{(2)}$ . In Russell-Saunders coupling, each trivalent lanthanide shows only one pronounced hypersensitive pseudoquadrupolar transition, from the ground state ( $S, L, J$ ) to the level ( $S, L-2, J-2$ ). However, because of the effects of intermediate coupling mixing different ( $S, L$ ) combinations in the same eigenvector, both  $4f^{10}\text{Ho}^{3+}$  and  $4f^{11}\text{Er}^{3+}$  have two such transitions, to levels with  $J=6$  and  $11/2$ , respectively. It is well recognized that the Judd-Ofelt theory works with a precision of some 20%, but also that the agreement in certain cases (16, 18, 19) is conspicuously ameliorated if one transition (say  $^3\text{H}_4 \rightarrow ^3\text{P}_2$  in  $\text{Pr}^{3+}$ ) is eliminated.

Whereas Eq. (2) originally was intended for absorption spectra only, the radiative lifetimes of excited states (related to the oscillator strength by Einstein's 1917 formula) and the branching ratios indicating the probability of forming various lower  $J$ -levels (1) (including the groundstate) can also be described by Eq. (2) to a reasonable approximation. Thus, the luminescence of  $\text{Ho}^{3+}$  (20),  $\text{Er}^{3+}$  (21), and  $\text{Tm}^{3+}$  (22) in various phosphate, silicate, germanate, and tellurite glasses can be treated along these lines. It is not surprising that the much larger number of data described by the same three  $\Omega_i$  and an "objective" set of  $U^{(n)}$  matrix elements produced a higher dispersion of the agreement, typically within a factor of 1.5 or 2.

The intensity parameters  $\Omega_i$  characterizing each material were derived by fitting the

experimentally observed oscillator strengths of the transitions obtained by integrating the absorption bands with the calculated values of  $U^{(4)2}$ . Their values (in the unit  $10^{-20} \text{ cm}^2$ ) are

	$\Omega_2$	$\Omega_4$	$\Omega_6$
Zirconium fluoride glass	0.93	2.61	2.17
Phosphate glass	4.12	4.69	1.83
Pentaphosphate crystal	3.66	1.43	3.07

(3)

The  $\text{Nd}^{3+}$  in the zirconium fluoride type B (5) shows  $\Omega_2 = 1.93$ ,  $\Omega_4 = 3.8$ , and  $\Omega_6 = 4.35$  for comparison. Table III gives the calculated luminescent properties of the zirconium fluoride glass, oscillator strength  $P$  (in the unit  $10^{-8}$ ), the radiative transition probability  $A$  (in the unit  $\text{sec}^{-1}$ ), and the branching ratio  $\beta = A_i / \sum A_i$ . Table IV gives the same type of data for the phosphate glass with  $n = 1.48$  (22) and Table V for crystalline  $\text{EuP}_5\text{O}_4$  having  $n = 1.62$ .

The nonradiative deexcitation from a given electronic level  $E_2$  to the next lower electronic level  $E_1$  is given by

$$W_{\text{NR}} = B \exp\{-\alpha(E_2 - E_1)\}, \quad (4)$$

where  $B$  and  $\alpha$  are phenomenological parameters (22) which are

	$\alpha$	$B (\text{sec}^{-1})$	$\hbar\omega (\text{cm}^{-1})$
$\text{ZrF}_4$	0.007	$4 \times 10^{-9}$	500
Phosphate	0.005	$5.4 \times 10^{-12}$	1300

and  $\hbar\omega$  is the phonon energy.

The nonradiative relaxation rates thus obtained for the deexcitation of the higher levels were higher than  $10^6 \text{ sec}^{-1}$  leading to a rapid depopulation of all higher levels to the  $^5\text{D}_0$  with a small contribution to the  $^5\text{D}_1$  and  $^5\text{D}_2$  levels.

Table VI combines the measured and calculated values of the radiative lifetimes and branching ratios from  $^5\text{D}_0$  to levels of the  $^7\text{F}$  multiplet in the zirconium fluoride and

page 6

TABLE III  
SPECTROSCOPIC PARAMETERS OF  $\text{Eu}^{3+}$  IN  
ZIRCONIUM FLUORIDE GLASS

Transition	$P \times 10^{-4}$	$A (\text{sec}^{-1})$	$\beta$
${}^7L_6 \rightarrow {}^7D_1$	0.36	0.004	0
${}^7D_2$	15.7	3.58	0.0162
${}^7D_1$	21.6	13.4	0.0604
${}^7D_0$	46.8	47.3	0.2141
${}^7F_6$	0.32	2.02	0.0091
${}^7F_5$	0.36	2.55	0.0115
${}^7F_4$	2.46	19.2	0.0868
${}^7F_3$	0.65	5.50	0.0249
${}^7F_2$	0.01	0.09	0.0004
${}^7F_1$	4.72	45.4	0.2057
${}^7F_0$	8.24	81.9	0.3707
${}^5D_2 \rightarrow {}^7D_1$	31.7	3.00	0.0279
${}^7D_2$	1.58	0.44	0.0041
${}^7F_6$	0.11	0.44	0.0041
${}^7F_5$	1.87	8.92	0.0830
${}^7F_4$	1.45	7.76	0.0722
${}^7F_3$	10.5	62.1	0.5781
${}^7F_2$	3.00	19.4	0.1805
${}^7F_1$	0.32	2.22	0.0206
${}^7F_0$	0.44	3.16	0.0294
${}^5D_1 \rightarrow {}^7D_1$	20.2	0.97	0.0089
${}^7F_6$	0.46	1.40	0.0129
${}^7F_5$	1.18	4.17	0.0385
${}^7F_4$	5.02	20.2	0.1866
${}^7F_3$	6.20	28.0	0.2590
${}^7F_2$	7.79	38.9	0.3592
${}^7F_1$	1.94	10.4	0.0964
${}^7F_0$	0.74	4.16	0.0384
${}^5D_0 \rightarrow {}^7F_6$	0.88	2.04	0.0197
${}^7F_5$	0	0	0
${}^7F_4$	10.9	34.8	0.3364
${}^7F_3$	0	0	0
${}^7F_2$	6.16	25.0	0.2419
${}^7F_1$	9.44	41.6	0.419
${}^7F_0$	0	0	0

phosphate glasses and pentaphosphate crystal. For the beryllium fluoride only the observed values are given.

Calculations of the results given in Table VI could not be performed for the beryllium fluoride glass, because the three  $\Omega_i$  from Eq. (3) evaluated from the absorption spectrum had a large uncertainty. It may be due to the fact (found by diffuse light scattering) that

TABLE IV  
SPECTROSCOPIC PARAMETERS OF  $\text{Eu}^{3+}$  IN  
PHOSPHATE GLASS

Transition	$P \times 10^{-4}$	$A (\text{sec}^{-1})$	$\beta$
${}^5D_2 \rightarrow {}^7D_1$	33.5	3.01	0.0150
${}^7D_2$	6.8	1.79	0.0089
${}^7F_6$	0.09	0.35	0.0018
${}^7F_5$	3.25	14.7	0.0732
${}^7F_4$	4.88	24.8	0.1233
${}^7F_3$	16.7	93.6	0.4655
${}^7F_2$	7.54	46.2	0.2299
${}^7F_1$	0.57	3.73	0.0185
${}^7F_0$	1.90	12.9	0.0641
${}^5D_1 \rightarrow {}^7D_1$	19.7	0.89	0.0043
${}^7F_6$	0.38	1.08	0.0052
${}^7F_5$	2.03	6.79	0.0327
${}^7F_4$	8.76	33.4	0.1607
${}^7F_3$	17.4	74.8	0.3597
${}^7F_2$	9.42	44.6	0.2145
${}^7F_1$	8.35	42.5	0.2045
${}^7F_0$	0.72	3.84	0.0185
${}^5D_0 \rightarrow {}^7F_6$	0.72	1.58	0.0079
${}^7F_5$	0	0	0
${}^7F_4$	19.0	57.6	0.2884
${}^7F_3$	0	0	0
${}^7F_2$	26.5	102.0	0.5113
${}^7F_1$	9.19	38.4	0.1924
${}^7F_0$	0	0	0

this glass was on the limit of heterogeneous precipitation, forming a vitro-ceramic (1). Nevertheless, we have included this material in the present paper, because we find the observed branching ratios and a few other experimental quantities interesting.

Two transitions play an unusual role in the specific case of  $\text{Eu}^{3+}$ . One is the pseudoquadrupolar hypersensitive emission  ${}^5D_0 \rightarrow {}^7F_2$  taking over a large proportion of the total luminescence intensity if  $\Omega_2$  is large. The other is (the usually very weak)  ${}^5D_0 \rightarrow {}^7F_0$  which is forbidden in all approximations in spherical symmetry. It is frequently argued that it occurs nevertheless because of mixing of sublevels belonging to different  $J$ -levels by nondiagonal elements of "ligand field" perturbations, but it is at the same time an experimental fact that "chem-

TABLE V  
SPECTROSCOPIC PARAMETERS OF  $\text{Eu}^{3+}$  IN  
CRYSTALLINE PENTAPHOSPHATE

Transition	$P (\times 10^{-6})$	$A (\text{sec}^{-1})$	$\beta$
${}^1\text{L}_6 \rightarrow {}^1\text{D}_2$	0.56	~0	0
${}^1\text{D}_2$	23.5	6.10	0.0160
${}^1\text{D}_1$	33.0	23.2	0.0607
${}^1\text{D}_0$	71.6	82.1	0.1148
${}^1\text{F}_6$	0.49	3.58	0.0094
${}^1\text{F}_5$	0.54	4.37	0.0114
${}^1\text{F}_4$	3.62	32.1	0.0839
${}^1\text{F}_3$	0.99	9.54	0.0250
${}^1\text{F}_2$	0.01	0.13	0.0004
${}^1\text{F}_1$	7.21	78.9	0.2065
${}^1\text{F}_0$	12.6	142.0	0.3720
${}^3\text{D}_3 \rightarrow {}^3\text{D}_2$	42.8	6.58	0.0407
${}^3\text{D}_1$	0.91	4.70	0.0291
${}^3\text{D}_0$	0	0	0
${}^3\text{F}_6$	0.02	0.15	0.0009
${}^3\text{F}_4$	1.08	7.99	0.0495
${}^3\text{F}_3$	10.6	86.7	0.5369
${}^3\text{F}_2$	2.29	20.4	0.1263
${}^3\text{F}_1$	1.83	17.6	0.1093
${}^3\text{F}_0$	1.70	17.3	0.1074
${}^3\text{F}_0$	0	0	0

TABLE V—Continued

${}^3\text{D}_2 \rightarrow {}^3\text{D}_1$	36.4	3.91	0.0213
${}^3\text{D}_0$	6.73	2.12	0.0115
${}^3\text{F}_6$	0.16	0.76	0.0042
${}^3\text{F}_5$	1.11	6.04	0.0329
${}^3\text{F}_4$	4.23	25.7	0.1402
${}^3\text{F}_3$	13.1	87.9	0.4785
${}^3\text{F}_2$	5.08	37.3	0.2032
${}^3\text{F}_1$	0.59	4.61	0.0251
${}^3\text{F}_0$	1.88	15.2	0.0830
${}^3\text{D}_1 \rightarrow {}^3\text{D}_0$	21.6	1.17	0.0058
${}^3\text{F}_6$	0.70	2.43	0.0121
${}^3\text{F}_5$	0.73	2.93	0.0146
${}^3\text{F}_4$	2.97	13.6	0.0678
${}^3\text{F}_3$	13.2	67.6	0.3377
${}^3\text{F}_2$	10.1	57.1	0.2851
${}^3\text{F}_1$	8.25	50.4	0.2516
${}^3\text{F}_0$	0.79	5.04	0.0252
${}^3\text{D}_0 \rightarrow {}^3\text{F}_6$	1.34	3.54	0.0179
${}^3\text{F}_5$	0	0	0
${}^3\text{F}_4$	6.45	23.4	0.1181
${}^3\text{F}_3$	0	0	0
${}^3\text{F}_2$	26.2	121.0	0.6099
${}^3\text{F}_1$	10.1	50.4	0.2541
${}^3\text{F}_0$	0	0	0

ically polarizable" materials (1) have a special propensity for showing both these transitions.

It is seen from Table VI that the branching ratio  $\beta$  for  ${}^3\text{D}_0 \rightarrow {}^3\text{F}_2$  agrees with experiment for the phosphate glass, but is under-

estimated for the zirconium fluoride glass, and overestimated for crystalline  $\text{EuP}_5\text{O}_{14}$ . With the exception of the latter case, the calculated and observed values of  $\beta$  usually agree within a factor of 1.5. This may not be as surprising as one would expect at first for

TABLE VI  
OBSERVED AND CALCULATED LIFETIMES (msec) OF EXCITED LEVELS OF  $\text{Eu}^{3+}$  AND BRANCHING RATIOS  $\beta$

	Zirconium fluoride glass		Beryllium fluoride glass		Phosphate glass		Pentaphosphate crystal	
	obs	calc	obs	calc	obs	calc	obs	calc
${}^3\text{D}_2$	0.50	—	—	—	—	—	—	—
${}^3\text{D}_1$	1.0	—	0.17	—	—	—	0.006	—
${}^3\text{D}_0$	5.0	9.7	8.78	—	2.95	5.00	4.8	5.05
$\beta {}^3\text{D}_0 \rightarrow {}^3\text{F}_4$	0.196	0.336	0.132	—	0.194	0.288	0.335	0.118
${}^3\text{F}_3$	0.010	0	0.015	—	0.041	0	0.029	0
${}^3\text{F}_2$	0.464	0.242	0.406	—	0.568	0.511	0.254	0.610
${}^3\text{F}_1$	0.290	0.419	0.422	—	0.189	0.192	0.374	0.254
${}^3\text{F}_0$	0.0017	0	0.005	—	0.007	0	0.007	0

page 8

the vitreous systems with a dispersion of local site symmetries, as clearly shown by the  $^4I_{9/2} \rightarrow ^2P_{1/2}$  band of  $Nd^{3+}$  in zirconium fluoride glass (5) having a half-width of  $93\text{ cm}^{-1}$  at liquid helium temperature, compared with 1 or  $2\text{ cm}^{-1}$  for crystalline  $NdF_3$  and  $NdZrF_6$ . This inhomogeneous line broadening is typical for glasses (1, 23) but does not, by itself, demonstrate that a distinction between network-forming and-modifying cations is well-defined in fluoride glasses. Both in fluoride and in oxide glasses, the individual site may deviate more, on the average, from spherical symmetry than would be true for the crystalline pentaphosphate; but at the same time, the consequences of deviations from spherical symmetry may cancel out to a large extent in the multiple sites in glasses.

## References

1. R. REISFELD AND C. K. JORGENSEN, "Lasers and Excited States of Rare Earths," Springer-Verlag, Berlin (1977).
2. M. J. WEBER, in "Handbook of the Physics and Chemistry of Rare Earths" (K. Gschneider and L. Eyring, Eds.), Vol. 4, North-Holland, Amsterdam (1979).
3. R. REISFELD, *Struct. Bonding (Berlin)* **13**, 53 (1973).
4. C. B. LAYNE AND M. J. WEBER, *Phys. Rev. B* **16**, 3529 (1977).
5. J. LUCAS, M. CHANTHANASINH, M. POULAIN, M. POULAIN, P. BRUN, AND M. J. WEBER, *J. Non-Cryst. Solids* **27**, 273 (1978).
6. R. REISFELD, R. A. VELAPOLDE, L. BOEHM, AND M. ISH-SHALOM, *J. Phys. Chem.* **75**, 3980 (1971).
7. R. REISFELD, R. A. VELAPOLDE, AND L. BOEHM, *J. Phys. Chem.* **76**, 1293 (1972).
8. R. REISFELD, H. MACK, A. EISENBERG, AND Y. ECKSTEIN, *J. Electrochem. Soc.* **122**, 273 (1975).
9. B. BLANZAT, J. P. DENIS, AND J. LORIER, in "Proceedings 10th Rare Earth Research Conference, Arizona, May 1973," p. 1170.
10. B. BLANZAT, J. P. DENIS, AND R. REISFELD, *Chem. Phys. Lett.* **51**, 403 (1977).
11. N. SPECTOR, R. REISFELD, AND L. BOEHM, *Chem. Phys. Lett.* **49**, 49, (1977).
12. N. SPECTOR, C. GUTTEL, AND R. REISFELD, *Opt. Pura Apl.* **10**, 197 (1977).
13. L. J. F. BROER, C. J. GORTER, AND J. HOOCHSCHAGEN, *Physica* **11**, 231 (1945).
14. B. R. JUDD, *Phys. Rev.* **127**, 750 (1962).
15. G. S. OFELT, *J. Chem. Phys.* **37**, 511 (1962).
16. W. T. CARNALL, P. R. FIELDS, AND K. RANJAK, *J. Chem. Phys.* **49**, 4412, 4424 (1968).
17. W. T. CARNALL, in "Handbook of the Physical and Chemistry Rare Earths" (K. Gschneider and L. Eyring, Eds.), Vol. 3, p. 111, Amsterdam (1979).
18. J. HORMADALY AND R. REISFELD, *J. Non Cryst Solids* **30**, 337 (1979).
19. R. REISFELD AND C. K. JORGENSEN, to be published.
20. R. REISFELD AND J. HORMADALY, *J. Chem. Phys.* **64**, 3207 (1976).
21. R. REISFELD AND Y. ECKSTEIN, *J. Chem. Phys.* **63**, 4001 (1975).
22. R. REISFELD, L. BOEHM, AND N. SPECTOR, in "The Rare Earths in Modern Science and Technology" (G. J. McCarthy and J. J. Rhyne, Eds.), p. 513, Plenum, (1978).
23. Y. KALISKY, R. REISFELD, AND Y. HAAS, *Chem. Phys. Lett.* **61**, 19 (1979).



## MULTIPHONON RELAXATION IN GLASSES

Renata Reisfeld

Department of Inorganic and Analytical Chemistry  
The Hebrew University of Jerusalem  
Jerusalem, Israel.

### ABSTRACT

Experimental data of multiphonon relaxation between electronic levels of rare earth ions in glasses are presented. These are based on measurements of the decay times or quantum efficiencies of the specific levels and subtracting the radiative transition probabilities in oxide, chalcogenide and fluoride glasses. It is shown that the nonradiative transfer in all glasses depends mainly on the energy gap between the emitting and next lower level of the ion incorporated in the glass and that the high energy phonons of the network formers are responsible for the relaxation permitting the lowest order process. The phenomenological parameters  $\alpha$ ,  $\beta$  and  $\epsilon$  appearing in the formulae of multiphonon transfer are computed and compared to these values in crystals. It is also shown that the Huang-Rhys number  $S$  being a measure of the electron-phonon coupling strengths is smaller than 0.1 for the oxide glasses as predicted by the theory of multiphonon relaxation. However it achieves a large value of about 2 in the chalcogenide glasses. The discrepancy in this high value is explained by the covalency of the rare earths incorporated in the chalcogenide glasses with the surrounding sulfur ions, thus the rare earth ions cannot be treated as isolated centers in these glasses. Experimental findings of phonon-assisted energy transfer between uranyl and rare earth ions in phosphate glasses are presented. It is shown that an experimental dependance between multiphonon relaxation rates and the energy gap is obtained similar to the multiphonon relaxation in a single ion. The coupling constant is higher in the case of the energy transfer due to the stronger coupling of uranyl to the glass.

## INTRODUCTION

The theory of multiphonon relaxation of ions in crystals, organic molecules and in semiconductors has attracted the interest of many researchers during the last two decades. A number of reviews have been written recently (1-6) dealing with these important phenomena. A unified treatment of multiphonon relaxation in both organic and inorganic systems as well as a critical review of the existing theories can be found in an excellent book by Englman (7). Excited electronic levels of rare earths (RE) in solids decay nonradiatively by exciting lattice vibrations (phonons). When the energy gap between the excited level and the next electronic level is larger than the phonon energy several lattice phonons are emitted in order to bridge the energy gap. It was recognized that the most energetical vibrations are responsible for the non-radiative decay since such a process can conserve energy in the lowest order. In glasses the most energetical vibrations are the stretching vibrations of the glass network polyhedron and it was shown that these distinct vibrations are active in the multiphonon process (8) rather than the less energetical vibrations of the bond between the RE and its surrounding ligands. Later (9) it was demonstrated that these less energetical vibrations may participate in cases when the energy gap is not bridged totally by the high energy vibrations. The experimental results reveal that the logarithm of the multiphonon decay rate decreases linearly with the energy gap, or the number of phonons bridging the gap. The theory of nonradiative decay by multiphonon mechanism was first proposed by Kubo and Toyozawa (10) who proposed that the basic mechanism allowing such transitions is the correction in the Born-Oppenheimer (BO) approximation due to vibrational motion of ions which admixes the electronic wave function and causes transitions that represent stationary states in the zero order BO approximation. For multiphonon processes one has to proceed to higher order being  $\Delta E/\hbar\omega$  to get real transitions between the electronic states (7). It should be noted that in contrast to the smallness of the radiative processes of high order the nonradiative high order processes are quite high.

From the point of view of theoretical treatment it is extremely difficult to calculate accurately the perturbation of a high order. However a considerable part of  $\Delta H_{\text{vibr}}$  can be eliminated as a perturbation by including it exactly in the wave function by a "renormalization". The part of  $\Delta H_{\text{vibr}}$  which still remains after renormalization is the nonadiabaticity of BO correction operator. At the end of the calculation an approximation is made of the interaction with only one phonon mode (1,5,11-13). For small coupling and low temperature a Poisson-like function is obtained (12) for the distribution of the multiphonon relaxation rate with the number of phonons

$$W_p \sim (\exp - S)(S^p/p!) \quad (1)$$

where  $S$  is the Huang-Rhys-Pekar number(7)

$$S(T=0) = \frac{1}{2} \Delta^2 \quad (2)$$

[ $S$  is the measure of electron phonon coupling strength]

The displacement  $\Delta$  measures the horizontal shift of the electronic state potentials in units of the zero point amplitude  $(\hbar/M\omega)^{1/2}$  where  $M$  is the mass of the vibrator. In the case of isolated RE  $S < 0.1$   $S$  can be incorporated in the exponential formula of Dexter

$$W = \beta \exp(-\alpha \Delta E) \text{ with} \quad (3)$$

$$\alpha = (\hbar\omega)^{-1} [\ln(p/S) - 1] \text{ for low temperature and} \quad (4)$$

$$\alpha = (\hbar\omega)^{-1} [\ln(p/S)(n+1) - 1] \text{ for } T > 0 \quad (5)$$

$n$  being the phonon occupancy number

$$n = (\exp(-\hbar\omega/kT) - 1)^{-1} \text{ as explained in ref.6} \quad (6)$$

Application of the multiphonon theory to glasses requires the knowledge of the structural units forming the glass. Similarly to the electronic spectra in glasses the vibrational frequencies show inhomogeneous broadening due to the variation of sites. Table I shows the average frequencies of the network formers. The vibrations involving the network formers are lower by a factor of 2 to 4. The lack of symmetry in a glass and the molecular character of the high energy vibration were taken into account by Layne et al (14) in developing the theory of multiphonon relaxation in glass by using higher order terms in the perturbation theory. The dependence of a multiphonon rate on the energy gap to be bridged results then from the ratio of  $p$ -phonon process to that for a  $p-1$  phonon decay. Assuming the average matrix elements to be the same for  $p$  and  $p-1$  order processes, the ratio of  $W_p$  to  $W_{p-1}$  is

$$W_p/W_{p-1} = (\hbar/2M\omega)(n+1)4m^2 | \langle a | V | b \rangle |^2 / \hbar\omega^2 \quad (7)$$

Since the perturbation is weak

$$W_p/W_{p-1} = \epsilon \ll 1 \quad (8)$$

This result leads to the following exponential dependence of the rate on energy gap:

$$W_p = W_0 \epsilon^p = W \exp[\ln(\epsilon)/\hbar\omega] \Delta E \quad (9)$$

Considering the dependence of  $W_p$  on the phonon occupation number

from Eq.6 the rate for a p-order multiphonon decay is at temperature  $T > 0$

$$W_p = W_0(n(T)+1)^p \exp(-\alpha \Delta E) \text{ where} \quad (10)$$

$$\alpha = -\ln(\epsilon)/h\nu \quad (11)$$

and  $W_0 = \beta$  of Eq.3 are dependent on the host but independent of the specific electronic level of RE from which the decay occurs.

By comparing Eq.4 with Eq.11 one obtains the connection

$$\ln S/p = \ln \epsilon - 1 \quad (12)$$

#### ANALYSIS OF THE EXPERIMENTAL RESULTS

The multiphonon relaxation rates of RE in oxide glasses were studied by us (3) and by Weber and his group(14). The results show an exponential behavior of W on energy gap. The low temperature results may be presented by a linear dependence of  $\ln W$  versus  $\Delta E$  or  $\ln W$  versus p as predicted by Eqs.10 and 11.

The spectral behavior of RE in chalcogenide glasses of the composition  $3Ga_2S_3-La_2S_3$  (GLS) and  $3Al_2S_3-La_2S_3$  (ALS) were studied by A. Bornstein and the author (15,18). The multiphonon relaxation rates for a number of levels of  $Ho^{3+}$  and  $Er^{3+}$  were obtained from lifetime measurements subtracting the radiative transition probabilities using the formula

$$1/\tau_{meas} = W + \Sigma A \quad (13)$$

where the radiative transition probabilities A were calculated by the Judd-Ofelt formula.

In cases where energy differences were higher than  $2500cm^{-1}$  and nonradiative probabilities small the values were obtained from measurements of quantum efficiencies using formula

$$\text{quantum yield} = \frac{\Sigma A}{\Sigma A + W} \quad (14)$$

Specifically the latter formula was applied to the nonradiative decays for the levels  $4S_{3/2}$  and  $4F_{9/2}$  of  $Er^{3+}$ . The low temperature values of multiphonon relaxations in the chalcogenide glasses versus energy gap are presented in Fig.1. Nonradiative rates for some levels of  $Nd^{3+}$  and  $Er^{3+}$  in fluoride glasses of the composition  $49BeF_2-27KF-14CaF_2-10AlF_3$  at room temperature were studied by Layne and Weber (20) by measurement of the transient fluorescence followed by pulsed laser excitation of selected levels. Their results can

also be presented by an exponential behavior.

The multiphonon decay rate for a given level to the next lower level decreases with the lowering of the energy of the stretching frequencies of the glass former since a large number of phonons is needed in fluoride glasses and more so in chalcogenide glasses in order to reach the same energy gap. Dependence of the multiphonon transition rate on the number of phonons from the emitting to the next lower level for a number of glasses and crystal hosts are presented in Fig.2.

The parameters  $\alpha$  and  $\beta$  of Eq.8 and  $\epsilon$  of Eq.11 are presented in Table I together with the phonon frequencies. The Huang-Rhys-Pekar (HRP) number  $S$  was calculated using Eq.12 for 4 and 5 phonons. Its values are presented in Table II. Our calculation differs slightly from that of Fonger and Struck (13) who used a different formula.

It should be noted that the measurement of lifetime and quantum efficiency from which the decay rates are calculated are reflecting an average of sites and Stark splittings of the specific levels thus the parameters presented in the Table reveal a gross behavior of variation of the level energies. When the glasses are selectively excited by line-narrowing techniques differences in multiphonon rates are observed (21) but even those cannot be attributed to specific sites having accidentally similar energies (22). Also when excited by line source various rare earth ions with the exception of  $\text{Eu}^{3+}$  having  $0 \rightarrow 0$  transitions transfer energy between them by multiphonon processes and both the lifetime and steady state fluorescence observed reflect the emission from a number of sites. Thus the numbers presented in the Table while not specific to a given site are still characteristic for a specific host. Low coupling constants in the oxide glasses are in accordance with the theory assuming weak coupling between the RE ion and its surroundings. A similar behavior is observed in the fluoride glasses. The chalcogenide glasses exhibit a much higher coupling constant while still showing exponential behavior between  $\ln W_0$  and the number of phonons. A plot of Eq.1 versus the number of phonons shows that an exponential behavior is observed only for  $S < 0.1$ . Higher values of  $S$  show deviation from exponentiality. From this it can be concluded that the multiphonon relaxation theory as finally reflected by Eq.1 is a good approximation for glasses in which mainly an ionic bond is formed between the RE ion and its surrounding ligands. In the chalcogenide glass the bond between the RE ion and the surrounding  $S$  ions is of a covalent type as reflected by the nephelauxetic effect(15,23). The covalency in the chalcogenide glasses is further reflected in the hypersensitive transitions in this glass (24).

Dr.W.H.Fonger has kindly sent us his computation of the orders of change of the function appearing in Eq.1 between 4 and 9 phonons

Table I. Parameters of nonradiative relaxations

The host	$\beta \text{ sec}^{-1}$	$\alpha \text{ cm}^{-1} \text{ sec}$	$\hbar\omega \text{ cm}^{-1}$	$\epsilon$
GLS, ALS <sup>x</sup>	$1 \times 10^6$	$2.9 \times 10^{-3}$	350	0.36
Tellurite <sup>#</sup>	$6.3 \times 10^{10}$	$4.7 \times 10^{-3}$	700	0.037
Germanate	$3.4 \times 10^{10}$	$4.9 \times 10^{-3}$	900	0.013
Phosphate	$5.4 \times 10^{12}$	$4.7 \times 10^{-3}$	1200	0.0037
Borate	$2.9 \times 10^{12}$	$3.8 \times 10^{-3}$	1400	0.0049
BeF <sub>2</sub> <sup>xx</sup>	$9 \times 10^{11}$	$6.3 \times 10^{-3}$	500	0.042
LaCl <sub>3</sub> <sup>*</sup>	$1.5 \times 10^{10}$	$13.0 \times 10^{-3}$	260	0.037
LaBr <sub>3</sub>	$1.2 \times 10^{10}$	$19.0 \times 10^{-3}$	175	0.037
LaF <sub>3</sub>	$6.6 \times 10^8$	$5.6 \times 10^{-3}$	350	0.14
Y <sub>2</sub> O <sub>3</sub>	$2.7 \times 10^8$	$3.8 \times 10^{-3}$	550	0.12
SrF <sub>2</sub>	$3.1 \times 10^8$	$4.0 \times 10^{-3}$	360	0.20
Y <sub>3</sub> Al <sub>5</sub> O <sub>12</sub>	$9.7 \times 10^7$	$3.1 \times 10^{-3}$	700	0.045
YAlO <sub>3</sub>	$5 \times 10^9$	$4.6 \times 10^{-3}$	600	0.063
LiYF <sub>4</sub>	$3.5 \times 10^7$	$3.8 \times 10^{-3}$	400	0.22
BaY <sub>2</sub> F <sub>8</sub>	$4.5 \times 10^7$	$4.1 \times 10^{-3}$		

<sup>x</sup> Ref. 18 <sup>#</sup>R. Reisfeld, L. Boehm and N. Spector. The Rare Earths in Modern Science and Technology. p.513 ed. G.J. McCarthy and J.J. Rhyne, Plenum Press 1978. <sup>xx</sup>C.B. Layne and M.J. Weber, Phys. Rev. B 16, 3259 1977. <sup>\*</sup> Ref 2. p.89.

Table II. Values of S for 4 and 5 phonons.

Host	GLS	Tell	Ger	Phos	Borate	BeF <sub>2</sub>	LaCl <sub>3</sub>
$\epsilon$	0.36	0.037	0.013	0.0037	0.0049	0.042	0.037
S(4p)	0.53	0.054	0.019	0.005	0.007	0.06	0.054
S(5p)	0.66	0.067	0.024	0.007	0.009	0.08	0.067

4p and 5p refer to 4 and 5 phonons respectively

as a function of values of  $S$ . From this calculation it is evident that the change in the oxide and fluoride glasses being of 10 orders of magnitude can be expressed as values smaller than 0.1. On the other hand the changes in the chalcogenide glasses are of 2 orders of magnitude corresponding to the high number of  $S=2$ . As mentioned above the high number in the chalcogenide glass maybe due to the covalency and inability to look on the RE incorporated in the chalcogenide glasses as a point charge.

Energy transfer from the  $UO_2^{2+}$  ion to various RE ions which are not in resonance with the electronic emitting state of the  $UO_2^{2+}$  ion (25) are presented as a function of energy gap between the uranyl level and the levels of the RE ions in which energy transfer is taking place. Here again an exponential behavior is observed according with the Dexter-Miyakawa theory (26) which predicts that the phonon-assisted energy transfer maybe described by formula

$$W_{PAT}(\Delta E) = W_{PAT}(0)e^{-\beta\Delta E} \quad (15)$$

where  $\Delta E$  is the energy gap between the levels of donor and acceptor ions and  $\beta$  is a parameter determined by the strength of electron-lattice coupling as well as by the nature of the phonon involved.

In reference (13) it is proposed that energy transfer probabilities should have the same functional dependence as Eq.1 where the HRP function is the sum of the donor and acceptor  $S$  values. Phonon-assisted energy transfer between trivalent RE ions in yttrium oxide was studied by Yamada, Shionoya and Kushida (27). An exponential behavior of energy transfer rate on energy gap resulted in  $\beta=2.5 \times 10^{-3}$ .  $\beta$  values obtained from Fig.3 for energy transfer between  $UO_2^{2+}$  ion to RE ion in phosphate glass equal  $2.3 \times 10^{-4}$ . The coupling constant obtained from these values using Eq.11 are  $\epsilon=0.3$  for yttrium oxide and  $\epsilon=0.76$  in phosphate glass. Since  $\epsilon$  in this case reveals the sum of the coupling constant of the donor and acceptor ions (28) it is not surprising that when the acceptor ion is uranyl which is much stronger coupled to the host, the coupling constant is higher.

In conclusion multiphonon processes in glasses can be expressed by an exponential behavior with the host dependent parameters  $\alpha$  and  $\beta$ . The coupling constants  $\epsilon$  and  $S$  obtained from  $\alpha$  reveal a weak interaction in the oxide and fluoride glasses and much stronger interaction in the chalcogenide glasses being a result of the covalency between the RE's in the chalcogenide host.

#### Acknowledgement

The author is deeply grateful to Professors R.Englman and C.K. Jørgensen, Dr.Fonger and Mr.A.Bornstein for valuable discussions and to Mrs.E.Greenberg for help in preparation of the manuscript.

# REFERENCES

1. Yu E.Perlin, Sov.Phys.Uspekhi 6 542 (1963)
2. L.A.Riseberg and M.J.Weber in "Progress in Optics" Vol XIV, ed. E.Wolf, North Holland (1976)
3. R.Reisfeld, Structure and Bonding 22 123 (1975)
4. K.F.Freed in "Radiationless Processes in Molecules and Condensed Phases" ed. F.K.Fong, Springer-Verlag (1976)
5. F.K.Fong "Theory of Molecular Relaxation" John Wiley & Sons (1975)
6. F.Auzel, Proc.Intl.School of Atomic and Molecular Spectroscopy, ed. B.DiBartolo (1978)
7. R.Englman, Nonradiative Decay of Ions and Molecules in Solids, North Holland Pub.Co.Amsterdam, New York, Oxford (1979)
8. R.Reisfeld and Y.Eckstein, J.Chem.Phys. 63 4001 (1975)
9. R.Reisfeld, J.Hormadaly and A.Muranevich, Chem.Phys.Lett. 38 188 (1976); J.Hormadaly and R.Reisfeld, ibid 45 436 (1977)
10. Y.Tozozawa in Dynamical Processes in Solid State Optics p.90, ed. R.Kubo (Benjamin 1976)
11. R.Englman and J.Jortner, Mol.Phys. 18 145 (1970)
12. T.Miyakawa and D.L.Dexter, Phys.Rev.B 1 2961 (1970)
13. W.H.Fonger and C.W.Struck, J.Luminescence 17 241 (1978)
14. C.B.Layne, W.H.Lowdermilk and M.J.Weber, Phys.Rev.B 16 10 (1977)
15. A.Bornstein, J.Flahaut, M.Guittard, S.Jaulmes, A.M.Loizeau-Lazac'h, G.Lucazeau and R.Reisfeld, The Rare Earths in Modern Science and Technology, ed.McCarthy and Rhyne, Plenum Press 599 (1978)
16. R.Reisfeld and A.Bornstein, J.Luminescence 18/19 253 (1979)
17. R.Reisfeld, A.Bornstein, J.Flahaut, M.Guittard and A.M.Loizeau-Lazac'h, Chem.Phys.Lett. 47 408 (1977)
18. A.Bornstein, PhD Thesis (1979)
19. R.Reisfeld and A.Bornstein, J.Noncryst.Solids 27 143 (1978)
20. C.B.Layne and M.J.Weber, Phys.Rev.B 16 3259 (1977)
21. C.Brecher, L.A.Riseberg and M.J.Weber, Phys.Rev.B. 18 5799 (1978)
22. Y.Kalisky, R.Reisfeld and Y.Haas, Chem.Phys.Lett. 61 19 (1979)
23. R.Reisfeld and C.K.Jørgensen, Lasers and Excited States of Rare Earths, ed. Springer-Verlag, Heidelberg (1977)
24. R.Reisfeld, A.Bornstein and J.Flahaut, The Rare Earths in Modern Science and Technology, ed.McCarthy and Rhyne, Plenum Press Vol.2. (1979)
25. C.K.Jørgensen and R.Reisfeld, Chem.Phys.Lett. 35 441 (1975)
26. R.Reisfeld and N.Lieblisch-Sofer, Phonon-assisted energy transfer in glasses. Dynamical Processes in the Excited States of Ions and Molecules in Solids, DPC Wisconsin, Madison June (1979)
27. N.Yamada, S.Shionoya and T.Kushida, J.Phys.Soc.Jap. 32 1577 (1972)
28. N.Lieblisch-Sofer, R.Reisfeld and C.K.Jørgensen, Inorg.Chim. Acta 30 259 (1978)



Fig.1. Nonradiative relaxation rates for chalcogenide glasses.

Fig.2. Nonradiative relaxation  $W_0$  versus number of phonons  $p$

Fig.3. Energy transfer probability from  $UO_2^{2+}$  to the rare earths.

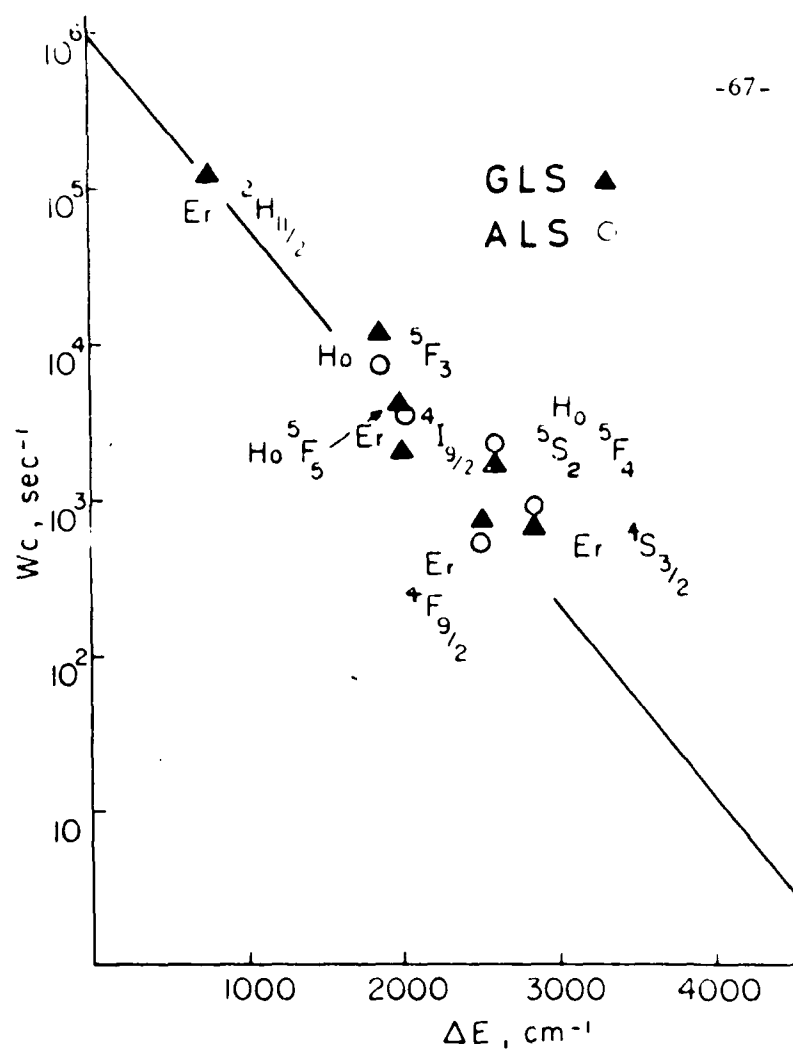


Fig. 1

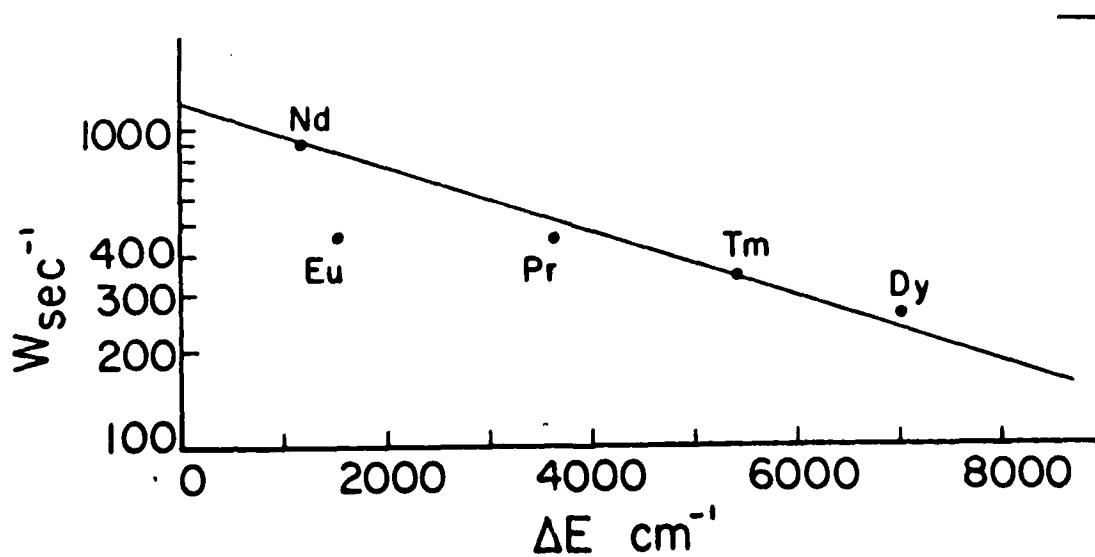
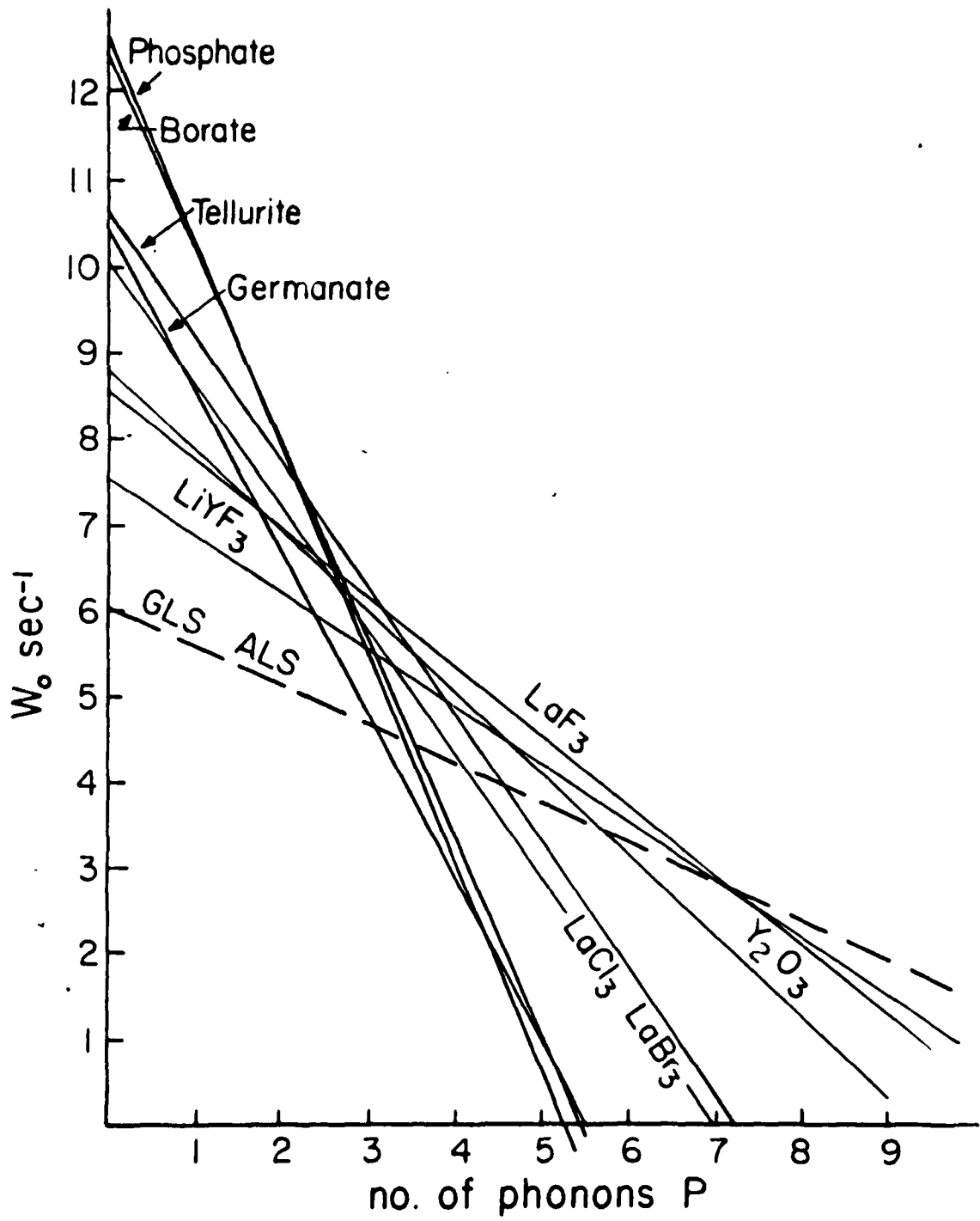


Fig. 3



F. 2

DATE  
FILMED  
-8